



PUBLISHED FOR SISSA BY SPRINGER

RECEIVED: February 12, 2018

REVISED: May 7, 2018

ACCEPTED: June 11, 2018

PUBLISHED: June 29, 2018

Search for Higgs boson decays to beyond-the-Standard-Model light bosons in four-lepton events with the ATLAS detector at $\sqrt{s} = 13$ TeV



The ATLAS collaboration

E-mail: atlas.publications@cern.ch

ABSTRACT: A search is conducted for a beyond-the-Standard-Model boson using events where a Higgs boson with mass 125 GeV decays to four leptons ($\ell = e$ or μ). This decay is presumed to occur via an intermediate state which contains one or two on-shell, promptly decaying bosons: $H \rightarrow ZX/XX \rightarrow 4\ell$, where X is a new vector boson Z_d or pseudoscalar a with mass between 1 and 60 GeV. The search uses pp collision data collected with the ATLAS detector at the LHC with an integrated luminosity of 36.1 fb^{-1} at a centre-of-mass energy $\sqrt{s} = 13$ TeV. No significant excess of events above Standard Model background predictions is observed; therefore, upper limits at 95% confidence level are set on model-independent fiducial cross-sections, and on the Higgs boson decay branching ratios to vector and pseudoscalar bosons in two benchmark models.

KEYWORDS: Beyond Standard Model, Hadron-Hadron scattering (experiments)

ARXIV EPRINT: [1802.03388](https://arxiv.org/abs/1802.03388)

Contents

1	Introduction	2
2	Benchmark models	3
2.1	Vector-boson model	3
2.2	Pseudoscalar-boson model	4
3	ATLAS detector	6
4	Event reconstruction	6
4.1	Trigger and event preselection	7
4.2	Lepton reconstruction	7
4.3	Definition of invariant-mass kinematic variables	8
4.4	Summary of analysis event selections	8
5	$H \rightarrow ZX \rightarrow 4\ell$ analysis	8
5.1	Monte Carlo simulation	8
5.2	Event selection	10
5.3	Background estimation	11
5.4	Systematic uncertainties	11
5.5	Results	12
6	$H \rightarrow XX \rightarrow 4\ell$ ($15 \text{ GeV} < m_X < 60 \text{ GeV}$) analysis	12
6.1	Monte Carlo simulation	12
6.2	Event selection	14
6.3	Background estimation	15
6.4	Systematic uncertainties	15
6.5	Results	16
7	$H \rightarrow XX \rightarrow 4\mu$ ($1 \text{ GeV} < m_X < 15 \text{ GeV}$) analysis	18
7.1	Monte Carlo simulation	18
7.2	Event selection	18
7.3	Background estimation	18
7.4	Systematic uncertainties	20
7.5	Results	20
8	Interpretation and discussion	21
8.1	Limits on fiducial cross-sections	22
8.2	Limits on branching ratios	22
9	Conclusion	25

1 Introduction

Following the discovery of the Higgs boson by the ATLAS and CMS collaborations [1, 2] at the Large Hadron Collider (LHC), a comprehensive programme of measurements of the properties of this particle is underway. These measurements could uncover deviations from the expected branching ratios for the decays of a Standard Model (SM) Higgs boson or allow for the possibility of decays into non-SM particles. Existing measurements constrain the non-SM or “exotic” branching ratio of the Higgs boson to less than approximately 30% at 95% confidence level (CL) [3–5].

Exotic Higgs boson decays have been proposed as a way to search for evidence of new physics. Due to the extremely narrow decay width of the Higgs boson predicted by the SM, the addition of even a small coupling to a new light state could open up sizeable new decay modes. In addition, new particles may couple preferentially to the Higgs boson since it provides a possible “portal” for hidden-sector particles to interact with SM particles [6–9]. Such decays are predicted by many theories of physics beyond the SM. For example, they are predicted in theories with a hidden (“dark”) sector [10–19] and in those with an extended Higgs sector such as the Next-to-Minimal Supersymmetric Standard Model (NMSSM) [20–24]. They are also predicted in several models of dark matter [25–30], models that explain astrophysical observations of positron excesses [31–33], models with a first-order electroweak phase transition [34, 35], and theories with neutral naturalness [36–38]. The processes under study here are referred to as $pp \rightarrow H \rightarrow ZX/XX \rightarrow 4\ell$, with Z being the SM Z boson and with X representing a possible new vector boson Z_d or a new pseudoscalar boson a . Section 2 provides an introduction to the theoretical background and specific models examined in this paper.

The search uses pp collision data at a centre-of-mass energy $\sqrt{s} = 13$ TeV collected by the ATLAS detector (described in section 3) at the LHC in 2015 and 2016 corresponding to an integrated luminosity of 36.1 fb^{-1} . Same-flavour decays of the new particle to pairs of electrons and muons are considered, giving rise to the $4e$, $2e2\mu$, and 4μ final states for particles in the mass range from 15 GeV to $m_H/2$, where $m_H = 125$ GeV. For lower masses, targeting the range from 1 GeV to 15 GeV, only the 4μ final state is explored. Final states including τ leptons are not considered in either mass range. The event reconstruction is discussed in section 4.

The search for $H \rightarrow ZX \rightarrow 4\ell$ in an X mass range between 15 GeV and 55 GeV is covered in section 5, while the $H \rightarrow XX \rightarrow 4\ell$ searches are included in sections 6 and 7 for $15 \text{ GeV} < m_X < 60 \text{ GeV}$ and $1 \text{ GeV} < m_X < 15 \text{ GeV}$, respectively.¹ Model interpreta-

¹The reason for the two ranges being different is that in the $H \rightarrow ZX \rightarrow 4\ell$ search the mass distributions of the X and the Z bosons begin to overlap significantly for values larger than 55 GeV, thus inhibiting unambiguous identification of the Z and the new bosons. This is not the case in the $H \rightarrow XX \rightarrow 4\ell$ search where a Z veto is applied.

tions and discussions are presented in section 8. Finally, the conclusions of the search are presented in section 9.

This paper builds on the previous work of ref. [39], in which a similar analysis is reported with data collected at $\sqrt{s} = 8$ TeV.

2 Benchmark models

Two well-motivated benchmark models that predict exotic decays to light beyond-the-Standard-Model (BSM) bosons are summarised below, and are used later in this paper when interpreting the results. In the first BSM benchmark model, the SM is extended with a dark-sector $U(1)$ group, denoted $U(1)_d$, leading to the appearance of a BSM vector boson, Z_d . In the second BSM benchmark model, there are two Higgs doublets and an additional singlet scalar field (2HDM+S). This leads to the appearance of a BSM pseudoscalar boson, a . The Z_d boson and the a pseudoscalar could each comprise the intermediate state in the decays $H \rightarrow ZX \rightarrow 4\ell$ and $H \rightarrow XX \rightarrow 4\ell$, where the first benchmark model is considered for a higher mass range and the second for a lower mass range.

2.1 Vector-boson model

Hidden- or dark-sector states appear in many extensions to the SM [10–19, 40]. The dark-sector states allow a theoretically plausible route for generation of the particle content necessary to account for the astrophysical evidence of dark matter. For example, fermionic dark-matter candidates [30] or dark-sector couplings to normal matter might explain astrophysical observations of positron excesses [31–33].

A dark sector is introduced with an additional $U(1)_d$ dark gauge symmetry [14–19], coupled to the SM through kinetic mixing with the hypercharge gauge field [41–43]. The gauge boson of the symmetry is the Z_d vector boson. In this hypercharge portal scenario, the kinetic mixing parameter ϵ controls the coupling strength of the dark vector boson to SM particles, which in turn determines the lifetime of the Z_d boson. The branching ratios of the Z_d are independent of the kinetic mixing strength and are instead determined by the gauge coupling. This coupling leads to a significant fraction of decays ($\approx 15\%$) to pairs of electrons or muons. For Z_d masses between 1 GeV and 60 GeV, the decay would be prompt (relative to the vertex resolution of the ATLAS detector) for $\epsilon \gtrsim 10^{-5}$ [14]. For smaller values of ϵ , the displaced decays provide a unique signature, which has been previously searched for with the ATLAS detector in 8 TeV collisions [44]. For Z_d masses below a few GeV and small values of ϵ , the decay products would be highly collimated and require a special analysis [45]. Another possibility involves a mass mixing between the Z boson and Z_d , facilitating the decay of the Z_d to SM particles. In this mechanism, the strength of the mixing is determined by mass mixing parameter δ [16, 17].

If the $U(1)_d$ symmetry is broken by the introduction of a dark Higgs boson, there could also be mixing between the SM Higgs boson and the dark Higgs boson [14–19]. In this scenario, the Higgs portal coupling κ controls the strength of the Higgs coupling to dark vector bosons. The observed Higgs boson would be the lighter one of an extended Higgs sector and could also decay into dark-sector particles.

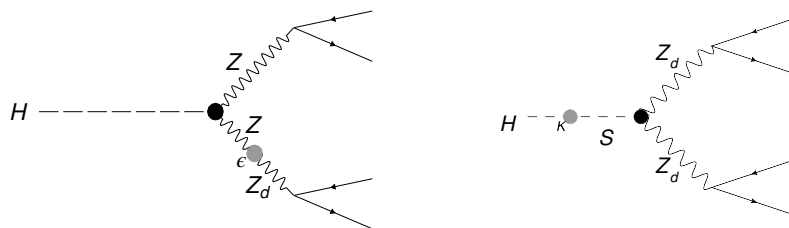


Figure 1. Exotic Higgs boson decays to four leptons induced by intermediate dark vector bosons via (left) the hypercharge portal and (right) the Higgs portal, where S is a dark Higgs boson [14]. The Z_d gauge boson decays to SM particles through kinetic mixing with the hypercharge field or through mass mixing with the Z boson. The HZZ_d vertex factor is proportional to ϵ whereas the HZ_dZ_d vertex factor is proportional to κ .

For the processes studied in this paper, the decay $H \rightarrow ZZ_d$ probes the parameter space of ϵ and m_{Z_d} , and does not depend on the presence of mixing between the SM Higgs boson and the dark-sector Higgs boson, κ . However, this BSM signal is indistinguishable from SM $H \rightarrow ZZ^*$ on an event-by-event basis, and therefore must emerge as a resonance in the dilepton mass above this background process. The SM background to the $H \rightarrow Z_dZ_d$ process, however, is more easily separated from the signal. This feature makes the latter channel potentially sensitive to much smaller values of kinetic mixing, where the only requirement is that the kinetic mixing must be large enough for the Z_d to decay promptly. However, this process depends on the presence of mixing between the SM Higgs boson and dark-sector Higgs boson, and therefore probes the parameter space of κ and m_{Z_d} .

Feynman diagrams of both processes are shown in figure 1. These processes are included in the Hidden Abelian Higgs Model (HAHM) that is used in this paper as the benchmark vector-boson model [14].

The presence of the dark sector could be inferred either from deviations from the SM-predicted rates of Drell-Yan (DY) events or from Higgs boson decays through exotic intermediate states. Model-independent upper bounds from electroweak constraints on the kinetic mixing parameter, ϵ , below 0.03 are reported in refs. [14, 46, 47] for dark vector bosons with masses between 1 GeV and 200 GeV. Upper bounds on the kinetic mixing parameter based on searches for dilepton resonances, $pp \rightarrow Z_d \rightarrow \ell\ell$, below the Z boson mass, are found to be in range of 0.005–0.020 for dark vector bosons with masses between 20 GeV and 80 GeV [48]. In the mass range of 10 MeV–10 GeV, values of ϵ above $\sim 10^{-3}$ are ruled out [49–54]. The experiments at the LHC are the only ones sensitive to the production of Higgs bosons, and this makes possible the search for the presence of a Higgs portal presented here. Constraints on the Higgs mixing parameter κ are probed through the $H \rightarrow Z_dZ_d \rightarrow 4\ell$ search while constraints on the kinetic mixing parameter and the mass-mixing parameter δ can be obtained through the $H \rightarrow ZZ_d \rightarrow 4\ell$ search.

2.2 Pseudoscalar-boson model

Another possibility to extend the SM with a hidden sector is to consider two-Higgs-doublet models extended by one complex scalar singlet field (2HDM+S) [15].

Two-Higgs-doublet models predict two charged scalars (H^\pm), two neutral scalars (H , \mathbb{H}) and one neutral pseudoscalar (A). The real mass eigenstate H is considered to be the observed Higgs boson, while other states are taken to be heavy in the decoupling limit to ensure that highly non-standard Higgs decays (e.g. involving CP-violation) which are significantly constrained by existing data, are avoided [55, 56]. The scalar singlet added to 2HDM only couples to the two Higgs complex fields in the potential and has no Yukawa couplings. Therefore, all of its couplings to SM fermions are acquired through mixing of the scalar field with the Higgs complex fields, which needs to be small to preserve the SM nature of the Higgs sector.

With these assumptions, the decay $H \rightarrow aa$ is allowed, where a is a light pseudoscalar mass eigenstate mostly composed of the imaginary part of the singlet field.² The aforementioned constraints on two-Higgs-doublet models can be incorporated in the 2HDM+S by choosing a region of the 2HDM phase space not yet excluded, and giving the real and imaginary components of the singlet separate masses and small mixings to the Higgs doublets. The branching ratios of a into fermions are determined by the Yukawa couplings of a to fermions, and lead to a rich decay phenomenology [15], albeit with typically negligible branching ratio to pairs of electrons, and smaller branching ratios to pairs of muons than the dark vector bosons described in the previous section. Among all the models predicting different decay possibilities, type II are theoretically well motivated,³ since light pseudoscalars can correspond to the R -symmetry limit of the NMSSM [57, 58], which elegantly solves the μ -problem of the MSSM [59] and greatly reduces the fine-tuning and little-hierarchy problems. Furthermore, in the NMSSM the branching ratio for $H \rightarrow aa$ can be significant. Type-II models can also predict a significant branching ratio for $a \rightarrow \mu\mu$, especially in the range $2m_\mu < m_a < 2m_\tau$, with values ranging from 10^{-2} to 10^{-1} for some regions of the parameter space [15].

Several searches for a Higgs boson decaying to electrons, muons, τ leptons or b -jets via two pseudoscalars have been performed at both the LHC and the Tevatron. The DØ and ATLAS collaborations have searched for a signal of $H \rightarrow aa \rightarrow 2\mu 2\tau$ in the a boson mass ranges $3.7 \leq m_a \leq 19 \text{ GeV}$ and $3.7 \leq m_a \leq 50 \text{ GeV}$, respectively [60, 61]. The DØ and CMS collaborations have searched for the signature $H \rightarrow aa \rightarrow 4\mu$ in the range $2m_\mu \leq m_a \leq 2m_\tau$ [60, 62]. The CMS collaboration has additionally searched for $H \rightarrow aa \rightarrow 4\tau, 2\mu 2\tau, 2\mu 2b$ in the range $5 \text{ GeV} \leq m_a \leq 62.5 \text{ GeV}$ [63] and the ATLAS collaboration for $H \rightarrow aa \rightarrow 4b$ in the range $20 \text{ GeV} \leq m_a \leq 60 \text{ GeV}$ [64]. These searches have led to limits on the branching ratio of the Higgs boson decaying to aa , scaled by the ratio of the production cross-section of the Higgs boson that is searched for to that predicted by the SM, $\sigma(H)/\sigma_{\text{SM}} \times \mathcal{B}(H \rightarrow aa)$, between 1% and 3% for pseudoscalar-boson masses between 1 GeV and 3 GeV and between 10% and 100% for masses larger than 5 GeV, assuming a 2HDM+S Type-II model with $\tan \beta = 5.0$.

²The pseudoscalar state is $a = \cos \theta_a S_I + \sin \theta_a A$, where $\theta_a \ll 1$ is a small mixing angle and S_I is the imaginary part of the complex singlet field.

³The right-handed states d_R and e_R couple to H_1 , u_R to H_2 , where H_1 and H_2 are the two Higgs doublets. See ref. [15] for more information.

3 ATLAS detector

The ATLAS experiment [65] is a multi-purpose particle physics detector with forward-backward symmetric cylindrical geometry and a near 4π coverage in solid angle.⁴ The interaction point is surrounded by an inner detector (ID) tracking system, a calorimeter system, and a muon spectrometer (MS). The ID covers $|\eta| < 2.5$ and consists of a silicon pixel detector, a silicon microstrip detector, and a transition radiation tracker. The ID is surrounded by a thin superconducting solenoid providing a 2 T axial magnetic field. One significant upgrade for Run 2 is the presence of the insertable B-layer (IBL) [66], an additional pixel layer close to the interaction point, which provides high-resolution measurements at small radius to improve the tracking performance. The calorimeter system features a high-granularity lead/liquid-argon (LAr) sampling calorimeter that measures the energy and the position of electromagnetic showers within $|\eta| < 4.9$. LAr sampling calorimeters are also used to measure hadronic showers in the endcap ($1.5 < |\eta| < 3.2$) and forward ($3.1 < |\eta| < 4.9$) regions, while a steel/scintillator tile calorimeter measures hadronic showers in the central region ($|\eta| < 1.7$). The MS surrounds the calorimeters and consists of three large superconducting air-core toroid magnets, each with eight coils, a system of precision tracking chambers ($|\eta| < 2.7$), and fast trigger chambers ($|\eta| < 2.4$). For Run 2 the ATLAS detector has a two-level trigger system. The first-level trigger (Level-1 trigger) is implemented in hardware and uses a subset of the detector information to reduce the accepted rate to 100 kHz. This is followed by a software-based trigger (called high-level trigger) that reduces the rate of events recorded to 1 kHz.

4 Event reconstruction

The three analyses presented in this paper all follow a similar event reconstruction and selection procedure. This section describes the basic event selection and lepton reconstruction requirements that are common to all three analyses. Table 1 summarises the event selection used in the three analyses that are described in further detail in sections 5–7.

Events are preselected in accord with trigger requirements and basic event requirements such as the existence of a reconstructed primary vertex [67], which has the largest sum of p_T^2 of the associated tracks. For each event, a selection is applied to the reconstructed final-state leptons. The event is required to have at least four leptons. These leptons are combined into dileptons, and the dileptons are paired into quadruplets. Quadruplets are then filtered by selection criteria specific to each analysis, and a single quadruplet (with a specific dilepton pairing) is selected according to a ranking metric that favours pairings

⁴ATLAS uses a right-handed coordinate system with its origin at the nominal interaction point (IP) in the centre of the detector and the z -axis along the beam pipe. The x -axis points from the IP to the centre of the LHC ring, and the y -axis points upward. Cylindrical coordinates (r, ϕ) are used in the transverse plane, ϕ being the azimuthal angle around the z -axis. The pseudorapidity is defined in terms of the polar angle θ as $\eta = -\ln \tan(\theta/2)$. The transverse momentum p_T and other transverse variables, are defined as the variables' component in the $x - y$ plane, the transverse energy E_T is defined as $\sqrt{m^2 + p_T^2}$, where m represents the mass of a considered object. The distance in the pseudorapidity-azimuthal-angle space is defined as dR or $\Delta R = \sqrt{(\Delta\eta)^2 + (\Delta\phi)^2}$.

compatible with either a ZX or XX intermediate state, depending on the analysis. If there are no quadruplets in the event that meet the selection criteria then the event is discarded. Final event selections are based on properties of this selected quadruplet and the corresponding dilepton pair.

4.1 Trigger and event preselection

Events are preselected by single-lepton, dilepton, or trilepton triggers [68], with a combined efficiency very close to 100% (relative to the signal region events surviving all other event selections). Trigger thresholds were increased slightly throughout the run to compensate for increasing peak instantaneous luminosity delivered by the LHC. The lowest p_T thresholds for the single-lepton triggers ranged from 24 GeV to 26 GeV. Dielectron (dimuon) trigger thresholds ranged from 2×12 GeV (2×10 GeV) to 2×17 GeV (22, 8 GeV). Trielectron (trimuon) triggers had thresholds of 17, 9, 9 GeV (3×6 GeV). In the low-mass selection, only the muon-based triggers are used. The events must have at least one primary vertex [67] with two or more associated tracks with $p_T > 400$ MeV and satisfy cleaning criteria [69] designed to reject events with excessive noise in the calorimeters.

4.2 Lepton reconstruction

An electron is reconstructed from a cluster of energy deposits in the electromagnetic calorimeter matched to a high-quality track in the ID. Its momentum is computed from the cluster energy and the direction of the track. Electrons are required to have $|\eta| < 2.47$ and $p_T > 7$ GeV. Electrons can be distinguished from other particles using several identification criteria that rely on the shapes of electromagnetic showers as well as tracking and track-to-cluster matching quantities. Following the description in ref. [70], the output of a likelihood function taking these quantities as input is used to identify electrons, choosing the loose working point, but with the additional requirement of a hit presence in the innermost layer of the ID.⁵

A muon is reconstructed by matching a track or track segment reconstructed in the MS to a track reconstructed in the ID [71]. Its momentum is calculated by combining the information from the two systems and correcting for energy deposited in the calorimeters. In regions of limited coverage by the MS ($|\eta| < 0.1$), muons can be reconstructed by matching ID tracks to calorimeter signals consistent with a minimum-ionising particle (calorimeter-tagged muons). In regions outside the ID acceptance ($2.5 < |\eta| < 2.7$), muon reconstruction can also be extended by using tracks in the MS (stand-alone muons). Reconstructed muons are required to pass the requirements of the loose working point to maximise the reconstruction efficiency while providing good-quality muon tracks [71]. Muons are required to have $|\eta| < 2.7$ and $p_T > 5$ GeV. Calorimeter-tagged muons must have $p_T > 15$ GeV.

Leptons are required to originate from the hard-scattering vertex, defined as the primary vertex in the pre-selection. The longitudinal impact parameter of each lepton track, calculated relative to the hard-scattering vertex and multiplied by $\sin \theta$ of the track, is

⁵When no measurement is expected in the innermost layer of the pixel detector, the requirement is transferred to the next-to-innermost pixel layer.

required to be smaller than 0.5 mm. Furthermore, muons must have a transverse impact parameter calculated relative to the beam line smaller than 1 mm in order to reject muons originating from cosmic rays. The significance of the transverse impact parameter calculated relative to the beam line is required to be less than three (five) for muons (electrons). Stand-alone muons are exempt from all three requirements, as they do not have an ID track.

The leptons are required to be isolated from other particles using ID track information and calorimeter information. The sum of the transverse energy ΣE_T of other topological clusters [72] in the cone of $\Delta R = 0.2$ around the electron (muon) is required to be less than 20% (30%) of the p_T of the electron (muon). The Σp_T of tracks within a variable-width cone of $\Delta R = \min(0.2, 10 \text{ GeV}/p_T)$ ($\Delta R < \min(0.3, 10 \text{ GeV}/p_T)$) of the electron (muon) must be less than 15% of the p_T of the electron (muon). Contributions to the isolation cones from other leptons in the quadruplet are subtracted before applying the requirements.

Overlap removal is applied to avoid identifying the same detector signature as multiple electrons, muons or jets. Electrons sharing an ID track with a selected muon are ignored, except if the muon is only calorimeter-tagged, in which case the muon is ignored instead. Electrons sharing their track or cluster in the calorimeter with a selected higher- p_T electron are ignored.

4.3 Definition of invariant-mass kinematic variables

For all three analyses, the convention is adopted that m_{12} and m_{34} are the invariant masses of the two dileptons that make up a quadruplet, with the defining constraint that $|m_{12} - m_Z| < |m_{34} - m_Z|$, where m_Z is the mass of the Z boson⁶ [73]. Thus m_{12} identifies the primary pair and m_{34} is the secondary pair.

In the case of quadruplets formed from four electrons or four muons, alternate pairings of same-flavour opposite-sign leptons can be formed. The invariant masses of these alternate pairings are denoted by m_{14} and m_{32} , where the positively charged lepton from the primary pair is paired with the negatively charged lepton from the secondary pair to compute m_{14} , and the positively charged lepton from the secondary pair is paired with the negatively charged lepton from the primary pair to compute m_{32} .

4.4 Summary of analysis event selections

Table 1 summarises the event selection used in the three analyses that are described in further detail in sections 5–7, and signal efficiencies of these selections with respect to a minimal fiducial volume are shown in figures 7a and 8a of section 8.1.

5 $H \rightarrow ZX \rightarrow 4\ell$ analysis

5.1 Monte Carlo simulation

Samples of events with $H \rightarrow ZZ_d \rightarrow 4\ell$, where the Higgs boson with mass $m_H = 125 \text{ GeV}$ was produced in the gluon-gluon fusion mode (ggF), were generated using the Hidden

⁶Put another way, m_{12} is the invariant mass of the dilepton that is closer to the Z boson mass, and m_{34} is the invariant mass of the other dilepton in the quadruplet.

	$H \rightarrow ZX \rightarrow 4\ell$ (15 GeV < m_X < 55 GeV)	$H \rightarrow XX \rightarrow 4\ell$ (15 GeV < m_X < 60 GeV)	$H \rightarrow XX \rightarrow 4\mu$ (1 GeV < m_X < 15 GeV)
QUADRUPLET SELECTION	- Require at least one quadruplet of leptons consisting of two pairs of same-flavour opposite-sign leptons - Three leading- p_T leptons satisfying $p_T > 20$ GeV, 15 GeV, 10 GeV - At least three muons are required to be reconstructed by combining ID and MS tracks in the 4μ channel		
	- Select best quadruplet (per channel) to be the one with the (sub)leading dilepton mass (second) closest to the Z mass - 50 GeV < m_{12} < 106 GeV - 12 GeV < m_{34} < 115 GeV - $m_{12,34,14,32} > 5$ GeV	Leptons in the quadruplet are responsible for firing at least one trigger. In the case of multi-lepton triggers, all leptons of the trigger must match to leptons in the quadruplet	
	$\Delta R(\ell, \ell') > 0.10$ (0.20) for same-flavour (different-flavour) leptons in the quadruplet		—
QUADRUPLET RANKING	Select first surviving quadruplet from channels, in the order: 4μ , $2e2\mu$, $2\mu2e$, $4e$	Select quadruplet with smallest $\Delta m_{\ell\ell} = m_{12} - m_{34} $	
EVENT SELECTION	115 GeV < $m_{4\ell}$ < 130 GeV		120 GeV < $m_{4\ell}$ < 130 GeV
		$m_{34}/m_{12} > 0.85$ Reject event if: $(m_{J/\Psi} - 0.25 \text{ GeV}) < m_{12,34,14,32} < (m_{\Psi(2S)} + 0.30 \text{ GeV})$, or $(m_{\Upsilon(1S)} - 0.70 \text{ GeV}) < m_{12,34,14,32} < (m_{\Upsilon(3S)} + 0.75 \text{ GeV})$	
		10 GeV < $m_{12,34}$ < 64 GeV 4e and 4μ channels: 5 GeV < $m_{14,32}$ < 75 GeV	0.88 GeV < $m_{12,34}$ < 20 GeV No restriction on alternative pairing

Table 1. Summary of the event selection of the different analyses described in this paper. The quarkonia resonance masses $m_{J/\Psi}$, $m_{\Psi(2S)}$, $m_{\Upsilon(1S)}$, and $m_{\Upsilon(3S)}$ are taken from ref. [73].

Abelian Higgs Model (HAHM) [18, 19]. The event generator MADGRAPH5_AMC@NLO v2.2.3 [74] with the NNPDF23 [75] parton distribution functions (PDFs) at leading order (LO) was used. PYTHIA8 [76] (v8.170) with the A14 parameter set [77] was used for the modelling of the parton shower, hadronisation and underlying event. Nine samples were generated in the range $15 \leq m_{Z_d} \leq 55$ GeV with a 5 GeV step corresponding to different Z_d mass hypotheses. The model parameters ϵ and κ were adjusted so that only $H \rightarrow ZZ_d \rightarrow 4\ell$ decays were generated ($\epsilon \gg \kappa$). The samples were normalised using the SM Higgs boson production cross-section $\sigma_{\text{SM}}(ggF) = 48.58$ pb and the $\mathcal{B}(H \rightarrow ZZ^* \rightarrow 4\ell) = 1.25 \times 10^{-4}$ taken from ref. [78], as this branching ratio corresponds approximately to the upper limit set in the previous search [39]. Final states with τ leptons are not considered in this analysis and thus were not generated. The background processes considered for this search follow those used in the $H \rightarrow ZZ^* \rightarrow 4\ell$ measurement [79], and consist of:

$H \rightarrow ZZ^* \rightarrow 4\ell$: the Higgs boson production through ggF [80], vector-boson fusion (VBF) [81], and in association with a vector boson (VH) [82], was simulated using the POWHEG-BOX v2 MC event generator [83–85] with the PDF4LHC NLO PDF set [86]. For Higgs boson production in association with a heavy quark pair, events were simulated with MADGRAPH5_AMC@NLO (v.2.2.3 for $t\bar{t}H$ and v.2.3.3 for $b\bar{b}H$) [74],

using the CT10 NLO PDF set [87] for $t\bar{t}H$ and the NNPDF23 PDF set [75] for $b\bar{b}H$. For the ggF , VBF , VH , and $b\bar{b}H$ production mechanisms, PYTHIA8 [88] was used for the $H \rightarrow ZZ^* \rightarrow 4\ell$ decay as well as for parton showering, hadronisation and underlying event using the AZNLO parameter set [89]. For showering in the $t\bar{t}H$ process, HERWIG++ [90] was used with the UEEE5 parameter set [91]. The Higgs boson production cross-sections and decay branching ratios, as well as their uncertainties, are taken from refs. [78, 92, 93]. This background is approximately 64% of the total background prediction.

$ZZ^* \rightarrow 4\ell$: the non-resonant SM $ZZ^* \rightarrow 4\ell$ process was simulated using SHERPA 2.2.2 [94–96] for quark-antiquark annihilation, using the NNPDF3.0 NNLO PDF set. The loop-induced gg -initiated ZZ^* production was modelled with GG2VV [97] interfaced to PYTHIA8, where s -channel H diagrams were omitted to avoid double-counting this contribution, using the CT10 PDFs. The latter process was calculated at LO and receives large QCD corrections at NLO. The cross-section of the sample was therefore multiplied by an NLO/LO K -factor of 1.70 ± 0.15 [98]. This background contributes with approximately 30% of the total prediction.

VVV , $t\bar{t}+V$: the triboson backgrounds ZZZ , WZZ , and WWZ with four or more leptons originating from the hard scatter were produced with SHERPA 2.1.1 [94–96, 99–102]. The all-leptonic $t\bar{t}Z$ and $t\bar{t}W$ processes were simulated with MADGRAPH5_AMC@NLO interfaced to PYTHIA8 with the A14 parameter set. This background is approximately 0.5% of the total prediction.

Reducible background: processes like $Z + \text{jets}$, $t\bar{t}$ and WZ , produce less than four prompt leptons but can contribute to the selection through jets misidentified as leptons. $Z + \text{jets}$ events were modelled using SHERPA 2.2.2. The $t\bar{t}$ background was generated with POWHEG-BOX interfaced to PYTHIA6 [103] for parton shower and hadronisation and underlying event. The WZ production was modelled using POWHEG-BOX plus PYTHIA8 and the AZNLO parameter set. This background is approximately 6% of the total prediction.

The generation of the simulated samples includes the effect of multiple pp interactions in the same and nearby bunch crossings (pile-up). This was simulated at LO with PYTHIA8 using MSTW 2008 PDFs [104] and the A2 tune [105]. The samples were then passed through a simulation of the ATLAS detector [106] based on GEANT4 [107]. Weights were applied to the simulated events to correct for the small differences relative to data in the reconstruction, identification, isolation, and impact parameter efficiencies for electrons and muons [70, 71]. Furthermore, the lepton momentum scales and resolutions were adjusted to match the data [71, 108].

5.2 Event selection

All possible combinations of quadruplets are formed by selecting two same-flavour opposite-sign (SFOS) lepton pairs. Each quadruplet must not include more than one stand-alone

or calorimeter-tagged muon, and its three leading leptons must have p_T (E_T) $> 20, 15, 10$ GeV.⁷ Then a quadruplet per final state is chosen so that the leading pair is defined as the SFOS pair with the mass m_{12} closest to the Z boson mass and the subleading pair is defined as the SFOS pair with the mass m_{34} second closest to the Z boson mass. From this point, the analysis selection proceeds in parallel for the four final states ($4\mu, 2e2\mu, 2\mu2e, 4e$).

For each final state, m_{12} is required to be in the range of $50 - 106$ GeV, while m_{34} is required to be in the range of $12 - 115$ GeV. A separation of $\Delta R > 0.10$ (0.20) is required for all possible pairings of same-flavour (different-flavour) leptons in the quadruplet. Quadruplets are removed if an alternative same-flavour opposite-sign dilepton mass is less than 5 GeV. Then the loose calorimeter- and track-based isolation as well as impact parameter requirements explained in section 4.2 are imposed on the leptons. As the four leptons should originate from a common vertex point, a requirement on the χ^2 value of a common-vertex fit is applied, corresponding to a signal efficiency of 99.5% for all decay channels. If more than one quadruplet passes the selection, the channel with the highest expected signal rate is selected, in the order: $4\mu, 2e2\mu, 2\mu2e$ and $4e$. At this point only one quadruplet remains. In order to improve the four-lepton mass reconstruction, final-state radiation photons arising from any of the lepton candidates in the quadruplet are added to the 4ℓ system using the same strategy as in ref. [109]. Events are then classified into $2\ell2\mu$ and $2\ell2e$ final states. The signal region is defined by the window of the four-lepton invariant mass $m_{4\ell} \in [115, 130]$ GeV.

5.3 Background estimation

The dominant background contribution comes from $H \rightarrow ZZ^* \rightarrow 4\ell$, followed by non-resonant SM ZZ^* production. Triboson processes as well as $t\bar{t} + V$ processes are sources of smaller backgrounds. The background processes described above are estimated from simulation and normalised with the theoretical calculations of their cross-section as described in section 5.1.

The reducible background is estimated using data-driven techniques. Different approaches are followed for the $2\ell2\mu$ and $2\ell2e$ final states [109]. The procedure to estimate the normalisation of these backgrounds is explained in ref. [79]. The shapes of the Z +jets and $t\bar{t}$ backgrounds for the m_{34} distribution are taken from simulation and normalised using the inclusive data-driven estimate. For the WZ production, as the background sources are different between the two channels, this background is included in the data-driven estimate for the $2\ell2e$ final state, while it is added from simulation for the $2\ell2\mu$ final state.

5.4 Systematic uncertainties

Imperfect knowledge of the parameters affecting the measurements either from simulated or from data-driven estimates leads to systematic uncertainties which affect the normalisation or the shape of the signal and background samples. Each source of systematic uncertainty is considered to be uncorrelated with other sources. They are listed below.

⁷The p_T requirement is applied to muons while the E_T requirement is applied to electrons.

Luminosity and pile-up: the uncertainty in the integrated luminosity is 3.2%, affecting the overall normalisation of all processes estimated from the simulation. It is derived, following a methodology similar to that detailed in ref. [110], from a calibration of the luminosity scale using x - y beam-separation scans performed in August 2015 and May 2016. The uncertainty associated with the modelling of pile-up arises mainly from differences between the expected and observed fraction of the visible pp cross-section.

Lepton-related uncertainties: uncertainties associated with leptons arise from the reconstruction and identification efficiencies [70, 71], as well as lepton momentum scales and resolutions [71, 108]. The efficiencies are measured using tag-and-probe techniques on $Z \rightarrow \ell^+\ell^-$, $J/\psi \rightarrow \ell^+\ell^-$ and $\Upsilon \rightarrow \mu^+\mu^-$ data and simulated events. The small differences found are corrected for in the simulation. The combined effect of all these uncertainties results in an overall normalisation uncertainty in the signal and background ranging up to 10%. The dominant uncertainties arise in the reconstruction and identification of leptons.

MC background modelling: uncertainties in the factorisation and renormalisation scales, the parton shower, the choice of PDF, and the hadronisation and underlying-event model affect those backgrounds normalised with their theory cross-sections. Uncertainties in the modelling of $H \rightarrow ZZ^* \rightarrow 4\ell$ are found to be between 3% and 9% depending on the Higgs boson production mode, while for Standard Model $q\bar{q}/gg \rightarrow ZZ^*$ processes uncertainties from these sources add in quadrature to 5%.

Signal modelling: several sources of systematic uncertainty affect the theoretical modelling of the signal acceptance. Uncertainties originating from the choice of PDFs, the factorisation and renormalisation scales, and the modelling of parton shower, hadronisation, and underlying-event account for a total effect of 9% [92, 93].

Data-driven estimation of the background: uncertainties coming from the data-driven estimation of the background are also considered. They depend on the channel and affect the normalisation of the reducible background [79].

5.5 Results

The distribution of the invariant mass of the subleading dilepton pair m_{34} in the selected events in all four final states is shown in figure 2. The numbers of events observed in each channel after the event selection, as well as the expected background, are presented in table 2. A total of 102 events are observed for an expected background of 86.8 ± 7.5 .

6 $H \rightarrow XX \rightarrow 4\ell$ ($15 \text{ GeV} < m_X < 60 \text{ GeV}$) analysis

6.1 Monte Carlo simulation

The signal process $H \rightarrow Z_d Z_d \rightarrow 4\ell$ was generated using the same model and event generator as in the $H \rightarrow ZZ_d \rightarrow 4\ell$ analysis. The model parameters ϵ and κ were adjusted so that only $H \rightarrow Z_d Z_d \rightarrow 4\ell$ decays were generated ($\kappa \gg \epsilon$). Contributions from final states with τ leptons are not considered. The mass of the Z_d boson was varied for different

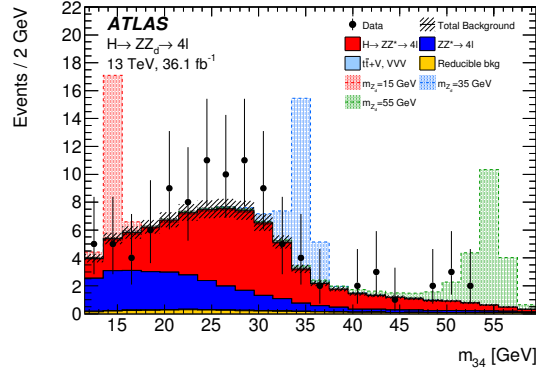


Figure 2. Distribution of m_{34} for data and background events in the mass range $m_{4\ell} \in [115, 130]$ GeV after the $H \rightarrow ZX \rightarrow 4\ell$ selection. Three signal points for the $H \rightarrow ZZ_d \rightarrow 4\ell$ model are shown. The signal strength corresponds to a branching ratio $\mathcal{B}(H \rightarrow ZZ_d \rightarrow 4\ell) = \frac{1}{3}\mathcal{B}(H \rightarrow ZZ^* \rightarrow 4\ell)$ (with $\mathcal{B}(H \rightarrow ZZ^* \rightarrow 4\ell)$ corresponding to the SM prediction [93]). The uncertainties include statistical and systematic contributions.

Process	$2\ell 2\mu$	$2\ell 2e$	Total
$H \rightarrow ZZ^* \rightarrow 4\ell$	34.3 ± 3.6	21.4 ± 3.0	55.7 ± 6.3
$ZZ^* \rightarrow 4\ell$	16.9 ± 1.2	9.0 ± 1.1	25.9 ± 2.0
Reducible background	2.1 ± 0.6	2.7 ± 0.7	4.8 ± 1.1
$VVV, t\bar{t} + V$	0.20 ± 0.05	0.20 ± 0.04	0.40 ± 0.06
Total expected	53.5 ± 4.3	33.3 ± 3.4	86.8 ± 7.5
Observed	65	37	102

Table 2. Expected and observed numbers of events in each channel after the $H \rightarrow ZX \rightarrow 4\ell$ event selection defined by the mass range $m_{4\ell} \in [115, 130]$ GeV. The uncertainties include MC-statistical and systematic components.

signal hypotheses in the range $15 \text{ GeV} < m_{Z_d} < 60 \text{ GeV}$ for $H \rightarrow Z_d Z_d \rightarrow 4\ell$, in steps of 5 GeV. The same signal normalisation was also applied (normalising to the SM Higgs boson production cross-section and $\mathcal{B}(H \rightarrow ZZ^* \rightarrow 4\ell)$).

For the signal process $H \rightarrow aa \rightarrow 4\mu$, the Higgs boson production was generated with the POWHEG-BOX v2 event generator [83–85] using the CT10 NLO PDFs [87]. Then this SM Higgs boson is replaced by a neutral scalar Higgs boson from the 2HDM+S [111] model. PYTHIA8 was used for the showering, hadronisation and underlying-event simulation in events generated where the Higgs boson decays to two pseudoscalar bosons that subsequently decay to pairs of muons, $H \rightarrow aa \rightarrow 4\mu$. The a -boson decay was done in the narrow-width approximation and the coupling to the muons is made to be that of a pseudoscalar. The mass of the a -boson was varied for five different signal hypotheses in the range $15 \text{ GeV} < m_a < 60 \text{ GeV}$.

The background processes considered in this analysis are similar to those featured in the $H \rightarrow ZZ_d \rightarrow 4\ell$ analysis described in section 5, however all the background processes

are now reducible by vetoing on lepton pairs consistent with a Z boson (see section 6.2 for more details). The background processes, in order of decreasing importance, are as follows:

$H \rightarrow ZZ^* \rightarrow 4\ell$: the modelling of this process is the same as for the $H \rightarrow ZZ_d \rightarrow 4\ell$ analysis, as described in section 5.3. This background is approximately 63% of the total background prediction for this analysis.

$ZZ^* \rightarrow 4\ell$: the dominant $q\bar{q}$ production mechanism was modelled by POWHEG-BOX interfaced to PYTHIA8. The gg -initiated production mechanism was modelled in the same way as described for the $H \rightarrow ZZ_d \rightarrow 4\ell$ analysis. Both production mechanisms use the CT10 PDFs. This background is approximately 19% of the total background prediction.

VVV/VBS: higher-order electroweak processes (with cross-sections proportional to α^6 at leading order) include triboson production and vector-boson scattering, which lead to four leptons in the final state, with two additional particles (quarks, neutrinos, or electrons and muons). These processes were modelled by SHERPA 2.1.1 with the CT10 PDFs. Higgs boson production through VBF is subtracted from the estimates obtained with this event generator, in order to avoid double-counting this process in final background estimates. This background is approximately 17% of the total background prediction.

$Z + (t\bar{t}/J/\psi/\Upsilon) \rightarrow 4\ell$: this background process corresponds to the production of a Z boson, in association with either a quarkonium state ($b\bar{b}$ or $c\bar{c}$) that decays to leptons, or $t\bar{t}$ production with leptonic decays of the prompt W bosons. The processes involving quarkonia were modelled using PYTHIA8 with the NNPDF 2.3 PDFs [75]. The $t\bar{t}Z$ process was modelled at leading order with MADGRAPH5 [112] interfaced to PYTHIA8, using the NNPDF 2.3 PDFs [75] and the A14 tune [77]. These backgrounds are approximately 1% of the total background prediction.

Other reducible backgrounds: the same three SM processes of diboson WZ production, production of $t\bar{t}$ which decay semileptonically or fully leptonically and single Z production with associated jets are considered as in the $H \rightarrow ZZ_d \rightarrow 4\ell$ analysis, with the same modelling for the first two. The last one however was modelled by POWHEG-BOX interfaced to PYTHIA8 and the CTEQ6L1 PDFs [113]. The contribution from these processes is estimated to be negligible.

6.2 Event selection

After forming the possible SFOS quadruplets in each event (as described in section 5.2), the following selections are applied to the quadruplets: each quadruplet must not include more than one stand-alone or calorimeter-tagged muon, and the three leading leptons in the quadruplet must have $p_T > 20, 15, 10$ GeV. Additionally, the leptons in the quadruplet must be matched to at least one of the triggers used to select the event at trigger-level, and a separation of $\Delta R > 0.1(0.2)$ is required for all same-flavour (different-flavour) leptons in the

quadruplet. The event is discarded if no quadruplets remain. From any quadruplets remaining, a single quadruplet is selected as the one with the smallest dilepton invariant mass difference $\delta m = |m_{12} - m_{34}|$. This procedure for selecting a single quadruplet can result in the incorrectly paired quadruplet being selected in $4e$ or 4μ signal events. The fraction of signal events where this occurs was estimated using the $Z_d Z_d$ MC samples to be approximately 2% (1%) in the $4e$ (4μ) channel for $m_X = 15$ GeV, rising to 8% (5%) at $m_X = 60$ GeV. Events are classified into three channels according to the flavours of the leptons in the selected quadruplet: $4e$, $2e2\mu$, and 4μ (no distinction is made between $2e2\mu$ and $2\mu2e$ permutations).

The remaining selections are applied to the selected quadruplet of the event, with the event discarded if any selection fails: the four-lepton invariant mass must be in the range $115 < m_{4\ell} < 130$ GeV, to select events consistent with a 125 GeV Higgs boson. The ratio of the secondary dilepton's mass to the primary dilepton's mass (m_{34}/m_{12}) must be greater than 0.85, which selects events where the dilepton masses are similar. Neither of the dilepton invariant masses is allowed to be in a mass range around the J/Ψ or Υ resonance masses (see table 1), with this requirement also applied to the alternative-pairing dilepton invariant masses (m_{14} and m_{32}) for events with a $4e$ or 4μ selected quadruplet. Finally, the dilepton invariant masses are required to be in the range $10 < m_{12,34} < 64$ GeV and in the case of $4e$ and 4μ quadruplets the alternative-pairing dilepton masses must be in the range $5 < m_{14,32} < 75$ GeV. These last two selections suppress backgrounds that contain a Z boson, and are referred to as the Z Veto in the following.

6.3 Background estimation

All background estimates for this analysis rely on using MC simulations, and are validated in regions that are orthogonal to the signal event selection described in the previous section.

The two main background processes ($H \rightarrow ZZ^* \rightarrow 4\ell$ and $ZZ^* \rightarrow 4\ell$) are validated by comparison of the background prediction to data in three validation regions that are orthogonal to the signal region. The first validation region (VR1) is defined by reversing part of the Z Veto requirement: VR1 requires m_{14} or m_{32} to be greater than 75 GeV. The second validation region (VR2) instead requires that m_{12} is greater than 64 GeV. These two regions primarily validate the $H \rightarrow ZZ^* \rightarrow 4\ell$ prediction. The third validation region (VR3) reverses the requirement on the four-lepton invariant mass window, i.e. requires $m_{4\ell} < 115$ GeV or $m_{4\ell} > 130$ GeV. In all three validation regions the $m_{34}/m_{12} > 0.85$ requirement is removed in order to increase the number of data events. Distributions of the average dilepton mass are shown for the three validation regions in figure 3.

The background estimates for the signal region are given in table 3, and include all systematic uncertainties described in section 6.4.

6.4 Systematic uncertainties

The systematic uncertainties in the signal and background modelling are the same as those described in section 5.4 (excluding the data-driven background uncertainties, which are not applicable to this search). It should be noted that fewer than four background events are predicted in the signal region for the $H \rightarrow XX \rightarrow 4\ell$ analysis, and therefore the dominant uncertainty in the background prediction is the statistical uncertainty.

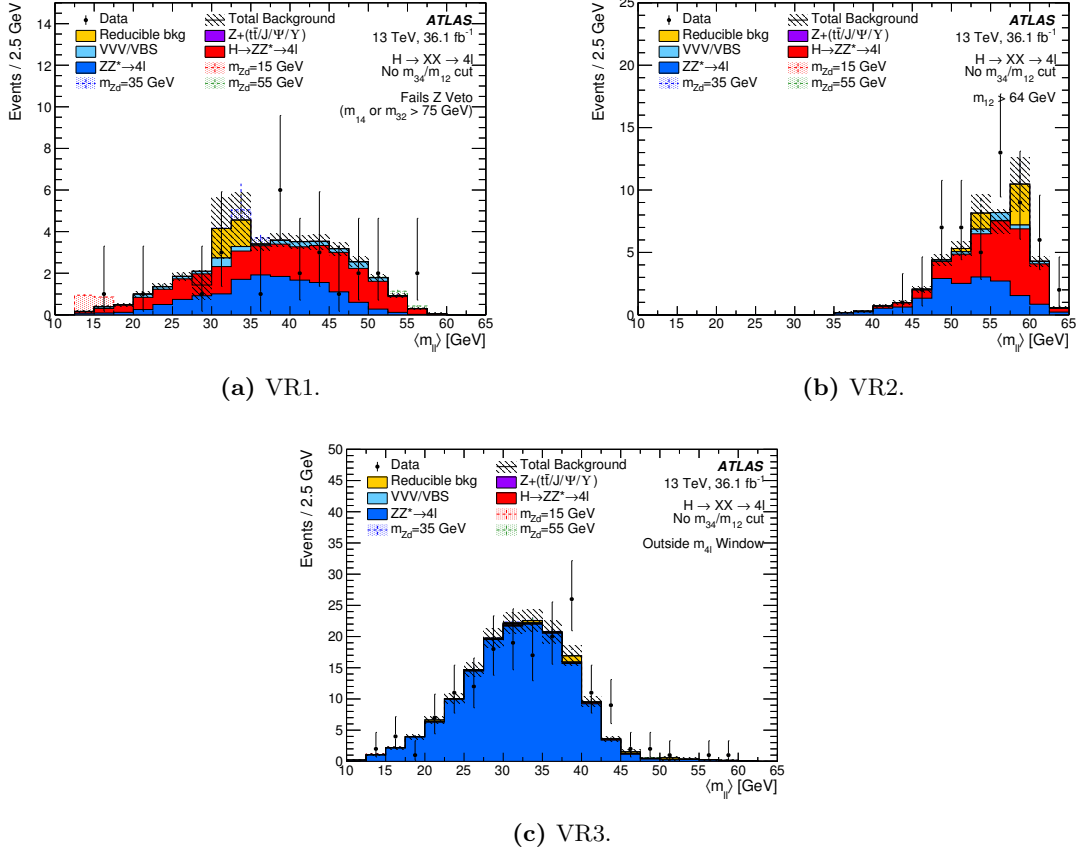


Figure 3. Distributions of $\langle m_{\ell\ell} \rangle = \frac{1}{2}(m_{12} + m_{34})$ in three background validation regions of the $H \rightarrow XX \rightarrow 4\ell$ ($15 < m_X < 60$ GeV) analysis: (a) events failing the Z Veto ($4e$ or 4μ events where m_{14} or $m_{32} > 75$ GeV), (b) events where $m_{12} > 64$ GeV, (c) events outside of the $115 < m_{4\ell} < 130$ GeV window. In all cases the m_{34}/m_{12} requirement is removed to increase the number of events. The (negligible) contamination by the signal in these validation regions is shown for three mass hypotheses of the vector-boson benchmark model: the signal strength corresponds to a branching ratio $\mathcal{B}(H \rightarrow Z_d Z_d \rightarrow 4\ell) = \frac{1}{10} \mathcal{B}(H \rightarrow ZZ^* \rightarrow 4\ell)$ (with $\mathcal{B}(H \rightarrow ZZ^* \rightarrow 4\ell)$ corresponding to the SM prediction [93]).

6.5 Results

The distributions of $\langle m_{\ell\ell} \rangle = \frac{1}{2}(m_{12} + m_{34})$ for the events selected in this analysis are shown in figure 4, and the total yields presented in table 3: six events are observed for a prediction of 3.9 ± 0.3 events in the high-mass selection.

The biggest deviation from the Standard Model expectation is from a single event at $\langle m_{\ell\ell} \rangle \approx 20$ GeV, with a local significance of 3.2σ . The corresponding global significance is approximately 1.9σ , estimated using an approximation [114] for the tail probability of the profile-likelihood-ratio test statistic. The significances are calculated using a Gaussian signal model with normalisation, yield, and standard deviation determined by interpolation between the corresponding fits to simulated signal samples (5 GeV intervals in Z_d mass). This statistical model, where the signal spans several bins of the $\langle m_{\ell\ell} \rangle$ distribution, means

Process	Yield
$ZZ^* \rightarrow 4\ell$	0.8 ± 0.1
$H \rightarrow ZZ^* \rightarrow 4\ell$	2.6 ± 0.3
VVV/VBS	0.51 ± 0.18
$Z + (t\bar{t}/J/\Psi) \rightarrow 4\ell$	0.004 ± 0.004
Other Reducible Background	Negligible
Total	3.9 ± 0.3
Data	6

Table 3. Expected event yields of the SM background processes and observed data in the $H \rightarrow XX \rightarrow 4\ell$ ($15 \text{ GeV} < m_X < 60 \text{ GeV}$) selection. The uncertainties include MC-statistical and systematic components.

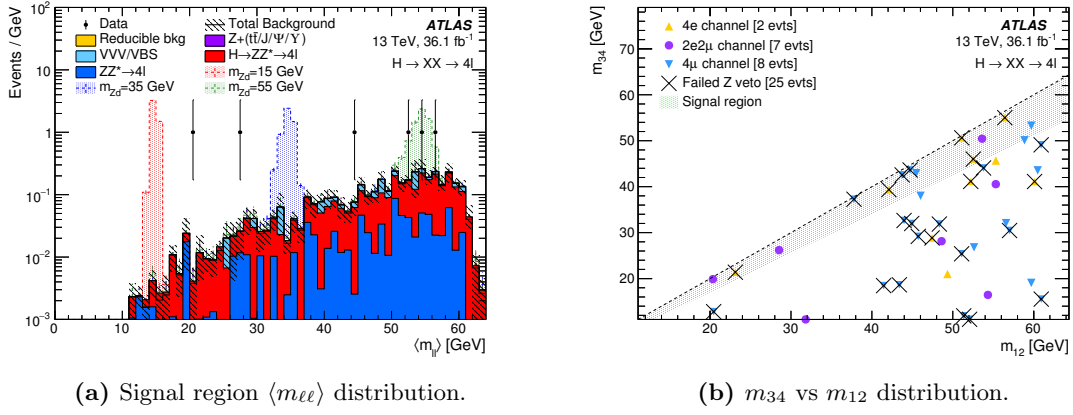


Figure 4. Distribution of (a) $\langle m_{\ell\ell} \rangle = \frac{1}{2}(m_{12} + m_{34})$ and (b) m_{34} vs m_{12} , for events selected in the $H \rightarrow XX \rightarrow 4\ell$ ($15 < m_X < 60 \text{ GeV}$) analysis. The example signal distributions in (a) correspond to the expected yield normalized with $\sigma(pp \rightarrow H \rightarrow Z_d Z_d \rightarrow 4\ell) = \frac{1}{10} \sigma_{\text{SM}}(pp \rightarrow H \rightarrow ZZ^* \rightarrow 4\ell)$. The crossed-through points in (b) fail the Z Veto. The events outside the (shaded green) signal region in figure (b) are events that fail the $m_{34}/m_{12} > 0.85$ requirement. The diagonal dashed line marks where $m_{12} = m_{34}$, and in this range of dilepton masses all events will have $m_{34} < m_{12}$.

that statistical fluctuations in the background estimate do not significantly impact the calculation of significance.

The m_{34} versus m_{12} distribution of the selected events is shown in figure 4b. In this figure, the crossed-through markers correspond to the events that fail the Z Veto, which required the alternative-pairing masses m_{32} and m_{14} (relevant only to the 4e and 4μ channels) to be less than 75 GeV. This requirement has a significant impact on the signal efficiency (up to $\approx 40\%$ loss) for m_X just above 15 GeV, but is applied in this analysis to mitigate any small contributions from SM processes involving Z boson production with large cross-sections. The 25 events that fail this veto are shown in validation region VR1 in figure 3, where there is a total background prediction of 38 ± 3 events.

7 $H \rightarrow XX \rightarrow 4\mu$ ($1 \text{ GeV} < m_X < 15 \text{ GeV}$) analysis

7.1 Monte Carlo simulation

The generation of the signal processes $H \rightarrow Z_d Z_d \rightarrow 4\ell$ and $H \rightarrow aa \rightarrow 4\mu$ follows the prescription described in section 6.1. Four samples were generated with Z_d masses of 1 GeV, 2 GeV, 5 GeV and 10 GeV, while the mass of the a -boson was varied for 10 different signal hypotheses in the range $0.5 \text{ GeV} \leq m_a \leq 15 \text{ GeV}$.

The background processes considered in this analysis are described in the following:

$H \rightarrow ZZ^* \rightarrow 4\ell$: the modelling of this process is the same as for the $H \rightarrow ZZ_d \rightarrow 4\ell$ analysis, described in section 5.1.

$ZZ^* \rightarrow 4\ell$: this process was simulated with SHERPA 2.1.1 due to an implicit particle-level requirement on the mass of the Z^* in the POWHEG-BOX MC sample used for the high-mass selection described in section 6.1. The gg -initiated production mechanism was modelled in the same way as for the $H \rightarrow ZZ_d \rightarrow 4\ell$ analysis, see section 5.1. Both production mechanisms are estimated using the CT10 PDFs.

VVV/VBS: the modelling of this process is described in section 6.1.

7.2 Event selection

In this search, only events with at least four muons are considered. Similarly to the searches described above, the selected muons are combined into 4μ quadruplets in all possible permutations of pairs of opposite-sign dimuons. In the case of having more than four muons, the different quadruplets that can be formed are all considered. Of the muons in each quadruplet, at least three must have $p_T > 10 \text{ GeV}$, at least two must have $p_T > 15 \text{ GeV}$, and at least one must have $p_T > 20 \text{ GeV}$, and there cannot be more than one stand-alone or calorimeter-tagged muon.

The quadruplet selection closely follows the selection described in section 6.2. Nonetheless, low-mass bosons are more boosted and muons less separated. For this reason, to keep signal efficiencies high, no ΔR requirement is applied to the muons of the quadruplets. If more than one quadruplet survives this selection, the one with the smallest $\Delta m_{\ell\ell}$ is selected.

Similarly to the $H \rightarrow XX \rightarrow 4\ell$ ($15 < m_X < 60 \text{ GeV}$) analysis, a set of requirements are applied to the quadruplet invariant masses as well as to the masses of the different muon pairings in the quadruplet. The quadruplet invariant mass must satisfy $120 \text{ GeV} < m_{4\ell} < 130 \text{ GeV}$. This window is tighter than the selections described in sections 5.2 and 6.2 because muons have smaller radiative losses than electrons. The dilepton masses must be in the range $0.88 \text{ GeV} < m_{12,34} < 20 \text{ GeV}$. No restriction is applied to the alternative-pairing dilepton masses because more than one third of signal events in this corner of the phase space contains an alternative-pairing dilepton mass that satisfies $75 \text{ GeV} < m_{14,32} < 125 \text{ GeV}$, and would therefore be lost if this selection was applied.

7.3 Background estimation

The main background contributions for this search come from the $ZZ^* \rightarrow 4\ell$ and $H \rightarrow ZZ^* \rightarrow 4\ell$ processes, as for the $H \rightarrow XX \rightarrow 4\ell$ ($15 < m_X < 60 \text{ GeV}$) case described in

section 6.3. These backgrounds, suppressed by the requirements on the lepton invariant mass, account for 30% each of the total background. Smaller background contributions come from higher-order electroweak processes (with cross-sections proportional to α^6 at leading order) and account for approximately 19% of the total background. Finally, events with multiple heavy flavour (bottom or charm) quark decays can also contribute to the total background yield. A leading part of this contribution comes from double semileptonic decays, where the b -quark decays to a muon and a c -quark which further decays into another muon and light hadrons. Resonances produced in the heavy flavour quark decay chain (i.e. ω , ρ , ϕ , J/ψ) that result in pairs of muons also become an important contribution of this background. Events with four heavy flavour quarks may pass the signal region requirements if each bottom or charm quark decays semileptonically.

The estimation method for the heavy flavour background was developed using fully data-driven inputs and inspired by a previous analysis from CMS [115]. Using data control samples, the background is modelled as a two-dimensional template in the plane of the invariant masses of the two dimuons. This template is constructed from the Cartesian product of two one-dimensional dimuon invariant mass spectra assuming that each muon pair is independent of the other. The one-dimensional templates are derived in control regions with three muons passing the same quality and isolation requirements used elsewhere in the analysis. The high- p_T selection requires three muons, with a muon pair with $p_T > 20$ GeV and $p_T > 10$ GeV matched to the dimuon trigger, and an additional muon with $p_T > 5$ GeV. The low- p_T selection also requires three muons, with a pair of muons, each with $p_T > 5$ GeV, and an additional muon with $p_T > 25$ GeV matched to the single-muon trigger. The choice of p_T thresholds for the templates was carefully studied and it is required that the first (second) dimuon pair always passes the high- p_T (low- p_T) selection. Estimations with alternative p_T threshold selections were found to be compatible with the current prescription. The Higgs boson mass requirement described in section 4 introduces a correlation between the dimuon pairs and therefore a correction to the two-dimensional template is necessary. This correction is extracted from data using a sample enriched in events with heavy flavour quarks, with inverted isolation and vertex requirements. The final template covers the full m_{34} vs m_{12} plane, including the signal region (defined by the condition $m_{34}/m_{12} > 0.85$). The normalisation of the template is computed in the region with $m_{34}/m_{12} < 0.85$, and its effect propagated to the signal region. The heavy flavour processes are negligible in the high-mass region, while they account for 22% of the total prediction in the low-mass region.

The modelling of the most important background processes ($ZZ^* \rightarrow 4\ell$ and $H \rightarrow ZZ^* \rightarrow 4\ell$) was validated in VR1, VR2 and VR3, defined in section 6.3 for the $H \rightarrow XX \rightarrow 4\ell$ ($15 < m_X < 60$ GeV) selection. The $ZZ^* \rightarrow 4\ell$ process can also be validated by comparing the background prediction to the data in a validation region (VR4) that is orthogonal to this signal region. This validation region is defined by reversing the four-lepton invariant mass window requirement, i.e. $m_{4\ell} < 120$ GeV or $m_{4\ell} > 130$ GeV. The average dilepton mass distribution for this region is shown in figure 5.

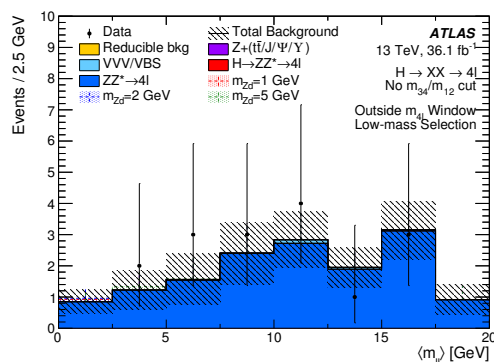


Figure 5. Distribution of $\langle m_{\ell\ell} \rangle = \frac{1}{2}(m_{12} + m_{34})$ in the validation region. The (negligible) contamination by the signal in these validation regions is shown for three mass hypotheses of the vector-boson benchmark model: the signal strength corresponds to a branching ratio $\mathcal{B}(H \rightarrow Z_d Z_d \rightarrow 4\ell) = \frac{1}{10} \mathcal{B}(H \rightarrow ZZ^* \rightarrow 4\ell)$ (with $\mathcal{B}(H \rightarrow ZZ^* \rightarrow 4\ell)$ corresponding to the SM prediction [93]).

7.4 Systematic uncertainties

In addition to the systematic uncertainties described in section 6.4, this analysis includes additional uncertainties for its data-driven background estimate.

Several sources of uncertainty are considered for the heavy flavour background data-driven estimation. Uncertainties in the shape of the one-dimensional templates are propagated to the two-dimensional template to account for shape variations in the dimuon invariant mass spectra. Different parameterisations of the Higgs boson mass requirement are also considered for modelling the effect of this condition on the shape of the distribution in the (m_{12}, m_{34}) plane. The previous two systematic uncertainties affect the shape of the two-dimensional plane, which propagates to a 63% effect on the yield of the heavy flavour background in the low-mass search signal region. Finally, the statistical uncertainty in the normalisation of the template in the signal region ($m_{34}/m_{12} < 0.85$ region of the two-dimensional plane) is also propagated to the signal region to account for fluctuations in the final heavy flavour background yields and has an effect of 13%. Uncertainties from the different sources are added in quadrature, and the total amounts to 65% for this background source.

7.5 Results

The $\langle m_{\ell\ell} \rangle$ distribution for the selected events is shown in figure 6a. Table 4 shows the resulting yields and uncertainties for this analysis: no events are observed to pass the selection, for a total background prediction of 0.4 ± 0.1 .

The m_{34} versus m_{12} distribution in figure 6b shows that there is no evidence of a signal-like resonance even outside of the $120 \text{ GeV} < m_{4\ell} < 130 \text{ GeV}$ window applied in this selection: 16 events are observed outside of this mass window, compared to a MC-based prediction of 15 ± 2 events from non-resonant SM ZZ processes. These 16 events are shown in the validation region in figure 5.

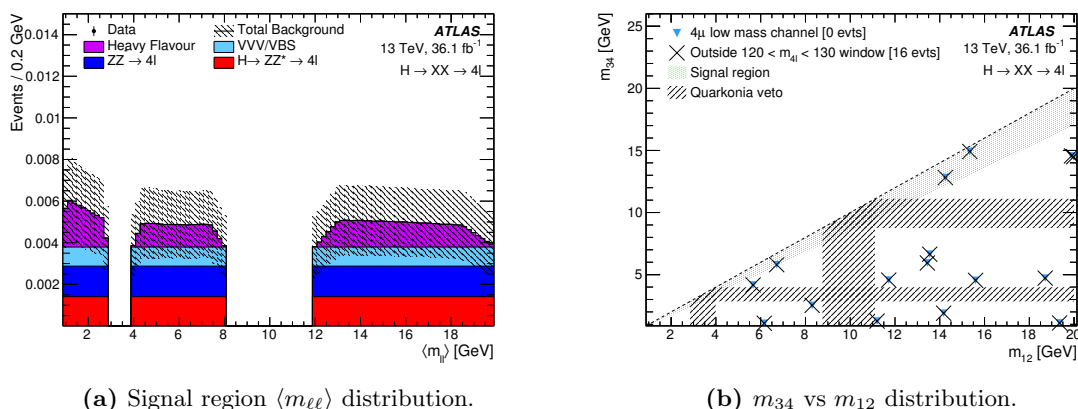


Figure 6. Distribution of (a) $\langle m_{\ell\ell} \rangle = \frac{1}{2}(m_{12} + m_{34})$ and (b) m_{34} vs m_{12} , for events selected in the $H \rightarrow XX \rightarrow 4\mu$ ($1 < m_X < 15$ GeV) analysis. The crossed-through points in figure (b) correspond to events that are outside the $m_{4\ell}$ mass window of $120 \text{ GeV} < m_{4\ell} < 130 \text{ GeV}$. The events outside the (shaded green) signal region are events that fail the $m_{34}/m_{12} > 0.85$ requirement.

Process	Yield
$ZZ^* \rightarrow 4\ell$	0.10 ± 0.01
$H \rightarrow ZZ^* \rightarrow 4\ell$	0.1 ± 0.1
VVV/VBS	0.06 ± 0.03
Heavy flavour	0.07 ± 0.04
Total	0.4 ± 0.1
Data	0

Table 4. Expected event yields of the SM background processes and observed data in the $H \rightarrow XX \rightarrow 4\mu$ ($1 \text{ GeV} < m_X < 15 \text{ GeV}$) selection. The uncertainties include MC-statistical and systematic components (systematic uncertainties are discussed in section 7.5).

8 Interpretation and discussion

The results do not show evidence for the signal processes of $H \rightarrow ZX \rightarrow 4\ell$ or $H \rightarrow XX \rightarrow 4\ell$. The results are therefore interpreted in terms of limits on the benchmark models presented in section 2.

For the $H \rightarrow ZX \rightarrow 4\ell$ analysis, the signal shape is obtained directly from simulation using the $Z_{(d)}Z_d$ benchmark model [14, 15]. For the $H \rightarrow XX \rightarrow 4\ell$ analysis, a simple Gaussian model is used for a generic signal in the $\langle m_{\ell\ell} \rangle$ observable, with the mean and standard deviation depending on the mass scale and resolution, respectively, in each decay channel. These scales and resolutions are estimated directly from simulation. The mass scale is found to have a -2% bias in $X \rightarrow ee$ decays, and -0.5% bias in $X \rightarrow \mu\mu$ decays (i.e. a -1% bias is used in the $ee\mu\mu$ channel). The mass resolutions are estimated to be 3.5% in $X \rightarrow ee$ decays and 1.9% in $X \rightarrow \mu\mu$ decays (meaning, for example, that the standard deviation in the 4μ channel is about $1/\sqrt{2} \times 1.9\% \approx 1.34\%$ of m_X). These scales and resolutions are valid across the full mass range considered (1–60 GeV).

8.1 Limits on fiducial cross-sections

The results were interpreted as limits on fiducial cross-sections by estimating the reconstruction efficiencies of each channel ϵ_c in the fiducial phase spaces defined in table 5. The fiducial selections were chosen to mimic the analysis selections described in sections 5.2 and 6.2. The leptons are “dressed”, i.e. in order to emulate the effects of quasi-collinear electromagnetic radiation from the charged leptons on their experimental reconstruction in the detector [116], the four-momenta of all prompt photons within $\Delta R = 0.1$ of a lepton are added to the four-momentum of the closest lepton. For the $H \rightarrow XX$ search the efficiencies (shown in figure 8a) are estimated with the $Z_d Z_d$ benchmark model and were verified to be compatible with the aa benchmark model to within 3% across the whole mass range. For the ZX search the efficiencies (shown in figure 7a) are estimated with the ZZ_d benchmark model, but no verification was explicitly made to confirm if these efficiencies are valid for a Za process. Assuming that the verified compatibility between efficiencies of $Z_d Z_d$ and aa processes applies equally to ZZ_d and Za processes, upper limits on the cross-sections corresponding to these fiducial phase spaces should be applicable to any models of 125 GeV Higgs boson decays to four leptons via one (with an associated Z boson) or two intermediate, on-shell, narrow, promptly decaying bosons. The fiducial requirements are applied to the four leptons in this decay. These efficiencies are used to compute 95% CL upper limits on the cross-sections in the fiducial phase spaces defined for the $H \rightarrow ZX \rightarrow 4\ell$ and $H \rightarrow XX \rightarrow 4\ell$ searches. These model-independent limits are computed using the CL_s frequentist formalism [117] with the profile-likelihood-ratio test statistic [118] (systematics are represented with nuisance parameters which are then profiled in the calculation of the test statistic). The results are shown in figures 7b and 8b, respectively. Impact of the systematic uncertainties on the limits is small.

For the $H \rightarrow ZX \rightarrow 4\ell$ search, a local excess of 3σ at $m_{Z_d} = 23 \text{ GeV}$ is observed in the $2\ell 2e$ channel. However, the total observed and predicted event counts in this channel agree within 0.5σ . No local excess is observed in the $2\ell 2\mu$ channel.

The width of the 2σ expected limit bands of figure 8b increases towards large values of m_X because more events are expected from background-only processes at this end of the mass spectrum; the larger expected background leads to a greater spread in the limits obtained with pseudoexperiments generated with the background-only hypothesis.

8.2 Limits on branching ratios

Model-dependent acceptances for the fiducial phase spaces are computed per channel for the $H \rightarrow ZZ_d \rightarrow 4\ell$ and $H \rightarrow XX \rightarrow 4\ell$ searches. The acceptance for the benchmark vector-boson model is estimated for both searches, whereas the acceptance for the benchmark pseudoscalar-boson model (type-II 2HDM+S model with $\tan \beta = 5$) is estimated only for the $H \rightarrow XX \rightarrow 4\ell$ search. The acceptances are used in a combined statistical model to compute upper limits on $\sigma_H \times \mathcal{B}(H \rightarrow ZZ_d \rightarrow 4\ell)$ and $\sigma_H \times \mathcal{B}(H \rightarrow XX \rightarrow 4\ell)$ for each model. The Z_d model assumes partial fractions of 0.25:0.25:0.25:0.25 for the $4e:2e2\mu:4\mu:2\mu 2e$ channels, whereas the a model assumes 100% decay to 4μ . These cross-section limits are converted into limits on the branching ratios of $H \rightarrow ZZ_d$, $H \rightarrow Z_d Z_d$

	$H \rightarrow ZX \rightarrow 4\ell$ (15 GeV < m_X < 55 GeV)	$H \rightarrow XX \rightarrow 4\ell$ (15 GeV < m_X < 60 GeV)	$H \rightarrow XX \rightarrow 4\mu$ (1 GeV < m_X < 15 GeV)
Electrons	Dressed with prompt photons within $\Delta R = 0.1$ $p_{\text{T}} > 7 \text{ GeV}$ $ \eta < 2.5$		
Muons	Dressed with prompt photons within $\Delta R = 0.1$ $p_{\text{T}} > 5 \text{ GeV}$ $ \eta < 2.7$		
Quadruplet	Three leading- p_{T} leptons satisfy $p_{\text{T}} > 20 \text{ GeV}$, 15 GeV, 10 GeV		
	$\Delta R > 0.1$ (0.2) between SF (OF) leptons		—
	50 GeV < m_{12} < 106 GeV 12 GeV < m_{34} < 115 GeV 115 GeV < $m_{4\ell}$ < 130 GeV $m_{12,34,14,32} > 5 \text{ GeV}$	$m_{34}/m_{12} > 0.85$	
		10 GeV < $m_{12,34}$ < 64 GeV 5 GeV < $m_{14,32}$ < 75 GeV if 4e or 4 μ	0.88 GeV < $m_{12,34}$ < 20 GeV
	Reject event if either of: $(m_{J/\psi} - 0.25 \text{ GeV}) < m_{12,34,14,32} < (m_{\psi(2S)} + 0.30 \text{ GeV})$ $(m_{\Upsilon(1S)} - 0.70 \text{ GeV}) < m_{12,34,14,32} < (m_{\Upsilon(3S)} + 0.75 \text{ GeV})$		

Table 5. Summary of the fiducial phase-space definitions used in this analysis, appropriate for processes of the form $H \rightarrow ZZ_d \rightarrow 4\ell$ and $H \rightarrow XX \rightarrow 4\ell$, where X is a promptly decaying, on-shell, narrow resonance.

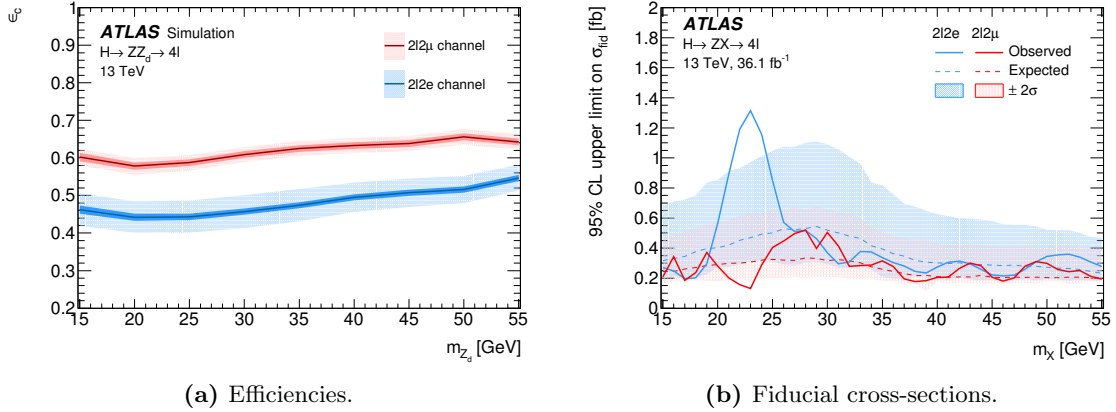


Figure 7. (a) Per-channel efficiencies ϵ_c calculated in the fiducial volume described in the $H \rightarrow ZX \rightarrow 4\ell$ column of table 5. The dark band is the statistical uncertainty and the lighter band is the systematic uncertainty. These efficiencies were computed using the $H \rightarrow ZZ_d \rightarrow 4\ell$ model. (b) Upper limits at the 95% CL on fiducial cross-sections for the $H \rightarrow ZX \rightarrow 4\ell$ process. The limits from the $H \rightarrow Za \rightarrow 4\ell$ search are valid only for the 2l2μ channel as the $H \rightarrow Za$ model assumes $\mathcal{B}(a \rightarrow \mu\mu) = 100\%$.

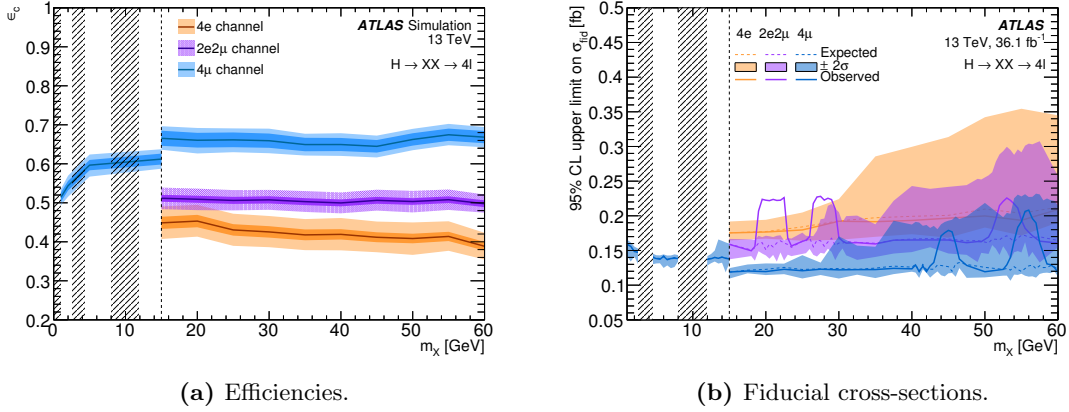


Figure 8. (a) Model-independent per-channel efficiencies ϵ_c calculated in the fiducial volumes described in the $1 \text{ GeV} < m_X < 15 \text{ GeV}$ and $15 \text{ GeV} < m_X < 60 \text{ GeV}$ columns of table 5 (i.e. separate phase spaces are defined for m_X above and below 15 GeV). The dark band is the statistical uncertainty and the lighter band is the systematic uncertainty. (b) Upper limits at the 95% CL on fiducial cross-sections for the $H \rightarrow XX \rightarrow 4\ell$ process. The step change in the fiducial cross-section limit in the 4 μ channel is due to the change in efficiency caused by the change in fiducial phase-space definition. The shaded areas are the quarkonia veto regions.

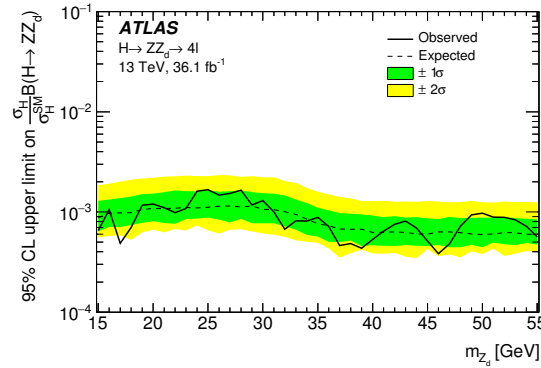


Figure 9. Upper limit at 95% CL on the branching ratio for the $H \rightarrow ZZ_d$ process.

and $H \rightarrow aa$ by using the theoretical branching ratios for $Z_d \rightarrow \ell\ell$ and $a \rightarrow \mu\mu$ from each benchmark model [14, 15], and assuming for σ_H the SM cross-section⁸ for Higgs boson production at $\sqrt{s} = 13 \text{ TeV}$ [93]. The limits on these branching ratios are shown in figures 9 and 10 for the $H \rightarrow ZZ_d \rightarrow 4\ell$ and $H \rightarrow XX \rightarrow 4\ell$ searches, respectively. The observed limit for $\mathcal{B}(H \rightarrow aa)$ (figure 10b) for $m_a > 15 \text{ GeV}$ is greater than 1 (i.e. this search has no sensitivity to this model in that mass range). The limit on the branching ratio for $H \rightarrow Z_d Z_d \rightarrow 4\ell$ improves on the Run 1 result of ref. [39] by about a factor of four, which corresponds to the increase in both luminosity and Higgs boson production cross-section between Run 1 and Run 2.

⁸This assumes that the presence of BSM decays of the Higgs boson does not significantly alter the Higgs boson production cross-section from the SM prediction.

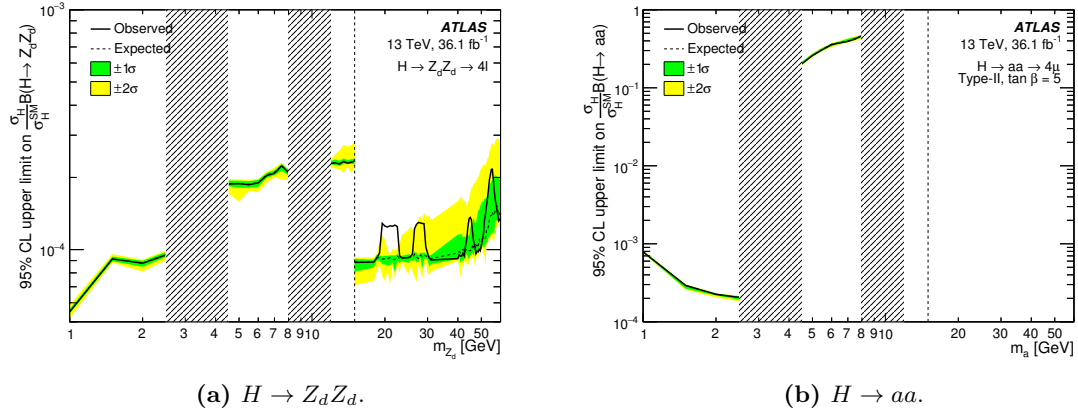


Figure 10. Upper limit at 95% CL on the branching ratios for processes (a) $H \rightarrow Z_d Z_d$ and (b) $H \rightarrow aa$, for the two benchmark models studied in this paper. The limit on $H \rightarrow aa$ is greater than 1 for $m_a > 15$ GeV. The step change in (a) at the $m_X = 15$ GeV boundary is due to the addition of sensitivity to $4e$ and $2e2\mu$ final states (lowering the limit). The shaded areas are the quarkonia veto regions.

9 Conclusion

Searches are performed for exotic decays of the Standard Model Higgs boson with a mass of 125 GeV to one or two new spin-1 particles, $H \rightarrow ZZ_d$ and $H \rightarrow Z_d Z_d$, or spin-0 particles, $H \rightarrow Za$ and $H \rightarrow aa$, using proton-proton collision data produced at $\sqrt{s} = 13$ TeV and recorded by the ATLAS detector at the LHC in 2015 and 2016. The data correspond to a combined integrated luminosity of 36.1 fb^{-1} . The searches explore the final state consisting of four leptons (electrons or muons) produced from the prompt decays of the intermediate boson states. The search targeting the ZX intermediate state is sensitive to Z_d masses between 15 and 55 GeV, and the search targeting the XX intermediate state is sensitive to Z_d masses between 15 and 60 GeV. Intermediate states of XX ($X = a$ or Z_d) where the boson mass m_X is between 1 and 15 GeV (excluding masses near known dilepton resonances from quarkonium states) are searched for in events with four muons.

The data are found to be globally consistent with SM background predictions. Upper limits (dependent on the mass of the intermediate exotic boson) are set on the branching ratio of Higgs boson to ZZ_d , $Z_d Z_d$, and aa , corresponding to $\mathcal{B}(H \rightarrow ZZ_d) \approx 0.1\%$, $\mathcal{B}(H \rightarrow Z_d Z_d) \approx 0.01\%$, and $\mathcal{B}(H \rightarrow aa) \approx 1\%$ respectively (depending on mass range). These limits are obtained under the assumption of a SM production cross-section for Higgs bosons, and assume prompt decay of the exotic bosons. Limits on fiducial cross-sections are also computed, which can be used for testing models different from the benchmark models used in this paper.

Acknowledgments

We thank CERN for the very successful operation of the LHC, as well as the support staff from our institutions without whom ATLAS could not be operated efficiently.

We acknowledge the support of ANPCyT, Argentina; YerPhI, Armenia; ARC, Australia; BMFWF and FWF, Austria; ANAS, Azerbaijan; SSTC, Belarus; CNPq and FAPESP, Brazil; NSERC, NRC and CFI, Canada; CERN; CONICYT, Chile; CAS, MOST and NSFC, China; COLCIENCIAS, Colombia; MSMT CR, MPO CR and VSC CR, Czech Republic; DNRF and DNSRC, Denmark; IN2P3-CNRS, CEA-DRF/IRFU, France; SRNSFG, Georgia; BMBF, HGF, and MPG, Germany; GSRT, Greece; RGC, Hong Kong SAR, China; ISF, I-CORE and Benoziyo Center, Israel; INFN, Italy; MEXT and JSPS, Japan; CNRST, Morocco; NWO, Netherlands; RCN, Norway; MNiSW and NCN, Poland; FCT, Portugal; MNE/IFA, Romania; MES of Russia and NRC KI, Russian Federation; JINR; MESTD, Serbia; MSSR, Slovakia; ARRS and MIZŠ, Slovenia; DST/NRF, South Africa; MINECO, Spain; SRC and Wallenberg Foundation, Sweden; SERI, SNSF and Cantons of Bern and Geneva, Switzerland; MOST, Taiwan; TAEK, Turkey; STFC, United Kingdom; DOE and NSF, United States of America. In addition, individual groups and members have received support from BCKDF, the Canada Council, CANARIE, CRC, Compute Canada, FQRNT, and the Ontario Innovation Trust, Canada; EPLANET, ERC, ERDF, FP7, Horizon 2020 and Marie Skłodowska-Curie Actions, European Union; Investissements d’Avenir Labex and Idex, ANR, Région Auvergne and Fondation Partager le Savoir, France; DFG and AvH Foundation, Germany; Herakleitos, Thales and Aristeia programmes co-financed by EU-ESF and the Greek NSRF; BSF, GIF and Minerva, Israel; BRF, Norway; CERCA Programme Generalitat de Catalunya, Generalitat Valenciana, Spain; the Royal Society and Leverhulme Trust, United Kingdom.

The crucial computing support from all WLCG partners is acknowledged gratefully, in particular from CERN, the ATLAS Tier-1 facilities at TRIUMF (Canada), NDGF (Denmark, Norway, Sweden), CC-IN2P3 (France), KIT/GridKA (Germany), INFN-CNAF (Italy), NL-T1 (Netherlands), PIC (Spain), ASGC (Taiwan), RAL (U.K.) and BNL (U.S.A.), the Tier-2 facilities worldwide and large non-WLCG resource providers. Major contributors of computing resources are listed in ref. [119].

Open Access. This article is distributed under the terms of the Creative Commons Attribution License ([CC-BY 4.0](https://creativecommons.org/licenses/by/4.0/)), which permits any use, distribution and reproduction in any medium, provided the original author(s) and source are credited.

References

- [1] ATLAS collaboration, *Observation of a new particle in the search for the Standard Model Higgs boson with the ATLAS detector at the LHC*, *Phys. Lett. B* **716** (2012) 1 [[arXiv:1207.7214](https://arxiv.org/abs/1207.7214)] [[INSPIRE](#)].
- [2] CMS collaboration, *Observation of a new boson at a mass of 125 GeV with the CMS experiment at the LHC*, *Phys. Lett. B* **716** (2012) 30 [[arXiv:1207.7235](https://arxiv.org/abs/1207.7235)] [[INSPIRE](#)].
- [3] ATLAS collaboration, *Measurements of the Higgs boson production and decay rates and coupling strengths using pp collision data at $\sqrt{s} = 7$ and 8 TeV in the ATLAS experiment*, *Eur. Phys. J. C* **76** (2016) 6 [[arXiv:1507.04548](https://arxiv.org/abs/1507.04548)] [[INSPIRE](#)].

- [4] CMS collaboration, *Precise determination of the mass of the Higgs boson and tests of compatibility of its couplings with the Standard Model predictions using proton collisions at 7 and 8 TeV*, *Eur. Phys. J. C* **75** (2015) 212 [[arXiv:1412.8662](#)] [[INSPIRE](#)].
- [5] ATLAS and CMS collaborations, *Measurements of the Higgs boson production and decay rates and constraints on its couplings from a combined ATLAS and CMS analysis of the LHC pp collision data at $\sqrt{s} = 7$ and 8 TeV*, *JHEP* **08** (2016) 045 [[arXiv:1606.02266](#)] [[INSPIRE](#)].
- [6] R.E. Shrock and M. Suzuki, *Invisible decays of Higgs bosons*, *Phys. Lett. B* **110** (1982) 250 [[INSPIRE](#)].
- [7] M.J. Strassler and K.M. Zurek, *Echoes of a hidden valley at hadron colliders*, *Phys. Lett. B* **651** (2007) 374 [[hep-ph/0604261](#)] [[INSPIRE](#)].
- [8] R.M. Schabinger and J.D. Wells, *A minimal spontaneously broken hidden sector and its impact on Higgs boson physics at the Large Hadron Collider*, *Phys. Rev. D* **72** (2005) 093007 [[hep-ph/0509209](#)] [[INSPIRE](#)].
- [9] B. Patt and F. Wilczek, *Higgs-field portal into hidden sectors*, [hep-ph/0605188](#) [[INSPIRE](#)].
- [10] P. Fayet, *Light spin 1/2 or spin 0 dark matter particles*, *Phys. Rev. D* **70** (2004) 023514 [[hep-ph/0403226](#)] [[INSPIRE](#)].
- [11] D.P. Finkbeiner and N. Weiner, *Exciting dark matter and the INTEGRAL/SPI 511 keV signal*, *Phys. Rev. D* **76** (2007) 083519 [[astro-ph/0702587](#)] [[INSPIRE](#)].
- [12] N. Arkani-Hamed, D.P. Finkbeiner, T.R. Slatyer and N. Weiner, *A theory of dark matter*, *Phys. Rev. D* **79** (2009) 015014 [[arXiv:0810.0713](#)] [[INSPIRE](#)].
- [13] E. Dudas, Y. Mambrini, S. Pokorski and A. Romagnoni, *Extra U(1) as natural source of a monochromatic gamma ray line*, *JHEP* **10** (2012) 123 [[arXiv:1205.1520](#)] [[INSPIRE](#)].
- [14] D. Curtin, R. Essig, S. Gori and J. Shelton, *Illuminating dark photons with high-energy colliders*, *JHEP* **02** (2015) 157 [[arXiv:1412.0018](#)] [[INSPIRE](#)].
- [15] D. Curtin et al., *Exotic decays of the 125 GeV Higgs boson*, *Phys. Rev. D* **90** (2014) 075004 [[arXiv:1312.4992](#)] [[INSPIRE](#)].
- [16] H. Davoudiasl, H.-S. Lee, I. Lewis and W.J. Marciano, *Higgs decays as a window into the dark sector*, *Phys. Rev. D* **88** (2013) 015022 [[arXiv:1304.4935](#)] [[INSPIRE](#)].
- [17] H. Davoudiasl, H.-S. Lee and W.J. Marciano, *‘Dark’ Z implications for parity violation, rare meson decays and Higgs physics*, *Phys. Rev. D* **85** (2012) 115019 [[arXiv:1203.2947](#)] [[INSPIRE](#)].
- [18] J.D. Wells, *How to find a hidden world at the Large Hadron Collider*, [arXiv:0803.1243](#) [[INSPIRE](#)].
- [19] S. Gopalakrishna, S. Jung and J.D. Wells, *Higgs boson decays to four fermions through an Abelian hidden sector*, *Phys. Rev. D* **78** (2008) 055002 [[arXiv:0801.3456](#)] [[INSPIRE](#)].
- [20] B.A. Dobrescu and K.T. Matchev, *Light axion within the next-to-minimal supersymmetric Standard Model*, *JHEP* **09** (2000) 031 [[hep-ph/0008192](#)] [[INSPIRE](#)].
- [21] U. Ellwanger, J.F. Gunion, C. Hugonie and S. Moretti, *Towards a no lose theorem for NMSSM Higgs discovery at the LHC*, [hep-ph/0305109](#) [[INSPIRE](#)].

- [22] R. Dermisek and J.F. Gunion, *Escaping the large fine tuning and little hierarchy problems in the next to minimal supersymmetric model and $h \rightarrow aa$ decays*, *Phys. Rev. Lett.* **95** (2005) 041801 [[hep-ph/0502105](#)] [[INSPIRE](#)].
- [23] S. Chang, R. Dermisek, J.F. Gunion and N. Weiner, *Nonstandard Higgs boson decays*, *Ann. Rev. Nucl. Part. Sci.* **58** (2008) 75 [[arXiv:0801.4554](#)] [[INSPIRE](#)].
- [24] D.E. Morrissey and A. Pierce, *Modified Higgs boson phenomenology from gauge or gaugino mediation in the NMSSM*, *Phys. Rev. D* **78** (2008) 075029 [[arXiv:0807.2259](#)] [[INSPIRE](#)].
- [25] V. Silveira and A. Zee, *Scalar phantoms*, *Phys. Lett. B* **161** (1985) 136 [[INSPIRE](#)].
- [26] M. Pospelov, A. Ritz and M.B. Voloshin, *Secluded WIMP dark matter*, *Phys. Lett. B* **662** (2008) 53 [[arXiv:0711.4866](#)] [[INSPIRE](#)].
- [27] P. Draper, T. Liu, C.E.M. Wagner, L.-T. Wang and H. Zhang, *Dark light Higgs*, *Phys. Rev. Lett.* **106** (2011) 121805 [[arXiv:1009.3963](#)] [[INSPIRE](#)].
- [28] S. Ipek, D. McKeen and A.E. Nelson, *A renormalizable model for the galactic center gamma ray excess from dark matter annihilation*, *Phys. Rev. D* **90** (2014) 055021 [[arXiv:1404.3716](#)] [[INSPIRE](#)].
- [29] A. Martin, J. Shelton and J. Unwin, *Fitting the galactic center gamma-ray excess with cascade annihilations*, *Phys. Rev. D* **90** (2014) 103513 [[arXiv:1405.0272](#)] [[INSPIRE](#)].
- [30] D. Clowe et al., *A direct empirical proof of the existence of dark matter*, *Astrophys. J.* **648** (2006) L109 [[astro-ph/0608407](#)] [[INSPIRE](#)].
- [31] PAMELA collaboration, O. Adriani et al., *An anomalous positron abundance in cosmic rays with energies 1.5–100 GeV*, *Nature* **458** (2009) 607 [[arXiv:0810.4995](#)] [[INSPIRE](#)].
- [32] J. Chang et al., *An excess of cosmic ray electrons at energies of 300–800 GeV*, *Nature* **456** (2008) 362 [[INSPIRE](#)].
- [33] AMS collaboration, M. Aguilar et al., *First result from the Alpha Magnetic Spectrometer on the International Space Station: precision measurement of the positron fraction in primary cosmic rays of 0.5–350 GeV*, *Phys. Rev. Lett.* **110** (2013) 141102 [[INSPIRE](#)].
- [34] S. Profumo, M.J. Ramsey-Musolf and G. Shaughnessy, *Singlet Higgs phenomenology and the electroweak phase transition*, *JHEP* **08** (2007) 010 [[arXiv:0705.2425](#)] [[INSPIRE](#)].
- [35] N. Blinov, J. Kozaczuk, D.E. Morrissey and C. Tamarit, *Electroweak baryogenesis from exotic electroweak symmetry breaking*, *Phys. Rev. D* **92** (2015) 035012 [[arXiv:1504.05195](#)] [[INSPIRE](#)].
- [36] G. Burdman, Z. Chacko, H.-S. Goh and R. Harnik, *Folded supersymmetry and the LEP paradox*, *JHEP* **02** (2007) 009 [[hep-ph/0609152](#)] [[INSPIRE](#)].
- [37] N. Craig, A. Katz, M. Strassler and R. Sundrum, *Naturalness in the dark at the LHC*, *JHEP* **07** (2015) 105 [[arXiv:1501.05310](#)] [[INSPIRE](#)].
- [38] D. Curtin and C.B. Verhaaren, *Discovering uncolored naturalness in exotic Higgs decays*, *JHEP* **12** (2015) 072 [[arXiv:1506.06141](#)] [[INSPIRE](#)].
- [39] ATLAS collaboration, *Search for new light gauge bosons in Higgs boson decays to four-lepton final states in pp collisions at $\sqrt{s} = 8$ TeV with the ATLAS detector at the LHC*, *Phys. Rev. D* **92** (2015) 092001 [[arXiv:1505.07645](#)] [[INSPIRE](#)].
- [40] J. Alexander et al., *Dark sectors 2016 workshop: community report*, [arXiv:1608.08632](#) [[INSPIRE](#)].

- [41] P. Galison and A. Manohar, *Two Z's or not two Z's?*, *Phys. Lett. B* **136** (1984) 279 [[INSPIRE](#)].
- [42] B. Holdom, *Two U(1)'s and ϵ charge shifts*, *Phys. Lett. B* **166** (1986) 196 [[INSPIRE](#)].
- [43] K.R. Dienes, C.F. Kolda and J. March-Russell, *Kinetic mixing and the supersymmetric gauge hierarchy*, *Nucl. Phys. B* **492** (1997) 104 [[hep-ph/9610479](#)] [[INSPIRE](#)].
- [44] ATLAS collaboration, *Search for long-lived neutral particles decaying into lepton jets in proton-proton collisions at $\sqrt{s} = 8$ TeV with the ATLAS detector*, *JHEP* **11** (2014) 088 [[arXiv:1409.0746](#)] [[INSPIRE](#)].
- [45] ATLAS collaboration, *A search for prompt lepton-jets in pp collisions at $\sqrt{s} = 8$ TeV with the ATLAS detector*, *JHEP* **02** (2016) 062 [[arXiv:1511.05542](#)] [[INSPIRE](#)].
- [46] A. Hook, E. Izaguirre and J.G. Wacker, *Model independent bounds on kinetic mixing*, *Adv. High Energy Phys.* **2011** (2011) 859762 [[arXiv:1006.0973](#)] [[INSPIRE](#)].
- [47] M. Pospelov, *Secluded U(1) below the weak scale*, *Phys. Rev. D* **80** (2009) 095002 [[arXiv:0811.1030](#)] [[INSPIRE](#)].
- [48] I. Hoenig, G. Samach and D. Tucker-Smith, *Searching for dilepton resonances below the Z mass at the LHC*, *Phys. Rev. D* **90** (2014) 075016 [[arXiv:1408.1075](#)] [[INSPIRE](#)].
- [49] NA48/2 collaboration, J.R. Batley et al., *Precise measurement of the $K^\pm \rightarrow \pi^\pm e^+ e^-$ decay*, *Phys. Lett. B* **677** (2009) 246 [[arXiv:0903.3130](#)] [[INSPIRE](#)].
- [50] BABAR collaboration, J.P. Lees et al., *Search for low-mass dark-sector Higgs bosons*, *Phys. Rev. Lett.* **108** (2012) 211801 [[arXiv:1202.1313](#)] [[INSPIRE](#)].
- [51] E.M. Riordan et al., *A search for short lived axions in an electron beam dump experiment*, *Phys. Rev. Lett.* **59** (1987) 755 [[INSPIRE](#)].
- [52] J.D. Bjorken et al., *Search for neutral metastable penetrating particles produced in the SLAC beam dump*, *Phys. Rev. D* **38** (1988) 3375 [[INSPIRE](#)].
- [53] A. Bross, M. Crisler, S.H. Pordes, J. Volk, S. Errede and J. Wrbanek, *A search for shortlived particles produced in an electron beam dump*, *Phys. Rev. Lett.* **67** (1991) 2942 [[INSPIRE](#)].
- [54] E787 collaboration, S. Adler et al., *Further search for the decay $K^+ \rightarrow \pi^+ \nu \bar{\nu}$ in the momentum region $P < 195$ MeV/c*, *Phys. Rev. D* **70** (2004) 037102 [[hep-ex/0403034](#)] [[INSPIRE](#)].
- [55] J.F. Gunion, B. Grzadkowski, H.E. Haber and J. Kalinowski, *LEP limits on CP-violating nonminimal Higgs sectors*, *Phys. Rev. Lett.* **79** (1997) 982 [[hep-ph/9704410](#)] [[INSPIRE](#)].
- [56] G. Bélanger, B. Dumont, U. Ellwanger, J.F. Gunion and S. Kraml, *Global fit to Higgs signal strengths and couplings and implications for extended Higgs sectors*, *Phys. Rev. D* **88** (2013) 075008 [[arXiv:1306.2941](#)] [[INSPIRE](#)].
- [57] R. Dermisek and J.F. Gunion, *The NMSSM close to the R-symmetry limit and naturalness in $h \rightarrow aa$ decays for $m_a < 2m_b$* , *Phys. Rev. D* **75** (2007) 075019 [[hep-ph/0611142](#)] [[INSPIRE](#)].
- [58] J.R. Ellis, J.F. Gunion, H.E. Haber, L. Roszkowski and F. Zwirner, *Higgs bosons in a nonminimal supersymmetric model*, *Phys. Rev. D* **39** (1989) 844 [[INSPIRE](#)].
- [59] G.F. Giudice and A. Masiero, *A natural solution to the μ problem in supergravity theories*, *Phys. Lett. B* **206** (1988) 480 [[INSPIRE](#)].

- [60] D0 collaboration, V.M. Abazov et al., *Search for NMSSM Higgs bosons in the $h \rightarrow aa \rightarrow \mu\mu\mu\mu, \mu\mu\tau\tau$ channels using $p\bar{p}$ collisions at $\sqrt{s} = 1.96$ TeV*, *Phys. Rev. Lett.* **103** (2009) 061801 [[arXiv:0905.3381](#)] [[INSPIRE](#)].
- [61] ATLAS collaboration, *Search for Higgs bosons decaying to aa in the $\mu\mu\tau\tau$ final state in pp collisions at $\sqrt{s} = 8$ TeV with the ATLAS experiment*, *Phys. Rev. D* **92** (2015) 052002 [[arXiv:1505.01609](#)] [[INSPIRE](#)].
- [62] CMS collaboration, *A search for pair production of new light bosons decaying into muons*, *Phys. Lett. B* **752** (2016) 146 [[arXiv:1506.00424](#)] [[INSPIRE](#)].
- [63] CMS collaboration, *Search for light bosons in decays of the 125 GeV Higgs boson in proton-proton collisions at $\sqrt{s} = 8$ TeV*, *JHEP* **10** (2017) 076 [[arXiv:1701.02032](#)] [[INSPIRE](#)].
- [64] ATLAS collaboration, *Search for the Higgs boson produced in association with a W boson and decaying to four b -quarks via two spin-zero particles in pp collisions at 13 TeV with the ATLAS detector*, *Eur. Phys. J. C* **76** (2016) 605 [[arXiv:1606.08391](#)] [[INSPIRE](#)].
- [65] ATLAS collaboration, *The ATLAS experiment at the CERN Large Hadron Collider*, 2008 *JINST* **3** S08003 [[INSPIRE](#)].
- [66] ATLAS collaboration, *ATLAS insertable B -layer technical design report*, CERN-LHCC-2010-013, CERN, Geneva Switzerland, (2010) [[ATLAS-TDR-19](#)].
- [67] ATLAS collaboration, *Vertex reconstruction performance of the ATLAS detector at $\sqrt{s} = 13$ TeV*, *ATL-PHYS-PUB-2015-026*, CERN, Geneva Switzerland, (2015).
- [68] ATLAS collaboration, *Performance of the ATLAS trigger system in 2015*, *Eur. Phys. J. C* **77** (2017) 317 [[arXiv:1611.09661](#)] [[INSPIRE](#)].
- [69] ATLAS collaboration, *Selection of jets produced in 13 TeV proton-proton collisions with the ATLAS detector*, *ATLAS-CONF-2015-029*, CERN, Geneva Switzerland, (2015).
- [70] ATLAS collaboration, *Electron efficiency measurements with the ATLAS detector using 2012 LHC proton-proton collision data*, *Eur. Phys. J. C* **77** (2017) 195 [[arXiv:1612.01456](#)] [[INSPIRE](#)].
- [71] ATLAS collaboration, *Muon reconstruction performance of the ATLAS detector in proton-proton collision data at $\sqrt{s} = 13$ TeV*, *Eur. Phys. J. C* **76** (2016) 292 [[arXiv:1603.05598](#)] [[INSPIRE](#)].
- [72] ATLAS collaboration, *Topological cell clustering in the ATLAS calorimeters and its performance in LHC run 1*, *Eur. Phys. J. C* **77** (2017) 490 [[arXiv:1603.02934](#)] [[INSPIRE](#)].
- [73] PARTICLE DATA GROUP collaboration, C. Patrignani et al., *Review of particle physics*, *Chin. Phys. C* **40** (2016) 100001 [[INSPIRE](#)].
- [74] J. Alwall et al., *The automated computation of tree-level and next-to-leading order differential cross sections and their matching to parton shower simulations*, *JHEP* **07** (2014) 079 [[arXiv:1405.0301](#)] [[INSPIRE](#)].
- [75] R.D. Ball et al., *Parton distributions with LHC data*, *Nucl. Phys. B* **867** (2013) 244 [[arXiv:1207.1303](#)] [[INSPIRE](#)].
- [76] T. Sjöstrand, S. Mrenna and P.Z. Skands, *A brief introduction to PYTHIA 8.1*, *Comput. Phys. Commun.* **178** (2008) 852 [[arXiv:0710.3820](#)] [[INSPIRE](#)].

- [77] ATLAS collaboration, *ATLAS run 1 PYTHIA8 tunes*, [ATL-PHYS-PUB-2014-021](#), CERN, Geneva Switzerland, (2014).
- [78] LHC HIGGS CROSS SECTION WORKING GROUP collaboration, J.R. Andersen et al., *Handbook of LHC Higgs cross sections: 3. Higgs properties*, [CERN-2013-004](#), CERN, Geneva Switzerland, (2013) [[arXiv:1307.1347](#)] [[INSPIRE](#)].
- [79] ATLAS collaboration, *Measurement of inclusive and differential cross sections in the $H \rightarrow ZZ^* \rightarrow 4\ell$ decay channel in pp collisions at $\sqrt{s} = 13$ TeV with the ATLAS detector*, *JHEP* **10** (2017) 132 [[arXiv:1708.02810](#)] [[INSPIRE](#)].
- [80] K. Hamilton, P. Nason, E. Re and G. Zanderighi, *NNLOPS simulation of Higgs boson production*, *JHEP* **10** (2013) 222 [[arXiv:1309.0017](#)] [[INSPIRE](#)].
- [81] P. Nason and C. Oleari, *NLO Higgs boson production via vector-boson fusion matched with shower in POWHEG*, *JHEP* **02** (2010) 037 [[arXiv:0911.5299](#)] [[INSPIRE](#)].
- [82] G. Luisoni, P. Nason, C. Oleari and F. Tramontano, *$HW^\pm/HZ + 0$ and 1 jet at NLO with the POWHEG BOX interfaced to GoSam and their merging within MiNLO*, *JHEP* **10** (2013) 083 [[arXiv:1306.2542](#)] [[INSPIRE](#)].
- [83] P. Nason, *A new method for combining NLO QCD with shower Monte Carlo algorithms*, *JHEP* **11** (2004) 040 [[hep-ph/0409146](#)] [[INSPIRE](#)].
- [84] S. Frixione, P. Nason and C. Oleari, *Matching NLO QCD computations with parton shower simulations: the POWHEG method*, *JHEP* **11** (2007) 070 [[arXiv:0709.2092](#)] [[INSPIRE](#)].
- [85] S. Alioli, P. Nason, C. Oleari and E. Re, *A general framework for implementing NLO calculations in shower Monte Carlo programs: the POWHEG BOX*, *JHEP* **06** (2010) 043 [[arXiv:1002.2581](#)] [[INSPIRE](#)].
- [86] J. Butterworth et al., *PDF4LHC recommendations for LHC run II*, *J. Phys. G* **43** (2016) 023001 [[arXiv:1510.03865](#)] [[INSPIRE](#)].
- [87] H.-L. Lai et al., *New parton distributions for collider physics*, *Phys. Rev. D* **82** (2010) 074024 [[arXiv:1007.2241](#)] [[INSPIRE](#)].
- [88] T. Sjöstrand, S. Mrenna and P.Z. Skands, *A brief introduction to PYTHIA 8.1*, *Comput. Phys. Commun.* **178** (2008) 852 [[arXiv:0710.3820](#)] [[INSPIRE](#)].
- [89] ATLAS collaboration, *Measurement of the Z/γ^* boson transverse momentum distribution in pp collisions at $\sqrt{s} = 7$ TeV with the ATLAS detector*, *JHEP* **09** (2014) 145 [[arXiv:1406.3660](#)] [[INSPIRE](#)].
- [90] M. Bahr et al., *HERWIG++ physics and manual*, *Eur. Phys. J. C* **58** (2008) 639 [[arXiv:0803.0883](#)] [[INSPIRE](#)].
- [91] M.H. Seymour and A. Siodmok, *Constraining MPI models using σ_{eff} and recent Tevatron and LHC underlying event data*, *JHEP* **10** (2013) 113 [[arXiv:1307.5015](#)] [[INSPIRE](#)].
- [92] LHC HIGGS CROSS SECTION WORKING GROUP collaboration, S. Dittmaier et al., *Handbook of LHC Higgs cross sections: 1. Inclusive observables*, [arXiv:1101.0593](#) [[INSPIRE](#)].
- [93] S. Dittmaier et al., *Handbook of LHC Higgs cross sections: 2. Differential distributions*, [arXiv:1201.3084](#) [[INSPIRE](#)].
- [94] T. Gleisberg et al., *Event generation with SHERPA 1.1*, *JHEP* **02** (2009) 007 [[arXiv:0811.4622](#)] [[INSPIRE](#)].

- [95] T. Gleisberg and S. Höche, *Comix, a new matrix element generator*, *JHEP* **12** (2008) 039 [[arXiv:0808.3674](#)] [[INSPIRE](#)].
- [96] F. Cascioli, P. Maierhofer and S. Pozzorini, *Scattering amplitudes with open loops*, *Phys. Rev. Lett.* **108** (2012) 111601 [[arXiv:1111.5206](#)] [[INSPIRE](#)].
- [97] N. Kauer, C. O'Brien and E. Vryonidou, *Interference effects for $H \rightarrow WW \rightarrow \ell\nu q\bar{q}'$ and $H \rightarrow ZZ \rightarrow \ell\bar{\ell}q\bar{q}$ searches in gluon fusion at the LHC*, *JHEP* **10** (2015) 074 [[arXiv:1506.01694](#)] [[INSPIRE](#)].
- [98] F. Caola, K. Melnikov, R. Röntsch and L. Tancredi, *QCD corrections to ZZ production in gluon fusion at the LHC*, *Phys. Rev. D* **92** (2015) 094028 [[arXiv:1509.06734](#)] [[INSPIRE](#)].
- [99] S. Höche, F. Krauss, S. Schumann and F. Siegert, *QCD matrix elements and truncated showers*, *JHEP* **05** (2009) 053 [[arXiv:0903.1219](#)] [[INSPIRE](#)].
- [100] S. Schumann and F. Krauss, *A parton shower algorithm based on Catani-Seymour dipole factorisation*, *JHEP* **03** (2008) 038 [[arXiv:0709.1027](#)] [[INSPIRE](#)].
- [101] M. Schönherr and F. Krauss, *Soft photon radiation in particle decays in SHERPA*, *JHEP* **12** (2008) 018 [[arXiv:0810.5071](#)] [[INSPIRE](#)].
- [102] S. Höche, F. Krauss, M. Schönherr and F. Siegert, *QCD matrix elements + parton showers: the NLO case*, *JHEP* **04** (2013) 027 [[arXiv:1207.5030](#)] [[INSPIRE](#)].
- [103] T. Sjöstrand, S. Mrenna and P.Z. Skands, *PYTHIA 6.4 physics and manual*, *JHEP* **05** (2006) 026 [[hep-ph/0603175](#)] [[INSPIRE](#)].
- [104] A.D. Martin, W.J. Stirling, R.S. Thorne and G. Watt, *Parton distributions for the LHC*, *Eur. Phys. J. C* **63** (2009) 189 [[arXiv:0901.0002](#)] [[INSPIRE](#)].
- [105] ATLAS collaboration, *Summary of ATLAS PYTHIA 8 tunes*, *ATL-PHYS-PUB-2012-003*, CERN, Geneva Switzerland, (2012).
- [106] ATLAS collaboration, *The ATLAS simulation infrastructure*, *Eur. Phys. J. C* **70** (2010) 823 [[arXiv:1005.4568](#)] [[INSPIRE](#)].
- [107] GEANT4 collaboration, S. Agostinelli et al., *GEANT4: a simulation toolkit*, *Nucl. Instrum. Meth. A* **506** (2003) 250 [[INSPIRE](#)].
- [108] ATLAS collaboration, *Electron and photon energy calibration with the ATLAS detector using data collected in 2015 at $\sqrt{s} = 13$ TeV*, *ATL-PHYS-PUB-2016-015*, CERN, Geneva Switzerland, (2016).
- [109] ATLAS collaboration, *Measurements of Higgs boson production and couplings in the four-lepton channel in pp collisions at center-of-mass energies of 7 and 8 TeV with the ATLAS detector*, *Phys. Rev. D* **91** (2015) 012006 [[arXiv:1408.5191](#)] [[INSPIRE](#)].
- [110] ATLAS collaboration, *Improved luminosity determination in pp collisions at $\sqrt{s} = 7$ TeV using the ATLAS detector at the LHC*, *Eur. Phys. J. C* **73** (2013) 2518 [[arXiv:1302.4393](#)] [[INSPIRE](#)].
- [111] A. Belyaev, J. Pivarski, A. Safonov, S. Senkin and A. Tatarinov, *LHC discovery potential of the lightest NMSSM Higgs in the $h_1 \rightarrow a_1 a_1 \rightarrow 4$ muons channel*, *Phys. Rev. D* **81** (2010) 075021 [[arXiv:1002.1956](#)] [[INSPIRE](#)].
- [112] J. Alwall, M. Herquet, F. Maltoni, O. Mattelaer and T. Stelzer, *MadGraph 5: going beyond*, *JHEP* **06** (2011) 128 [[arXiv:1106.0522](#)] [[INSPIRE](#)].

- [113] J. Pumplin, D.R. Stump, J. Huston, H.L. Lai, P.M. Nadolsky and W.K. Tung, *New generation of parton distributions with uncertainties from global QCD analysis*, *JHEP* **07** (2002) 012 [[hep-ph/0201195](#)] [[INSPIRE](#)].
- [114] E. Gross and O. Vitells, *Trial factors for the look elsewhere effect in high energy physics*, *Eur. Phys. J. C* **70** (2010) 525 [[arXiv:1005.1891](#)] [[INSPIRE](#)].
- [115] CMS collaboration, *A search for pair production of new light bosons decaying into muons*, *Phys. Lett. B* **752** (2016) 146 [[arXiv:1506.00424](#)] [[INSPIRE](#)].
- [116] ATLAS collaboration, *Proposal for truth particle observable definitions in physics measurements*, [ATL-PHYS-PUB-2015-013](#), CERN, Geneva Switzerland, (2015).
- [117] A.L. Read, *Presentation of search results: the CL_s technique*, *J. Phys. G* **28** (2002) 2693 [[INSPIRE](#)].
- [118] G. Cowan, K. Cranmer, E. Gross and O. Vitells, *Asymptotic formulae for likelihood-based tests of new physics*, *Eur. Phys. J. C* **71** (2011) 1554 [*Erratum ibid.* **C 73** (2013) 2501] [[arXiv:1007.1727](#)] [[INSPIRE](#)].
- [119] ATLAS collaboration, *ATLAS computing acknowledgements*, [ATL-GEN-PUB-2016-002](#), CERN, Geneva Switzerland, (2016).

The ATLAS collaboration

M. Aaboud^{137d}, G. Aad⁸⁸, B. Abbott¹¹⁵, O. Abidinov^{12,*}, B. Abeloos¹¹⁹, S.H. Abidi¹⁶¹, O.S. AbouZeid¹³⁹, N.L. Abraham¹⁵¹, H. Abramowicz¹⁵⁵, H. Abreu¹⁵⁴, R. Abreu¹¹⁸, Y. Abulaiti^{148a,148b}, B.S. Acharya^{167a,167b,a}, S. Adachi¹⁵⁷, L. Adamczyk^{41a}, J. Adelman¹¹⁰, M. Adersberger¹⁰², T. Adye¹³³, A.A. Affolder¹³⁹, Y. Afik¹⁵⁴, T. Agatonovic-Jovin¹⁴, C. Agheorghiesei^{28c}, J.A. Aguilar-Saavedra^{128a,128f}, S.P. Ahlen²⁴, F. Ahmadov^{68,b}, G. Aielli^{135a,135b}, S. Akatsuka⁷¹, H. Akerstedt^{148a,148b}, T.P.A. Åkesson⁸⁴, E. Akilli⁵², A.V. Akimov⁹⁸, G.L. Alberghi^{22a,22b}, J. Albert¹⁷², P. Albicocco⁵⁰, M.J. Alconada Verzini⁷⁴, S.C. Alderweireldt¹⁰⁸, M. Aleksa³², I.N. Aleksandrov⁶⁸, C. Alexa^{28b}, G. Alexander¹⁵⁵, T. Alexopoulos¹⁰, M. Alhroob¹¹⁵, B. Ali¹³⁰, M. Aliev^{76a,76b}, G. Alimonti^{94a}, J. Alison³³, S.P. Alkire³⁸, B.M.M. Allbrooke¹⁵¹, B.W. Allen¹¹⁸, P.P. Allport¹⁹, A. Aloisio^{106a,106b}, A. Alonso³⁹, F. Alonso⁷⁴, C. Alpigiani¹⁴⁰, A.A. Alshehri⁵⁶, M.I. Alstady⁸⁸, B. Alvarez Gonzalez³², D. Álvarez Piqueras¹⁷⁰, M.G. Alviggi^{106a,106b}, B.T. Amadio¹⁶, Y. Amaral Coutinho^{26a}, C. Amelung²⁵, D. Amidei⁹², S.P. Amor Dos Santos^{128a,128c}, S. Amoroso³², G. Amundsen²⁵, C. Anastopoulos¹⁴¹, L.S. Ancu⁵², N. Andari¹⁹, T. Andeen¹¹, C.F. Anders^{60b}, J.K. Anders⁷⁷, K.J. Anderson³³, A. Andreazza^{94a,94b}, V. Andrei^{60a}, S. Angelidakis³⁷, I. Angelozzi¹⁰⁹, A. Angerami³⁸, A.V. Anisenkov^{111,c}, N. Anjos¹³, A. Annovi^{126a}, C. Antel^{60a}, M. Antonelli⁵⁰, A. Antonov^{100,*}, D.J. Antrim¹⁶⁶, F. Anulli^{134a}, M. Aoki⁶⁹, L. Aperio Bella³², G. Arabidze⁹³, Y. Arai⁶⁹, J.P. Araque^{128a}, V. Araujo Ferraz^{26a}, A.T.H. Arce⁴⁸, R.E. Ardell⁸⁰, F.A. Arduh⁷⁴, J-F. Arguin⁹⁷, S. Argyropoulos⁶⁶, M. Arik^{20a}, A.J. Armbruster³², L.J. Armitage⁷⁹, O. Arnaez¹⁶¹, H. Arnold⁵¹, M. Arratia³⁰, O. Arslan²³, A. Artamonov^{99,*}, G. Artoni¹²², S. Artz⁸⁶, S. Asai¹⁵⁷, N. Asbah⁴⁵, A. Ashkenazi¹⁵⁵, L. Asquith¹⁵¹, K. Assamagan²⁷, R. Astalos^{146a}, M. Atkinson¹⁶⁹, N.B. Atlay¹⁴³, K. Augsten¹³⁰, G. Avolio³², B. Axen¹⁶, M.K. Ayoub^{35a}, G. Azuelos^{97,d}, A.E. Baas^{60a}, M.J. Baca¹⁹, H. Bachacou¹³⁸, K. Bachas^{76a,76b}, M. Backes¹²², P. Bagnaia^{134a,134b}, M. Bahmani⁴², H. Bahrasemani¹⁴⁴, J.T. Baines¹³³, M. Bajic³⁹, O.K. Baker¹⁷⁹, P.J. Bakker¹⁰⁹, E.M. Baldin^{111,c}, P. Balek¹⁷⁵, F. Balli¹³⁸, W.K. Balunas¹²⁴, E. Banas⁴², A. Bandyopadhyay²³, Sw. Banerjee^{176,e}, A.A.E. Bannoura¹⁷⁸, L. Barak¹⁵⁵, E.L. Barberio⁹¹, D. Barberis^{53a,53b}, M. Barbero⁸⁸, T. Barillari¹⁰³, M-S Barisits³², J.T. Barkeloo¹¹⁸, T. Barklow¹⁴⁵, N. Barlow³⁰, S.L. Barnes^{36b}, B.M. Barnett¹³³, R.M. Barnett¹⁶, Z. Barnovska-Blenessy^{36c}, A. Baroncelli^{136a}, G. Barone²⁵, A.J. Barr¹²², L. Barranco Navarro¹⁷⁰, F. Barreiro⁸⁵, J. Barreiro Guimarães da Costa^{35a}, R. Bartoldus¹⁴⁵, A.E. Barton⁷⁵, P. Bartos^{146a}, A. Basalae¹²⁵, A. Bassalat^{119,f}, R.L. Bates⁵⁶, S.J. Batista¹⁶¹, J.R. Batley³⁰, M. Battaglia¹³⁹, M. Bause^{134a,134b}, F. Bauer¹³⁸, H.S. Bawa^{145,g}, J.B. Beacham¹¹³, M.D. Beattie⁷⁵, T. Beau⁸³, P.H. Beauchemin¹⁶⁵, P. Bechtel²³, H.P. Beck^{18,h}, H.C. Beck⁵⁷, K. Becker¹²², M. Becker⁸⁶, C. Becot¹¹², A.J. Beddall^{20e}, A. Beddall^{20b}, V.A. Bednyakov⁶⁸, M. Bedognetti¹⁰⁹, C.P. Bee¹⁵⁰, T.A. Beermann³², M. Begalli^{26a}, M. Bégel²⁷, J.K. Behr⁴⁵, A.S. Bell⁸¹, G. Bella¹⁵⁵, L. Bellagamba^{22a}, A. Bellerive³¹, M. Bellomo¹⁵⁴, K. Belotskiy¹⁰⁰, O. Beltramello³², N.L. Belyaev¹⁰⁰, O. Benary^{155,*}, D. Bencheikroun^{137a}, M. Bender¹⁰², N. Benekos¹⁰, Y. Benhammou¹⁵⁵, E. Benhar Noccioli¹⁷⁹, J. Benitez⁶⁶, D.P. Benjamin⁴⁸, M. Benoit⁵², J.R. Bensinger²⁵, S. Bentvelsen¹⁰⁹, L. Beresford¹²², M. Beretta⁵⁰, D. Berge¹⁰⁹, E. Bergeas Kuutmann¹⁶⁸, N. Berger⁵, J. Beringer¹⁶, S. Berlendis⁵⁸, N.R. Bernard⁸⁹, G. Bernardi⁸³, C. Bernius¹⁴⁵, F.U. Bernlochner²³, T. Berry⁸⁰, P. Berta⁸⁶, C. Bertella^{35a}, G. Bertoli^{148a,148b}, I.A. Bertram⁷⁵, C. Bertsche⁴⁵, D. Bertsche¹¹⁵, G.J. Besjes³⁹, O. Bessidskaia Bylund^{148a,148b}, M. Bessner⁴⁵, N. Besson¹³⁸, A. Bethani⁸⁷, S. Bethke¹⁰³, A. Betti²³, A.J. Bevan⁷⁹, J. Beyer¹⁰³, R.M. Bianchi¹²⁷, O. Biebel¹⁰², D. Biedermann¹⁷, R. Bielski⁸⁷, K. Bierwagen⁸⁶, N.V. Biesuz^{126a,126b}, M. Biglietti^{136a}, T.R.V. Billoud⁹⁷, H. Bilokon⁵⁰, M. Bindi⁵⁷, A. Bingul^{20b}, C. Bini^{134a,134b}, S. Biondi^{22a,22b}, T. Bisanz⁵⁷, C. Bittrich⁴⁷, D.M. Bjergaard⁴⁸, J.E. Black¹⁴⁵, K.M. Black²⁴, R.E. Blair⁶, T. Blazek^{146a},

I. Bloch⁴⁵, C. Blocker²⁵, A. Blue⁵⁶, U. Blumenschein⁷⁹, Dr. Blunier^{34a}, G.J. Bobbink¹⁰⁹, V.S. Bobrovnikov^{111,c}, S.S. Bocchetta⁸⁴, A. Bocci⁴⁸, C. Bock¹⁰², M. Boehler⁵¹, D. Boerner¹⁷⁸, D. Bogavac¹⁰², A.G. Bogdanchikov¹¹¹, C. Bohm^{148a}, V. Boisvert⁸⁰, P. Bokan^{168,i}, T. Bold^{41a}, A.S. Boldyrev¹⁰¹, A.E. Bolz^{60b}, M. Bomben⁸³, M. Bona⁷⁹, M. Boonekamp¹³⁸, A. Borisov¹³², G. Borissov⁷⁵, J. Bortfeldt³², D. Bortoletto¹²², V. Bortolotto^{62a}, D. Boscherini^{22a}, M. Bosman¹³, J.D. Bossio Sola²⁹, J. Boudreau¹²⁷, E.V. Bouhova-Thacker⁷⁵, D. Boumediene³⁷, C. Bourdarios¹¹⁹, S.K. Boutle⁵⁶, A. Boveia¹¹³, J. Boyd³², I.R. Boyko⁶⁸, A.J. Bozson⁸⁰, J. Bracinik¹⁹, A. Brandt⁸, G. Brandt⁵⁷, O. Brandt^{60a}, F. Braren⁴⁵, U. Bratzler¹⁵⁸, B. Brau⁸⁹, J.E. Brau¹¹⁸, W.D. Breaden Madden⁵⁶, K. Brendlinger⁴⁵, A.J. Brennan⁹¹, L. Brenner¹⁰⁹, R. Brenner¹⁶⁸, S. Bressler¹⁷⁵, D.L. Briglin¹⁹, T.M. Bristow⁴⁹, D. Britton⁵⁶, D. Britzger⁴⁵, F.M. Brochu³⁰, I. Brock²³, R. Brock⁹³, G. Brooijmans³⁸, T. Brooks⁸⁰, W.K. Brooks^{34b}, J. Brosamer¹⁶, E. Brost¹¹⁰, J.H. Broughton¹⁹, P.A. Bruckman de Renstrom⁴², D. Bruncko^{146b}, A. Bruni^{22a}, G. Bruni^{22a}, L.S. Bruni¹⁰⁹, S. Bruno^{135a,135b}, BH Brunt³⁰, M. Bruschi^{22a}, N. Bruscino¹²⁷, P. Bryant³³, L. Bryngemark⁴⁵, T. Buanes¹⁵, Q. Buat¹⁴⁴, P. Buchholz¹⁴³, A.G. Buckley⁵⁶, I.A. Budagov⁶⁸, F. Buehrer⁵¹, M.K. Bugge¹²¹, O. Bulekov¹⁰⁰, D. Bullock⁸, T.J. Burch¹¹⁰, S. Burdin⁷⁷, C.D. Burgard⁵¹, A.M. Burger⁵, B. Burghgrave¹¹⁰, K. Burka⁴², S. Burke¹³³, I. Burmeister⁴⁶, J.T.P. Burr¹²², E. Busato³⁷, D. Büscher⁵¹, V. Büscher⁸⁶, P. Bussey⁵⁶, J.M. Butler²⁴, C.M. Buttar⁵⁶, J.M. Butterworth⁸¹, P. Butti³², W. Buttinger²⁷, A. Buzatu¹⁵³, A.R. Buzykaev^{111,c}, Changqiao C.-Q.^{36c}, S. Cabrera Urbán¹⁷⁰, D. Caforio¹³⁰, H. Cai¹⁶⁹, V.M.M. Cairo^{40a,40b}, O. Cakir^{4a}, N. Calace⁵², P. Calafiura¹⁶, A. Calandri⁸⁸, G. Calderini⁸³, P. Calfayan⁶⁴, G. Callea^{40a,40b}, L.P. Caloba^{26a}, S. Calvente Lopez⁸⁵, D. Calvet³⁷, S. Calvet³⁷, T.P. Calvet⁸⁸, R. Camacho Toro³³, S. Camarda³², P. Camarri^{135a,135b}, D. Cameron¹²¹, R. Caminal Armadans¹⁶⁹, C. Camincher⁵⁸, S. Campana³², M. Campanelli⁸¹, A. Camplani^{94a,94b}, A. Campoverde¹⁴³, V. Canale^{106a,106b}, M. Cano Bret^{36b}, J. Cantero¹¹⁶, T. Cao¹⁵⁵, M.D.M. Capeans Garrido³², I. Caprini^{28b}, M. Caprini^{28b}, M. Capua^{40a,40b}, R.M. Carbone³⁸, R. Cardarelli^{135a}, F. Cardillo⁵¹, I. Carli¹³¹, T. Carli³², G. Carlino^{106a}, B.T. Carlson¹²⁷, L. Carminati^{94a,94b}, R.M.D. Carney^{148a,148b}, S. Caron¹⁰⁸, E. Carquin^{34b}, S. Carrá^{94a,94b}, G.D. Carrillo-Montoya³², D. Casadei¹⁹, M.P. Casado^{13,j}, A.F. Casha¹⁶¹, M. Casolino¹³, D.W. Casper¹⁶⁶, R. Castelijns¹⁰⁹, V. Castillo Gimenez¹⁷⁰, N.F. Castro^{128a,k}, A. Catinaccio³², J.R. Catmore¹²¹, A. Cattai³², J. Caudron²³, V. Cavaliere¹⁶⁹, E. Cavallaro¹³, D. Cavalli^{94a}, M. Cavalli-Sforza¹³, V. Cavasinni^{126a,126b}, E. Celebi^{20d}, F. Ceradini^{136a,136b}, L. Cerda Alberich¹⁷⁰, A.S. Cerqueira^{26b}, A. Cerri¹⁵¹, L. Cerrito^{135a,135b}, F. Cerutti¹⁶, A. Cervelli^{22a,22b}, S.A. Cetin^{20d}, A. Chafaq^{137a}, D. Chakraborty¹¹⁰, S.K. Chan⁵⁹, W.S. Chan¹⁰⁹, Y.L. Chan^{62a}, P. Chang¹⁶⁹, J.D. Chapman³⁰, D.G. Charlton¹⁹, C.C. Chau³¹, C.A. Chavez Barajas¹⁵¹, S. Che¹¹³, S. Cheatham^{167a,167c}, A. Chegwidien⁹³, S. Chekanov⁶, S.V. Chekulaev^{163a}, G.A. Chelkov^{68,l}, M.A. Chelstowska³², C. Chen^{36c}, C. Chen⁶⁷, H. Chen²⁷, J. Chen^{36c}, S. Chen^{35b}, S. Chen¹⁵⁷, X. Chen^{35c,m}, Y. Chen⁷⁰, H.C. Cheng⁹², H.J. Cheng^{35a,35d}, A. Cheplakov⁶⁸, E. Cheremushkina¹³², R. Cherkoui El Moursli^{137e}, E. Cheu⁷, K. Cheung⁶³, L. Chevalier¹³⁸, V. Chiarella⁵⁰, G. Chiarelli^{126a}, G. Chiodini^{76a}, A.S. Chisholm³², A. Chitan^{28b}, Y.H. Chiu¹⁷², M.V. Chizhov⁶⁸, K. Choi⁶⁴, A.R. Chomont³⁷, S. Chouridou¹⁵⁶, Y.S. Chow^{62a}, V. Christodoulou⁸¹, M.C. Chu^{62a}, J. Chudoba¹²⁹, A.J. Chuinard⁹⁰, J.J. Chwastowski⁴², L. Chytka¹¹⁷, A.K. Ciftci^{4a}, D. Cinca⁴⁶, V. Cindro⁷⁸, I.A. Cioară²³, A. Ciocio¹⁶, F. Ciotto^{106a,106b}, Z.H. Citron¹⁷⁵, M. Citterio^{94a}, M. Ciubancan^{28b}, A. Clark⁵², B.L. Clark⁵⁹, M.R. Clark³⁸, P.J. Clark⁴⁹, R.N. Clarke¹⁶, C. Clement^{148a,148b}, Y. Coadou⁸⁸, M. Cobal^{167a,167c}, A. Coccaro⁵², J. Cochran⁶⁷, L. Colasurdo¹⁰⁸, B. Cole³⁸, A.P. Colijn¹⁰⁹, J. Collot⁵⁸, T. Colombo¹⁶⁶, P. Conde Muino^{128a,128b}, E. Coniavitis⁵¹, S.H. Connell^{147b}, I.A. Connelly⁸⁷, S. Constantinescu^{28b}, G. Conti³², F. Conventi^{106a,n}, M. Cooke¹⁶, A.M. Cooper-Sarkar¹²², F. Cormier¹⁷¹, K.J.R. Cormier¹⁶¹, M. Corradi^{134a,134b}, F. Corriveau^{90,o}, A. Cortes-Gonzalez³², G. Costa^{94a}, M.J. Costa¹⁷⁰, D. Costanzo¹⁴¹, G. Cottin³⁰,

G. Cowan⁸⁰, B.E. Cox⁸⁷, K. Cranmer¹¹², S.J. Crawley⁵⁶, R.A. Creager¹²⁴, G. Cree³¹, S. Crépé-Renaudin⁵⁸, F. Crescioli⁸³, W.A. Cribbs^{148a,148b}, M. Cristinziani²³, V. Croft¹¹², G. Crosetti^{40a,40b}, A. Cueto⁸⁵, T. Cuhadar Donszelmann¹⁴¹, A.R. Cukierman¹⁴⁵, J. Cummings¹⁷⁹, M. Curatolo⁵⁰, J. Cúth⁸⁶, S. Czekierda⁴², P. Czodrowski³², G. D'amen^{22a,22b}, S. D'Auria⁵⁶, L. D'era⁸³, M. D'Onofrio⁷⁷, M.J. Da Cunha Sargedas De Sousa^{128a,128b}, C. Da Via⁸⁷, W. Dabrowski^{41a}, T. Dado^{146a}, T. Dai⁹², O. Dale¹⁵, F. Dallaire⁹⁷, C. Dallapiccola⁸⁹, M. Dam³⁹, J.R. Dandoy¹²⁴, M.F. Daneri²⁹, N.P. Dang^{176,e}, A.C. Daniells¹⁹, N.S. Dann⁸⁷, M. Danninger¹⁷¹, M. Dano Hoffmann¹³⁸, V. Dao¹⁵⁰, G. Darbo^{53a}, S. Darmora⁸, J. Dassoulas³, A. Dattagupta¹¹⁸, T. Daubney⁴⁵, W. Davey²³, C. David⁴⁵, T. Davidek¹³¹, D.R. Davis⁴⁸, P. Davison⁸¹, E. Dawe⁹¹, I. Dawson¹⁴¹, K. De⁸, R. de Asmundis^{106a}, A. De Benedetti¹¹⁵, S. De Castro^{22a,22b}, S. De Cecco⁸³, N. De Groot¹⁰⁸, P. de Jong¹⁰⁹, H. De la Torre⁹³, F. De Lorenzi⁶⁷, A. De Maria⁵⁷, D. De Pedis^{134a}, A. De Salvo^{134a}, U. De Sanctis^{135a,135b}, A. De Santo¹⁵¹, K. De Vasconcelos Corga⁸⁸, J.B. De Vivie De Regie¹¹⁹, R. Debbé²⁷, C. Debenedetti¹³⁹, D.V. Dedovich⁶⁸, N. Dehghanian³, I. Deigaard¹⁰⁹, M. Del Gaudio^{40a,40b}, J. Del Peso⁸⁵, D. Delgove¹¹⁹, F. Deliot¹³⁸, C.M. Delitzsch⁷, A. Dell'Acqua³², L. Dell'Asta²⁴, M. Dell'Orso^{126a,126b}, M. Della Pietra^{106a,106b}, D. della Volpe⁵², M. Delmastro⁵, C. Delporte¹¹⁹, P.A. Delsart⁵⁸, D.A. DeMarco¹⁶¹, S. Demers¹⁷⁹, M. Demichev⁶⁸, A. Demilly⁸³, S.P. Denisov¹³², D. Denysiuk¹³⁸, D. Derendarz⁴², J.E. Derkaoui^{137d}, F. Derue⁸³, P. Dervan⁷⁷, K. Desch²³, C. Deterre⁴⁵, K. Dette¹⁶¹, M.R. Devesa²⁹, P.O. Deviveiros³², A. Dewhurst¹³³, S. Dhaliwal²⁵, F.A. Di Bello⁵², A. Di Ciaccio^{135a,135b}, L. Di Ciaccio⁵, W.K. Di Clemente¹²⁴, C. Di Donato^{106a,106b}, A. Di Girolamo³², B. Di Girolamo³², B. Di Micco^{136a,136b}, R. Di Nardo³², K.F. Di Petrillo⁵⁹, A. Di Simone⁵¹, R. Di Sipio¹⁶¹, D. Di Valentino³¹, C. Diaconu⁸⁸, M. Diamond¹⁶¹, F.A. Dias³⁹, M.A. Diaz^{34a}, E.B. Diehl⁹², J. Dietrich¹⁷, S. Díez Cornell⁴⁵, A. Dimitrievska¹⁴, J. Dingfelder²³, P. Dita^{28b}, S. Dita^{28b}, F. Dittus³², F. Djama⁸⁸, T. Djobava^{54b}, J.I. Djuvsland^{60a}, M.A.B. do Vale^{26c}, D. Dobos³², M. Dobre^{28b}, D. Dodsworth²⁵, C. Doglioni⁸⁴, J. Dolejsi¹³¹, Z. Dolezal¹³¹, M. Donadelli^{26d}, S. Donati^{126a,126b}, P. Dondero^{123a,123b}, J. Donini³⁷, J. Dopke¹³³, A. Doria^{106a}, M.T. Dova⁷⁴, A.T. Doyle⁵⁶, E. Drechsler⁵⁷, M. Dris¹⁰, Y. Du^{36a}, J. Duarte-Campderros¹⁵⁵, F. Dubinin⁹⁸, A. Dubreuil⁵², E. Duchovni¹⁷⁵, G. Duckeck¹⁰², A. Ducourthial⁸³, O.A. Ducu^{97,p}, D. Duda¹⁰⁹, A. Dudarev³², A.Ch. Dudder⁸⁶, E.M. Duffield¹⁶, L. Duflot¹¹⁹, M. Dührssen³², C. Dulsen¹⁷⁸, M. Dumancic¹⁷⁵, A.E. Dumitriu^{28b,q}, A.K. Duncan⁵⁶, M. Dunford^{60a}, A. Duperrin⁸⁸, H. Duran Yildiz^{4a}, M. Düren⁵⁵, A. Durglishvili^{54b}, D. Duschinger⁴⁷, B. Dutta⁴⁵, D. Duvnjak¹, M. Dyndal⁴⁵, B.S. Dziedzic⁴², C. Eckardt⁴⁵, K.M. Ecker¹⁰³, R.C. Edgar⁹², T. Eifert³², G. Eigen¹⁵, K. Einsweiler¹⁶, T. Ekelof¹⁶⁸, M. El Kacimi^{137c}, R. El Kosseifi⁸⁸, V. Ellajosyula⁸⁸, M. Ellert¹⁶⁸, S. Elles⁵, F. Ellinghaus¹⁷⁸, A.A. Elliot¹⁷², N. Ellis³², J. Elmsheuser²⁷, M. Elsing³², D. Emeliyanov¹³³, Y. Enari¹⁵⁷, J.S. Ennis¹⁷³, M.B. Epland⁴⁸, J. Erdmann⁴⁶, A. Ereditato¹⁸, M. Ernst²⁷, S. Errede¹⁶⁹, M. Escalier¹¹⁹, C. Escobar¹⁷⁰, B. Esposito⁵⁰, O. Estrada Pastor¹⁷⁰, A.I. Etienvre¹³⁸, E. Etzion¹⁵⁵, H. Evans⁶⁴, A. Ezhilov¹²⁵, M. Ezzi^{137e}, F. Fabbri^{22a,22b}, L. Fabbri^{22a,22b}, V. Fabiani¹⁰⁸, G. Facini⁸¹, R.M. Fakhruddinov¹³², S. Falciano^{134a}, R.J. Falla⁸¹, J. Faltova³², Y. Fang^{35a}, M. Fanti^{94a,94b}, A. Farbin⁸, A. Farilla^{136a}, C. Farina¹²⁷, E.M. Farina^{123a,123b}, T. Farooque⁹³, S. Farrell¹⁶, S.M. Farrington¹⁷³, P. Farthouat³², F. Fassi^{137e}, P. Fassnacht³², D. Fassouliotis⁹, M. Fauci Giannelli⁴⁹, A. Favareto^{53a,53b}, W.J. Fawcett¹²², L. Fayard¹¹⁹, O.L. Fedin^{125,r}, W. Fedorko¹⁷¹, S. Feigl¹²¹, L. Feligioni⁸⁸, C. Feng^{36a}, E.J. Feng³², M.J. Fenton⁵⁶, A.B. Fenjuk¹³², L. Feremenga⁸, P. Fernandez Martinez¹⁷⁰, J. Ferrando⁴⁵, A. Ferrari¹⁶⁸, P. Ferrari¹⁰⁹, R. Ferrari^{123a}, D.E. Ferreira de Lima^{60b}, A. Ferrer¹⁷⁰, D. Ferrere⁵², C. Ferretti⁹², F. Fiedler⁸⁶, A. Filipčić⁷⁸, M. Filipuzzi⁴⁵, F. Filthaut¹⁰⁸, M. Fincke-Keeler¹⁷², K.D. Finelli²⁴, M.C.N. Fiolhais^{128a,128c,s}, L. Fiorini¹⁷⁰, A. Fischer², C. Fischer¹³, J. Fischer¹⁷⁸, W.C. Fisher⁹³, N. Flaschel⁴⁵, I. Fleck¹⁴³, P. Fleischmann⁹², R.R.M. Fletcher¹²⁴, T. Flick¹⁷⁸, B.M. Flierl¹⁰², L.R. Flores Castillo^{62a}, M.J. Flowerdew¹⁰³, G.T. Forcolin⁸⁷, A. Formica¹³⁸,

F.A. Förster¹³, A. Forti⁸⁷, A.G. Foster¹⁹, D. Fournier¹¹⁹, H. Fox⁷⁵, S. Fracchia¹⁴¹,
P. Francavilla^{126a,126b}, M. Franchini^{22a,22b}, S. Franchino^{60a}, D. Francis³², L. Franconi¹²¹,
M. Franklin⁵⁹, M. Frate¹⁶⁶, M. Fraternali^{123a,123b}, D. Freeborn⁸¹, S.M. Fressard-Batraneanu³²,
B. Freund⁹⁷, D. Froidevaux³², J.A. Frost¹²², C. Fukunaga¹⁵⁸, T. Fusayasu¹⁰⁴, J. Fuster¹⁷⁰,
O. Gabizon¹⁵⁴, A. Gabrielli^{22a,22b}, A. Gabrielli¹⁶, G.P. Gach^{41a}, S. Gadatsch³², S. Gadomski⁸⁰,
G. Gagliardi^{53a,53b}, L.G. Gagnon⁹⁷, C. Galea¹⁰⁸, B. Galhardo^{128a,128c}, E.J. Gallas¹²²,
B.J. Gallop¹³³, P. Gallus¹³⁰, G. Galster³⁹, K.K. Gan¹¹³, S. Ganguly³⁷, Y. Gao⁷⁷, Y.S. Gao^{145,g},
F.M. Garay Walls^{34a}, C. García¹⁷⁰, J.E. García Navarro¹⁷⁰, J.A. García Pascual^{35a},
M. Garcia-Sciveres¹⁶, R.W. Gardner³³, N. Garelli¹⁴⁵, V. Garonne¹²¹, A. Gascon Bravo⁴⁵,
K. Gasnikova⁴⁵, C. Gatti⁵⁰, A. Gaudiello^{53a,53b}, G. Gaudio^{123a}, I.L. Gavrilenko⁹⁸, C. Gay¹⁷¹,
G. Gaycken²³, E.N. Gazis¹⁰, C.N.P. Gee¹³³, J. Geisen⁵⁷, M. Geisen⁸⁶, M.P. Geisler^{60a},
K. Gellerstedt^{148a,148b}, C. Gemme^{53a}, M.H. Genest⁵⁸, C. Geng⁹², S. Gentile^{134a,134b},
C. Gentsos¹⁵⁶, S. George⁸⁰, D. Gerbaudo¹³, G. Geßner⁴⁶, S. Ghasemi¹⁴³, M. Ghneimat²³,
B. Giacobbe^{22a}, S. Giagu^{134a,134b}, N. Giangiacomi^{22a,22b}, P. Giannetti^{126a}, S.M. Gibson⁸⁰,
M. Gignac¹⁷¹, M. Gilchriese¹⁶, D. Gillberg³¹, G. Gilles¹⁷⁸, D.M. Gingrich^{3,d},
M.P. Giordani^{167a,167c}, F.M. Giorgi^{22a}, P.F. Giraud¹³⁸, P. Giromini⁵⁹, G. Giugliarelli^{167a,167c},
D. Giugni^{94a}, F. Giuli¹²², C. Giuliani¹⁰³, M. Giulini^{60b}, B.K. Gjølsten¹²¹, S. Gkaitatzis¹⁵⁶,
I. Gkialas^{9,t}, E.L. Gkoukousis¹³, P. Gkoutoumis¹⁰, L.K. Gladilin¹⁰¹, C. Glasman⁸⁵,
J. Glatzer¹³, P.C.F. Glaysheer⁴⁵, A. Glazov⁴⁵, M. Goblirsch-Kolb²⁵, J. Godlewski⁴², S. Goldfarb⁹¹,
T. Golling⁵², D. Golubkov¹³², A. Gomes^{128a,128b,128d}, R. Gonçalo^{128a}, R. Goncalves Gama^{26a},
J. Goncalves Pinto Firmino Da Costa¹³⁸, G. Gonella⁵¹, L. Gonella¹⁹, A. Gongadze⁶⁸,
J.L. Gonski⁵⁹, S. González de la Hoz¹⁷⁰, S. Gonzalez-Sevilla⁵², L. Goossens³², P.A. Gorbounov⁹⁹,
H.A. Gordon²⁷, I. Gorelov¹⁰⁷, B. Gorini³², E. Gorini^{76a,76b}, A. Gorišek⁷⁸, A.T. Goshaw⁴⁸,
C. Gössling⁴⁶, M.I. Gostkin⁶⁸, C.A. Gottardo²³, C.R. Goudet¹¹⁹, D. Goujdami^{137c},
A.G. Goussiou¹⁴⁰, N. Govender^{147b,u}, E. Gozani¹⁵⁴, I. Grabowska-Bold^{41a}, P.O.J. Gradin¹⁶⁸,
J. Gramling¹⁶⁶, E. Gramstad¹²¹, S. Grancagnolo¹⁷, V. Gratchev¹²⁵, P.M. Gravila^{28f}, C. Gray⁵⁶,
H.M. Gray¹⁶, Z.D. Greenwood^{82,v}, C. Grefe²³, K. Gregersen⁸¹, I.M. Gregor⁴⁵, P. Grenier¹⁴⁵,
K. Grevtsov⁵, J. Griffiths⁸, A.A. Grillo¹³⁹, K. Grimm⁷⁵, S. Grinstein^{13,w}, Ph. Gris³⁷,
J.-F. Grivaz¹¹⁹, S. Groh⁸⁶, E. Gross¹⁷⁵, J. Grosse-Knetter⁵⁷, G.C. Grossi⁸², Z.J. Grout⁸¹,
A. Grummer¹⁰⁷, L. Guan⁹², W. Guan¹⁷⁶, J. Guenther³², F. Guescini^{163a}, D. Guest¹⁶⁶,
O. Gueta¹⁵⁵, B. Gui¹¹³, E. Guido^{53a,53b}, T. Guillemin⁵, S. Guindon³², U. Gul⁵⁶, C. Gumpert³²,
J. Guo^{36b}, W. Guo⁹², Y. Guo^{36c,x}, R. Gupta⁴³, S. Gurbuz^{20a}, G. Gustavino¹¹⁵, B.J. Gutelman¹⁵⁴,
P. Gutierrez¹¹⁵, N.G. Gutierrez Ortiz⁸¹, C. Gutsche⁸¹, C. Guyot¹³⁸, M.P. Guzik^{41a},
C. Gwenlan¹²², C.B. Gwilliam⁷⁷, A. Haas¹¹², C. Haber¹⁶, H.K. Hadavand⁸, N. Haddad^{137e},
A. Hade⁸⁸, S. Hageböck²³, M. Hagihara¹⁶⁴, H. Hakobyan^{180,*}, M. Haleem⁴⁵, J. Haley¹¹⁶,
G. Halladjian⁹³, G.D. Hallewell⁸⁸, K. Hamacher¹⁷⁸, P. Hamal¹¹⁷, K. Hamano¹⁷², A. Hamilton^{147a},
G.N. Hamity¹⁴¹, P.G. Hamnett⁴⁵, L. Han^{36c}, S. Han^{35a,35d}, K. Hanagaki^{69,y}, K. Hanawa¹⁵⁷,
M. Hance¹³⁹, D.M. Handl¹⁰², B. Haney¹²⁴, P. Hanke^{60a}, J.B. Hansen³⁹, J.D. Hansen³⁹,
M.C. Hansen²³, P.H. Hansen³⁹, K. Hara¹⁶⁴, A.S. Hard¹⁷⁶, T. Harenberg¹⁷⁸, F. Hariri¹¹⁹,
S. Harkusha⁹⁵, P.F. Harrison¹⁷³, N.M. Hartmann¹⁰², Y. Hasegawa¹⁴², A. Hasib⁴⁹, S. Hassani¹³⁸,
S. Haug¹⁸, R. Hauser⁹³, L. Hauswald⁴⁷, L.B. Havener³⁸, M. Havranek¹³⁰, C.M. Hawkes¹⁹,
R.J. Hawkins³², D. Hayakawa¹⁵⁹, D. Hayden⁹³, C.P. Hays¹²², J.M. Hays⁷⁹, H.S. Hayward⁷⁷,
S.J. Haywood¹³³, S.J. Head¹⁹, T. Heck⁸⁶, V. Hedberg⁸⁴, L. Heelan⁸, S. Heer²³, K.K. Heidegger⁵¹,
S. Heim⁴⁵, T. Heim¹⁶, B. Heinemann^{45,z}, J.J. Heinrich¹⁰², L. Heinrich¹¹², C. Heinz⁵⁵,
J. Hejbal¹²⁹, L. Helary³², A. Held¹⁷¹, S. Hellman^{148a,148b}, C. Helsens³², R.C.W. Henderson⁷⁵,
Y. Heng¹⁷⁶, S. Henkelmann¹⁷¹, A.M. Henriques Correia³², S. Henrot-Versille¹¹⁹, G.H. Herbert¹⁷,
H. Herde²⁵, V. Herget¹⁷⁷, Y. Hernández Jiménez^{147c}, H. Herr⁸⁶, G. Hertel⁵¹, R. Hertenberger¹⁰²,
L. Hervas³², T.C. Herwig¹²⁴, G.G. Hesketh⁸¹, N.P. Hessey^{163a}, J.W. Hetherly⁴³, S. Higashino⁶⁹,

E. Higón-Rodríguez¹⁷⁰, K. Hildebrand³³, E. Hill¹⁷², J.C. Hill³⁰, K.H. Hiller⁴⁵, S.J. Hillier¹⁹, M. Hils⁴⁷, I. Hinchliffe¹⁶, M. Hirose⁵¹, D. Hirschbuehl¹⁷⁸, B. Hiti⁷⁸, O. Hladik¹²⁹, D.R. Hlaluku^{147c}, X. Hoad⁴⁹, J. Hobbs¹⁵⁰, N. Hod^{163a}, M.C. Hodgkinson¹⁴¹, P. Hodgson¹⁴¹, A. Hoecker³², M.R. Hoferkamp¹⁰⁷, F. Hoenig¹⁰², D. Hohn²³, T.R. Holmes³³, M. Holzbock¹⁰², M. Homann⁴⁶, S. Honda¹⁶⁴, T. Honda⁶⁹, T.M. Hong¹²⁷, B.H. Hooberman¹⁶⁹, W.H. Hopkins¹¹⁸, Y. Horii¹⁰⁵, A.J. Horton¹⁴⁴, J.-Y. Hostachy⁵⁸, A. Hostiuc¹⁴⁰, S. Hou¹⁵³, A. Hoummada^{137a}, J. Howarth⁸⁷, J. Hoya⁷⁴, M. Hrabovsky¹¹⁷, J. Hrdinka³², I. Hristova¹⁷, J. Hrivnac¹¹⁹, T. Hryn'ova⁵, A. Hrynevich⁹⁶, P.J. Hsu⁶³, S.-C. Hsu¹⁴⁰, Q. Hu²⁷, S. Hu^{36b}, Y. Huang^{35a}, Z. Hubacek¹³⁰, F. Hubaut⁸⁸, F. Huegging²³, T.B. Huffman¹²², E.W. Hughes³⁸, M. Huhtinen³², R.F.H. Hunter³¹, P. Huo¹⁵⁰, N. Huseynov^{68,b}, J. Huston⁹³, J. Huth⁵⁹, R. Hyneman⁹², G. Iacobucci⁵², G. Iakovidis²⁷, I. Ibragimov¹⁴³, L. Iconomidou-Fayard¹¹⁹, Z. Idrissi^{137e}, P. Iengo³², O. Igonkina^{109,aa}, T. Iizawa¹⁷⁴, Y. Ikegami⁶⁹, M. Ikeno⁶⁹, Y. Ilchenko^{11,ab}, D. Iliadis¹⁵⁶, N. Ilic¹⁴⁵, F. Iltzsche⁴⁷, G. Introzzi^{123a,123b}, P. Ioannou^{9,*}, M. Iodice^{136a}, K. Iordanidou³⁸, V. Ippolito⁵⁹, M.F. Isacson¹⁶⁸, N. Ishijima¹²⁰, M. Ishino¹⁵⁷, M. Ishitsuka¹⁵⁹, C. Issever¹²², S. Istin^{20a}, F. Ito¹⁶⁴, J.M. Iturbe Ponce^{62a}, R. Iuppa^{162a,162b}, H. Iwasaki⁶⁹, J.M. Izen⁴⁴, V. Izzo^{106a}, S. Jabbar³, P. Jackson¹, R.M. Jacobs²³, V. Jain², K.B. Jakobi⁸⁶, K. Jakobs⁵¹, S. Jakobsen⁶⁵, T. Jakoubek¹²⁹, D.O. Jamin¹¹⁶, D.K. Jana⁸², R. Jansky⁵², J. Janssen²³, M. Janus⁵⁷, P.A. Janus^{41a}, G. Jarlskog⁸⁴, N. Javadov^{68,b}, T. Javůrek⁵¹, M. Javurkova⁵¹, F. Jeanneau¹³⁸, L. Jeanty¹⁶, J. Jejelava^{54a,ac}, A. Jelinskas¹⁷³, P. Jenni^{51,ad}, C. Jeske¹⁷³, S. Jézéquel⁵, H. Ji¹⁷⁶, J. Jia¹⁵⁰, H. Jiang⁶⁷, Y. Jiang^{36c}, Z. Jiang¹⁴⁵, S. Jiggins⁸¹, J. Jimenez Pena¹⁷⁰, S. Jin^{35b}, A. Jinaru^{28b}, O. Jinnouchi¹⁵⁹, H. Jivan^{147c}, P. Johansson¹⁴¹, K.A. Johns⁷, C.A. Johnson⁶⁴, W.J. Johnson¹⁴⁰, K. Jon-And^{148a,148b}, R.W.L. Jones⁷⁵, S.D. Jones¹⁵¹, S. Jones⁷, T.J. Jones⁷⁷, J. Jongmanns^{60a}, P.M. Jorge^{128a,128b}, J. Jovicevic^{163a}, X. Ju¹⁷⁶, A. Juste Rozas^{13,w}, M.K. Köhler¹⁷⁵, A. Kaczmarzka⁴², M. Kado¹¹⁹, H. Kagan¹¹³, M. Kagan¹⁴⁵, S.J. Kahn⁸⁸, T. Kaji¹⁷⁴, E. Kajomovitz¹⁵⁴, C.W. Kalderon⁸⁴, A. Kaluza⁸⁶, S. Kama⁴³, A. Kamenshchikov¹³², N. Kanaya¹⁵⁷, L. Kanjir⁷⁸, V.A. Kantserov¹⁰⁰, J. Kanzaki⁶⁹, B. Kaplan¹¹², L.S. Kaplan¹⁷⁶, D. Kar^{147c}, K. Karakostas¹⁰, N. Karastathis¹⁰, M.J. Kareem^{163b}, E. Karentzos¹⁰, S.N. Karpov⁶⁸, Z.M. Karpova⁶⁸, K. Karthik¹¹², V. Kartvelishvili⁷⁵, A.N. Karyukhin¹³², K. Kasahara¹⁶⁴, L. Kashif¹⁷⁶, R.D. Kass¹¹³, A. Kastanas¹⁴⁹, Y. Kataoka¹⁵⁷, C. Kato¹⁵⁷, A. Katre⁵², J. Katzy⁴⁵, K. Kawade⁷⁰, K. Kawagoe⁷³, T. Kawamoto¹⁵⁷, G. Kawamura⁵⁷, E.F. Kay⁷⁷, V.F. Kazanin^{111,c}, R. Keeler¹⁷², R. Kehoe⁴³, J.S. Keller³¹, E. Kellermann⁸⁴, J.J. Kempster⁸⁰, J. Kendrick¹⁹, H. Keoshkerian¹⁶¹, O. Kepka¹²⁹, B.P. Kerševan⁷⁸, S. Kersten¹⁷⁸, R.A. Keyes⁹⁰, M. Khader¹⁶⁹, F. Khalil-zada¹², A. Khanov¹¹⁶, A.G. Kharlamov^{111,c}, T. Kharlamova^{111,c}, A. Khodinov¹⁶⁰, T.J. Khoo⁵², V. Khovanskiy^{99,*}, E. Khramov⁶⁸, J. Khubua^{54b,ae}, S. Kido⁷⁰, C.R. Kilby⁸⁰, H.Y. Kim⁸, S.H. Kim¹⁶⁴, Y.K. Kim³³, N. Kimura¹⁵⁶, O.M. Kind¹⁷, B.T. King⁷⁷, D. Kirchmeier⁴⁷, J. Kirk¹³³, A.E. Kiryunin¹⁰³, T. Kishimoto¹⁵⁷, D. Kisielewska^{41a}, V. Kitali⁴⁵, O. Kivernyk⁵, E. Kladiva^{146b}, T. Klapdor-Kleingrothaus⁵¹, M.H. Klein⁹², M. Klein⁷⁷, U. Klein⁷⁷, K. Kleinknecht⁸⁶, P. Klimek¹¹⁰, A. Klimentov²⁷, R. Klingenberg^{46,*}, T. Klingl²³, T. Klioutchnikova³², E.-E. Kluge^{60a}, P. Kluit¹⁰⁹, S. Kluth¹⁰³, E. Kneringer⁶⁵, E.B.F.G. Knoops⁸⁸, A. Knue¹⁰³, A. Kobayashi¹⁵⁷, D. Kobayashi⁷³, T. Kobayashi¹⁵⁷, M. Kobel⁴⁷, M. Kocian¹⁴⁵, P. Kodys¹³¹, T. Koffas³¹, E. Koffeman¹⁰⁹, N.M. Köhler¹⁰³, T. Koi¹⁴⁵, M. Kolb^{60b}, I. Koletsou⁵, A.A. Komar^{98,*}, T. Kondo⁶⁹, N. Kondrashova^{36b}, K. Köneke⁵¹, A.C. König¹⁰⁸, T. Kono^{69,af}, R. Konoplich^{112,ag}, N. Konstantinidis⁸¹, R. Kopeliansky⁶⁴, S. Koperny^{41a}, A.K. Kopp⁵¹, K. Korcyl⁴², K. Kordas¹⁵⁶, A. Korn⁸¹, A.A. Korol^{111,c}, I. Korolkov¹³, E.V. Korolkova¹⁴¹, O. Kortner¹⁰³, S. Kortner¹⁰³, T. Kosek¹³¹, V.V. Kostyukhin²³, A. Kotwal⁴⁸, A. Koulouris¹⁰, A. Kourkumeli-Charalampidi^{123a,123b}, C. Kourkumelis⁹, E. Kourlitis¹⁴¹, V. Kouskoura²⁷, A.B. Kowalewska⁴², R. Kowalewski¹⁷², T.Z. Kowalski^{41a}, C. Kozakai¹⁵⁷, W. Kozanecki¹³⁸, A.S. Kozhin¹³², V.A. Kramarenko¹⁰¹, G. Kramberger⁷⁸, D. Krasnopevtsev¹⁰⁰, M.W. Krasny⁸³,

A. Krasznahorkay³², D. Krauss¹⁰³, J.A. Kremer^{41a}, J. Kretzschmar⁷⁷, K. Kreutzfeldt⁵⁵,
P. Krieger¹⁶¹, K. Krizka¹⁶, K. Kroeninger⁴⁶, H. Kroha¹⁰³, J. Kroll¹²⁹, J. Kroll¹²⁴, J. Kroseberg²³,
J. Krstic¹⁴, U. Kruchonak⁶⁸, H. Krüger²³, N. Krumnack⁶⁷, M.C. Kruse⁴⁸, T. Kubota⁹¹,
H. Kucuk⁸¹, S. Kuday^{4b}, J.T. Kuechler¹⁷⁸, S. Kuehn³², A. Kugel^{60a}, F. Kuger¹⁷⁷, T. Kuhl⁴⁵,
V. Kukhtin⁶⁸, R. Kukla⁸⁸, Y. Kulchitsky⁹⁵, S. Kuleshov^{34b}, Y.P. Kulinich¹⁶⁹, M. Kuna^{134a,134b},
T. Kunigo⁷¹, A. Kupco¹²⁹, T. Kupfer⁴⁶, O. Kuprash¹⁵⁵, H. Kurashige⁷⁰, L.L. Kurchaninov^{163a},
Y.A. Kurochkin⁹⁵, M.G. Kurth^{35a,35d}, E.S. Kuwertz¹⁷², M. Kuze¹⁵⁹, J. Kvita¹¹⁷, T. Kwan¹⁷²,
D. Kyriazopoulos¹⁴¹, A. La Rosa¹⁰³, J.L. La Rosa Navarro^{26d}, L. La Rotonda^{40a,40b},
F. La Ruffa^{40a,40b}, C. Lacasta¹⁷⁰, F. Lacava^{134a,134b}, J. Lacey⁴⁵, D.P.J. Lack⁸⁷, H. Lacker¹⁷,
D. Lacour⁸³, E. Ladygin⁶⁸, R. Lafaye⁵, B. Laforge⁸³, S. Lai⁵⁷, S. Lammers⁶⁴, W. Lampl⁷,
E. Lançon²⁷, U. Landgraf⁵¹, M.P.J. Landon⁷⁹, M.C. Lanfermann⁵², V.S. Lang⁴⁵, J.C. Lange¹³,
R.J. Langenberg³², A.J. Lankford¹⁶⁶, F. Lanni²⁷, K. Lantzsch²³, A. Lanza^{123a},
A. Lapertosa^{53a,53b}, S. Laplace⁸³, J.F. Laporte¹³⁸, T. Lari^{94a}, F. Lasagni Manghi^{22a,22b},
M. Lassnig³², T.S. Lau^{62a}, P. Laurelli⁵⁰, W. Lavrijsen¹⁶, A.T. Law¹³⁹, P. Laycock⁷⁷,
T. Lazovich⁵⁹, M. Lazzaroni^{94a,94b}, B. Le⁹¹, O. Le Dortz⁸³, E. Le Guirrec⁸⁸, E.P. Le Quilleuc¹³⁸,
M. LeBlanc¹⁷², T. LeCompte⁶, F. Ledroit-Guillon⁵⁸, C.A. Lee²⁷, G.R. Lee^{34a}, S.C. Lee¹⁵³,
L. Lee⁵⁹, B. Lefebvre⁹⁰, G. Lefebvre⁸³, M. Lefebvre¹⁷², F. Legger¹⁰², C. Leggett¹⁶,
G. Lehmann Miotto³², X. Lei⁷, W.A. Leight⁴⁵, M.A.L. Leite^{26d}, R. Leitner¹³¹, D. Lellouch¹⁷⁵,
B. Lemmer⁵⁷, K.J.C. Leney⁸¹, T. Lenz²³, B. Lenzi³², R. Leone⁷, S. Leone^{126a}, C. Leonidopoulos⁴⁹,
G. Lerner¹⁵¹, C. Leroy⁹⁷, R. Les¹⁶¹, A.A.J. Lesage¹³⁸, C.G. Lester³⁰, M. Levchenko¹²⁵,
J. Levêque⁵, D. Levin⁹², L.J. Levinson¹⁷⁵, M. Levy¹⁹, D. Lewis⁷⁹, B. Li^{36c,x}, H. Li¹⁵⁰, L. Li^{36b},
Q. Li^{35a,35d}, Q. Li^{36c}, S. Li⁴⁸, X. Li^{36b}, Y. Li¹⁴³, Z. Liang^{35a}, B. Liberti^{135a}, A. Liblong¹⁶¹,
K. Lie^{62c}, J. Liebal²³, W. Liebig¹⁵, A. Limosani¹⁵², C.Y. Lin³⁰, K. Lin⁹³, S.C. Lin¹⁸², T.H. Lin⁸⁶,
R.A. Linck⁶⁴, B.E. Lindquist¹⁵⁰, A.E. Lioni⁵², E. Lipeles¹²⁴, A. Lipniacka¹⁵, M. Lisovyi^{60b},
T.M. Liss^{169,ah}, A. Lister¹⁷¹, A.M. Litke¹³⁹, B. Liu⁶⁷, H. Liu⁹², H. Liu²⁷, J.K.K. Liu¹²², J. Liu^{36a},
J.B. Liu^{36c}, K. Liu⁸⁸, L. Liu¹⁶⁹, M. Liu^{36c}, Y.L. Liu^{36c}, Y. Liu^{36c}, M. Livan^{123a,123b}, A. Lleres⁵⁸,
J. Llorente Merino^{35a}, S.L. Lloyd⁷⁹, C.Y. Lo^{62b}, F. Lo Sterzo⁴³, E.M. Lobodzinska⁴⁵, P. Loch⁷,
F.K. Loebinger⁸⁷, A. Loesle⁵¹, K.M. Loew²⁵, T. Lohse¹⁷, K. Lohwasser¹⁴¹, M. Lokajicek¹²⁹,
B.A. Long²⁴, J.D. Long¹⁶⁹, R.E. Long⁷⁵, L. Longo^{76a,76b}, K.A. Looper¹¹³, J.A. Lopez^{34b},
I. Lopez Paz¹³, A. Lopez Solis⁸³, J. Lorenz¹⁰², N. Lorenzo Martinez⁵, M. Losada²¹, P.J. Lösel¹⁰²,
X. Lou^{35a}, A. Lounis¹¹⁹, J. Love⁶, P.A. Love⁷⁵, H. Lu^{62a}, N. Lu⁹², Y.J. Lu⁶³, H.J. Lubatti¹⁴⁰,
C. Luci^{134a,134b}, A. Lucotte⁵⁸, C. Luedtke⁵¹, F. Luehring⁶⁴, W. Lukas⁶⁵, L. Luminari^{134a},
O. Lundberg^{148a,148b}, B. Lund-Jensen¹⁴⁹, M.S. Lutz⁸⁹, P.M. Luzi⁸³, D. Lynn²⁷, R. Lysak¹²⁹,
E. Lytken⁸⁴, F. Lyu^{35a}, V. Lyubushkin⁶⁸, H. Ma²⁷, L.L. Ma^{36a}, Y. Ma^{36a}, G. Maccarrone⁵⁰,
A. Macchiolo¹⁰³, C.M. Macdonald¹⁴¹, B. Maček⁷⁸, J. Machado Miguens^{124,128b}, D. Madaffari¹⁷⁰,
R. Madar³⁷, W.F. Mader⁴⁷, A. Madsen⁴⁵, N. Madysa⁴⁷, J. Maeda⁷⁰, S. Maeland¹⁵, T. Maeno²⁷,
A.S. Maevskiy¹⁰¹, V. Magerl⁵¹, C. Maiani¹¹⁹, C. Maidantchik^{26a}, T. Maier¹⁰²,
A. Maio^{128a,128b,128d}, O. Majersky^{146a}, S. Majewski¹¹⁸, Y. Makida⁶⁹, N. Makovec¹¹⁹,
B. Malaescu⁸³, Pa. Malecki⁴², V.P. Maleev¹²⁵, F. Malek⁵⁸, U. Mallik⁶⁶, D. Malon⁶, C. Malone³⁰,
S. Maltezos¹⁰, S. Malyukov³², J. Mamuzic¹⁷⁰, G. Mancini⁵⁰, I. Mandić⁷⁸, J. Maneira^{128a,128b},
L. Manhaes de Andrade Filho^{26b}, J. Manjarres Ramos⁴⁷, K.H. Mankinen⁸⁴, A. Mann¹⁰²,
A. Manousos³², B. Mansoulie¹³⁸, J.D. Mansour^{35a}, R. Mantifel⁹⁰, M. Mantoani⁵⁷,
S. Manzoni^{94a,94b}, L. Mapelli³², G. Marceca²⁹, L. March⁵², L. Marchese¹²², G. Marchiori⁸³,
M. Marcisovsky¹²⁹, C.A. Marin Tobon³², M. Marjanovic³⁷, D.E. Marley⁹², F. Marroquim^{26a},
S.P. Marsden⁸⁷, Z. Marshall¹⁶, M.U.F. Martensson¹⁶⁸, S. Marti-Garcia¹⁷⁰, C.B. Martin¹¹³,
T.A. Martin¹⁷³, V.J. Martin⁴⁹, B. Martin dit Latour¹⁵, M. Martinez^{13,w},
V.I. Martinez Outschoorn¹⁶⁹, S. Martin-Haugh¹³³, V.S. Martoiu^{28b}, A.C. Martyniuk⁸¹,
A. Marzin³², L. Masetti⁸⁶, T. Mashimo¹⁵⁷, R. Mashinistov⁹⁸, J. Masik⁸⁷, A.L. Maslennikov^{111,c},

L.H. Mason⁹¹, L. Massa^{135a,135b}, P. Mastrandrea⁵, A. Mastroberardino^{40a,40b}, T. Masubuchi¹⁵⁷, P. Mättig¹⁷⁸, J. Maurer^{28b}, S.J. Maxfield⁷⁷, D.A. Maximov^{111,c}, R. Mazini¹⁵³, I. Maznas¹⁵⁶, S.M. Mazza^{94a,94b}, N.C. Mc Fadden¹⁰⁷, G. Mc Goldrick¹⁶¹, S.P. Mc Kee⁹², A. McCarn⁹², R.L. McCarthy¹⁵⁰, T.G. McCarthy¹⁰³, L.I. McClymont⁸¹, E.F. McDonald⁹¹, J.A. Mcfayden³², G. Mchedlidze⁵⁷, S.J. McMahon¹³³, P.C. McNamara⁹¹, C.J. McNicol¹⁷³, R.A. McPherson^{172,o}, S. Meehan¹⁴⁰, T.J. Megy⁵¹, S. Mehlhase¹⁰², A. Mehta⁷⁷, T. Meideck⁵⁸, K. Meier^{60a}, B. Meirose⁴⁴, D. Melini^{170,ai}, B.R. Mellado Garcia^{147c}, J.D. Mellenthin⁵⁷, M. Melo^{146a}, F. Meloni¹⁸, A. Melzer²³, S.B. Menary⁸⁷, L. Meng⁷⁷, X.T. Meng⁹², A. Mengarelli^{22a,22b}, S. Menke¹⁰³, E. Meoni^{40a,40b}, S. Mergelmeyer¹⁷, C. Merlassino¹⁸, P. Mermod⁵², L. Merola^{106a,106b}, C. Meroni^{94a}, F.S. Merritt³³, A. Messina^{134a,134b}, J. Metcalfe⁶, A.S. Mete¹⁶⁶, C. Meyer¹²⁴, J-P. Meyer¹³⁸, J. Meyer¹⁰⁹, H. Meyer Zu Theenhausen^{60a}, F. Miano¹⁵¹, R.P. Middleton¹³³, S. Miglioranza^{53a,53b}, L. Mijović⁴⁹, G. Mikenberg¹⁷⁵, M. Mikestikova¹²⁹, M. Mikuž⁷⁸, M. Milesi⁹¹, A. Milic¹⁶¹, D.A. Millar⁷⁹, D.W. Miller³³, C. Mills⁴⁹, A. Milov¹⁷⁵, D.A. Milstead^{148a,148b}, A.A. Minaenko¹³², Y. Minami¹⁵⁷, I.A. Minashvili^{54b}, A.I. Mincer¹¹², B. Mindur^{41a}, M. Mineev⁶⁸, Y. Minegishi¹⁵⁷, Y. Ming¹⁷⁶, L.M. Mir¹³, A. Mirto^{76a,76b}, K.P. Mistry¹²⁴, T. Mitani¹⁷⁴, J. Mitrevski¹⁰², V.A. Mitsou¹⁷⁰, A. Miucci¹⁸, P.S. Miyagawa¹⁴¹, A. Mizukami⁶⁹, J.U. Mjörnmark⁸⁴, T. Mkrtchyan¹⁸⁰, M. Mlynarikova¹³¹, T. Moa^{148a,148b}, K. Mochizuki⁹⁷, P. Mogg⁵¹, S. Mohapatra³⁸, S. Molander^{148a,148b}, R. Moles-Valls²³, M.C. Mondragon⁹³, K. Mönig⁴⁵, J. Monk³⁹, E. Monnier⁸⁸, A. Montalbano¹⁵⁰, J. Montejo Berlingen³², F. Monticelli⁷⁴, S. Monzani^{94a}, R.W. Moore³, N. Morange¹¹⁹, D. Moreno²¹, M. Moreno Llácer³², P. Morettini^{53a}, S. Morgenstern³², D. Mori¹⁴⁴, T. Mori¹⁵⁷, M. Morii⁵⁹, M. Morinaga¹⁷⁴, V. Morisbak¹²¹, A.K. Morley³², G. Mornacchi³², J.D. Morris⁷⁹, L. Morvaj¹⁵⁰, P. Moschovakos¹⁰, M. Mosidze^{54b}, H.J. Moss¹⁴¹, J. Moss^{145,aj}, K. Motohashi¹⁵⁹, R. Mount¹⁴⁵, E. Mountricha²⁷, E.J.W. Moyses⁸⁹, S. Muanza⁸⁸, F. Mueller¹⁰³, J. Mueller¹²⁷, R.S.P. Mueller¹⁰², D. Muenstermann⁷⁵, P. Mullen⁵⁶, G.A. Mullier¹⁸, F.J. Munoz Sanchez⁸⁷, W.J. Murray^{173,133}, H. Musheghyan³², M. Muškinja⁷⁸, A.G. Myagkov^{132,ak}, M. Myska¹³⁰, B.P. Nachman¹⁶, O. Nackenhorst⁵², K. Nagai¹²², R. Nagai^{69,af}, K. Nagano⁶⁹, Y. Nagasaka⁶¹, K. Nagata¹⁶⁴, M. Nagel⁵¹, E. Nagy⁸⁸, A.M. Nairz³², Y. Nakahama¹⁰⁵, K. Nakamura⁶⁹, T. Nakamura¹⁵⁷, I. Nakano¹¹⁴, R.F. Naranjo Garcia⁴⁵, R. Narayan¹¹, D.I. Narrias Villar^{60a}, I. Naryshkin¹²⁵, T. Naumann⁴⁵, G. Navarro²¹, R. Nayyar⁷, H.A. Neal⁹², P.Yu. Nechaeva⁹⁸, T.J. Neep¹³⁸, A. Negri^{123a,123b}, M. Negrini^{22a}, S. Nektarijevic¹⁰⁸, C. Nellist⁵⁷, A. Nelson¹⁶⁶, M.E. Nelson¹²², S. Nemecek¹²⁹, P. Nemethy¹¹², M. Nessi^{32,al}, M.S. Neubauer¹⁶⁹, M. Neumann¹⁷⁸, P.R. Newman¹⁹, T.Y. Ng^{62c}, Y.S. Ng¹⁷, T. Nguyen Manh⁹⁷, R.B. Nickerson¹²², R. Nicolaidou¹³⁸, J. Nielsen¹³⁹, N. Nikiforou¹¹, V. Nikolaenko^{132,ak}, I. Nikolic-Audit⁸³, K. Nikolopoulos¹⁹, J.K. Nilsen¹²¹, P. Nilsson²⁷, Y. Ninomiya⁶⁹, A. Nisati^{134a}, N. Nishu^{36b}, R. Nisius¹⁰³, I. Nitsche⁴⁶, T. Nitta¹⁷⁴, T. Nobe¹⁵⁷, Y. Noguchi⁷¹, M. Nomachi¹²⁰, I. Nomidis³¹, M.A. Nomura²⁷, T. Nooney⁷⁹, M. Nordberg³², N. Norjoharuddeen¹²², O. Novgorodova⁴⁷, M. Nozaki⁶⁹, L. Nozka¹¹⁷, K. Ntekas¹⁶⁶, E. Nurse⁸¹, F. Nuti⁹¹, K. O'connor²⁵, D.C. O'Neil¹⁴⁴, A.A. O'Rourke⁴⁵, V. O'Shea⁵⁶, F.G. Oakham^{31,d}, H. Oberlack¹⁰³, T. Obermann²³, J. Ocariz⁸³, A. Ochi⁷⁰, I. Ochoa³⁸, J.P. Ochoa-Ricoux^{34a}, S. Oda⁷³, S. Odaka⁶⁹, A. Oh⁸⁷, S.H. Oh⁴⁸, C.C. Ohm¹⁴⁹, H. Ohman¹⁶⁸, H. Oide^{53a,53b}, H. Okawa¹⁶⁴, Y. Okumura¹⁵⁷, T. Okuyama⁶⁹, A. Olariu^{28b}, L.F. Oleiro Seabra^{128a}, S.A. Olivares Pino^{34a}, D. Oliveira Damazio²⁷, A. Olszewski⁴², J. Olszowska⁴², A. Onofre^{128a,128e}, K. Onogi¹⁰⁵, P.U.E. Onyisi^{11,ab}, H. Oppen¹²¹, M.J. Oreglia³³, Y. Oren¹⁵⁵, D. Orestano^{136a,136b}, N. Orlando^{62b}, R.S. Orr¹⁶¹, B. Osculati^{53a,53b,*}, R. Ospanov^{36c}, G. Otero y Garzon²⁹, H. Otono⁷³, M. Ouchrif^{137d}, F. Ould-Saada¹²¹, A. Ouraou¹³⁸, K.P. Oussoren¹⁰⁹, Q. Ouyang^{35a}, M. Owen⁵⁶, R.E. Owen¹⁹, V.E. Ozcan^{20a}, N. Ozturk⁸, K. Pachal¹⁴⁴, A. Pacheco Pages¹³, L. Pacheco Rodriguez¹³⁸, C. Padilla Aranda¹³, S. Pagan Griso¹⁶, M. Paganini¹⁷⁹, F. Paige²⁷, G. Palacino⁶⁴, S. Palazzo^{40a,40b}, S. Palestini³², M. Palka^{41b}, D. Pallin³⁷, E.St. Panagiotopoulou¹⁰, I. Panagoulas¹⁰, C.E. Pandini⁵²,

J.G. Panduro Vazquez⁸⁰, P. Pani³², S. Panitkin²⁷, D. Pantea^{28b}, L. Paolozzi⁵²,
 Th.D. Papadopoulou¹⁰, K. Papageorgiou^{9,t}, A. Paramonov⁶, D. Paredes Hernandez¹⁷⁹,
 A.J. Parker⁷⁵, M.A. Parker³⁰, K.A. Parker⁴⁵, F. Parodi^{53a,53b}, J.A. Parsons³⁸, U. Parzefall⁵¹,
 V.R. Pascuzzi¹⁶¹, J.M. Pasner¹³⁹, E. Pasqualucci^{134a}, S. Passaggio^{53a}, Fr. Pastore⁸⁰,
 S. Patariaia⁸⁶, J.R. Pater⁸⁷, T. Pauly³², B. Pearson¹⁰³, S. Pedraza Lopez¹⁷⁰, R. Pedro^{128a,128b},
 S.V. Peleganchuk^{111,c}, O. Penc¹²⁹, C. Peng^{35a,35d}, H. Peng^{36c}, J. Penwell⁶⁴, B.S. Peralva^{26b},
 M.M. Perego¹³⁸, D.V. Perepelitsa²⁷, F. Peri¹⁷, L. Perini^{94a,94b}, H. Pernegger³²,
 S. Perrella^{106a,106b}, R. Peschke⁴⁵, V.D. Peshekhonov^{68,*}, K. Peters⁴⁵, R.F.Y. Peters⁸⁷,
 B.A. Petersen³², T.C. Petersen³⁹, E. Petit⁵⁸, A. Petridis¹, C. Petridou¹⁵⁶, P. Petroff¹¹⁹,
 E. Petrolo^{134a}, M. Petrov¹²², F. Petrucci^{136a,136b}, N.E. Pettersson⁸⁹, A. Peyaud¹³⁸, R. Pezoa^{34b},
 F.H. Phillips⁹³, P.W. Phillips¹³³, G. Piacquadio¹⁵⁰, E. Pianori¹⁷³, A. Picazio⁸⁹, M.A. Pickering¹²²,
 R. Piegaia²⁹, J.E. Pilcher³³, A.D. Pilkington⁸⁷, M. Pinamonti^{135a,135b}, J.L. Pinfold³,
 H. Pirumov⁴⁵, M. Pitt¹⁷⁵, L. Plazak^{146a}, M.-A. Pleier²⁷, V. Pleskot⁸⁶, E. Plotnikova⁶⁸,
 D. Pluth⁶⁷, P. Podberezko¹¹¹, R. Poettgen⁸⁴, R. Poggi^{123a,123b}, L. Poggioli¹¹⁹, I. Pogrebnyak⁹³,
 D. Pohl²³, I. Pokharel⁵⁷, G. Polesello^{123a}, A. Poley⁴⁵, A. Policicchio^{40a,40b}, R. Polifka³²,
 A. Polini^{22a}, C.S. Pollard⁵⁶, V. Polychronakos²⁷, K. Pommès³², D. Ponomarenko¹⁰⁰,
 L. Pontecorvo^{134a}, G.A. Popeneciu^{28d}, D.M. Portillo Quintero⁸³, S. Pospisil¹³⁰, K. Potamianos⁴⁵,
 I.N. Potrap⁶⁸, C.J. Potter³⁰, H. Potti¹¹, T. Poulsen⁸⁴, J. Poveda³², M.E. Pozo Astigarraga³²,
 P. Pralavorio⁸⁸, A. Pranko¹⁶, S. Prell⁶⁷, D. Price⁸⁷, M. Primavera^{76a}, S. Prince⁹⁰, N. Proklova¹⁰⁰,
 K. Prokofiev^{62c}, F. Prokoshin^{34b}, S. Protopopescu²⁷, J. Proudfoot⁶, M. Przybycien^{41a}, A. Puri¹⁶⁹,
 P. Puzo¹¹⁹, J. Qian⁹², G. Qin⁵⁶, Y. Qin⁸⁷, A. Quadt⁵⁷, M. Queitsch-Maitland⁴⁵, D. Quilty⁵⁶,
 S. Raddum¹²¹, V. Radeka²⁷, V. Radescu¹²², S.K. Radhakrishnan¹⁵⁰, P. Radloff¹¹⁸, P. Rados⁹¹,
 F. Ragusa^{94a,94b}, G. Rahal¹⁸¹, J.A. Raine⁸⁷, S. Rajagopalan²⁷, C. Rangel-Smith¹⁶⁸, T. Rashid¹¹⁹,
 S. Raspopov⁵, M.G. Ratti^{94a,94b}, D.M. Rauch⁴⁵, F. Rauscher¹⁰², S. Rave⁸⁶, I. Ravinovich¹⁷⁵,
 J.H. Rawling⁸⁷, M. Raymond³², A.L. Read¹²¹, N.P. Readioff⁵⁸, M. Reale^{76a,76b},
 D.M. Rebuzzi^{123a,123b}, A. Redelbach¹⁷⁷, G. Redlinger²⁷, R. Reece¹³⁹, R.G. Reed^{147c}, K. Reeves⁴⁴,
 L. Rehnisch¹⁷, J. Reichert¹²⁴, A. Reiss⁸⁶, C. Rembser³², H. Ren^{35a,35d}, M. Rescigno^{134a},
 S. Resconi^{94a}, E.D. Resseguie¹²⁴, S. Rettie¹⁷¹, E. Reynolds¹⁹, O.L. Rezanova^{111,c}, P. Reznicek¹³¹,
 R. Rezvani⁹⁷, R. Richter¹⁰³, S. Richter⁸¹, E. Richter-Was^{41b}, O. Ricken²³, M. Ridel⁸³, P. Rieck¹⁰³,
 C.J. Riegel¹⁷⁸, J. Rieger⁵⁷, O. Rifki¹¹⁵, M. Rijssenbeek¹⁵⁰, A. Rimoldi^{123a,123b}, M. Rimoldi¹⁸,
 L. Rinaldi^{22a}, G. Ripellino¹⁴⁹, B. Ristić³², E. Ritsch³², I. Riu¹³, F. Rizatdinova¹¹⁶, E. Rizvi⁷⁹,
 C. Rizzi¹³, R.T. Roberts⁸⁷, S.H. Robertson^{90,o}, A. Robichaud-Veronneau⁹⁰, D. Robinson³⁰,
 J.E.M. Robinson⁴⁵, A. Robson⁵⁶, E. Rocco⁸⁶, C. Roda^{126a,126b}, Y. Rodina^{88,am},
 S. Rodriguez Bosca¹⁷⁰, A. Rodriguez Perez¹³, D. Rodriguez Rodriguez¹⁷⁰, S. Roe³², C.S. Rogan⁵⁹,
 O. Röhne¹²¹, J. Roloff⁵⁹, A. Romanouk¹⁰⁰, M. Romano^{22a,22b}, S.M. Romano Saez³⁷,
 E. Romero Adam¹⁷⁰, N. Rompotis⁷⁷, M. Ronzani⁵¹, L. Roos⁸³, S. Rosati^{134a}, K. Rosbach⁵¹,
 P. Rose¹³⁹, N.-A. Rosien⁵⁷, E. Rossi^{106a,106b}, L.P. Rossi^{53a}, J.H.N. Rosten³⁰, R. Rosten¹⁴⁰,
 M. Rotaru^{28b}, J. Rothberg¹⁴⁰, D. Rousseau¹¹⁹, A. Rozanov⁸⁸, Y. Rozen¹⁵⁴, X. Ruan^{147c},
 F. Rubbo¹⁴⁵, F. Rühr⁵¹, A. Ruiz-Martinez³¹, Z. Rurikova⁵¹, N.A. Rusakovich⁶⁸, H.L. Russell⁹⁰,
 J.P. Rutherford⁷, N. Ruthmann³², E.M. Rüttinger⁴⁵, Y.F. Ryabov¹²⁵, M. Rybar¹⁶⁹,
 G. Rybkin¹¹⁹, S. Ryu⁶, A. Ryzhov¹³², G.F. Rzehorz⁵⁷, A.F. Saavedra¹⁵², G. Sabato¹⁰⁹,
 S. Sacerdoti²⁹, H.F.-W. Sadrozinski¹³⁹, R. Sadykov⁶⁸, F. Safai Tehrani^{134a}, P. Saha¹¹⁰,
 M. Sahinsoy^{60a}, M. Saimpert⁴⁵, M. Saito¹⁵⁷, T. Saito¹⁵⁷, H. Sakamoto¹⁵⁷, Y. Sakurai¹⁷⁴,
 G. Salamanna^{136a,136b}, J.E. Salazar Loyola^{34b}, D. Salek¹⁰⁹, P.H. Sales De Bruin¹⁶⁸,
 D. Salihagic¹⁰³, A. Salnikov¹⁴⁵, J. Salt¹⁷⁰, D. Salvatore^{40a,40b}, F. Salvatore¹⁵¹,
 A. Salvucci^{62a,62b,62c}, A. Salzburger³², D. Sammel⁵¹, D. Sampsonidis¹⁵⁶, D. Sampsonidou¹⁵⁶,
 J. Sánchez¹⁷⁰, V. Sanchez Martinez¹⁷⁰, A. Sanchez Pineda^{167a,167c}, H. Sandaker¹²¹,
 R.L. Sandbach⁷⁹, C.O. Sander⁴⁵, M. Sandhoff¹⁷⁸, C. Sandoval²¹, D.P.C. Sankey¹³³,

M. Sannino^{53a,53b}, Y. Sano¹⁰⁵, A. Sansoni⁵⁰, C. Santoni³⁷, H. Santos^{128a}, I. Santoyo Castillo¹⁵¹,
 A. Sapronov⁶⁸, J.G. Saraiva^{128a,128d}, B. Sarrazin²³, O. Sasaki⁶⁹, K. Sato¹⁶⁴, E. Sauvan⁵,
 G. Savage⁸⁰, P. Savard^{161,d}, N. Savic¹⁰³, C. Sawyer¹³³, L. Sawyer^{82,v}, J. Saxon³³, C. Sbarra^{22a},
 A. Sbrizzi^{22a,22b}, T. Scanlon⁸¹, D.A. Scannicchio¹⁶⁶, J. Schaarschmidt¹⁴⁰, P. Schacht¹⁰³,
 B.M. Schachtner¹⁰², D. Schaefer³³, L. Schaefer¹²⁴, R. Schaefer⁴⁵, J. Schaeffer⁸⁶, S. Schaepe³²,
 S. Schaetzel^{60b}, U. Schäfer⁸⁶, A.C. Schaffer¹¹⁹, D. Schaile¹⁰², R.D. Schamberger¹⁵⁰,
 V.A. Schegelsky¹²⁵, D. Scheirich¹³¹, M. Schernau¹⁶⁶, C. Schiavi^{53a,53b}, S. Schier¹³⁹,
 L.K. Schildgen²³, C. Schillo⁵¹, M. Schioppa^{40a,40b}, S. Schlenker³², K.R. Schmidt-Sommerfeld¹⁰³,
 K. Schmieden³², C. Schmitt⁸⁶, S. Schmitt⁴⁵, S. Schmitz⁸⁶, U. Schnoor⁵¹, L. Schoeffel¹³⁸,
 A. Schoening^{60b}, B.D. Schoenrock⁹³, E. Schopf²³, M. Schott⁸⁶, J.F.P. Schouwenberg¹⁰⁸,
 J. Schovancova³², S. Schramm⁵², N. Schuh⁸⁶, A. Schulte⁸⁶, M.J. Schultens²³,
 H.-C. Schultz-Coulon^{60a}, H. Schulz¹⁷, M. Schumacher⁵¹, B.A. Schumm¹³⁹, Ph. Schune¹³⁸,
 A. Schwartzman¹⁴⁵, T.A. Schwarz⁹², H. Schweiger⁸⁷, Ph. Schwemling¹³⁸, R. Schwienhorst⁹³,
 J. Schwindling¹³⁸, A. Sciandra²³, G. Sciolla²⁵, M. Scornajenghi^{40a,40b}, F. Scuri^{126a}, F. Scutti⁹¹,
 J. Searcy⁹², P. Seema²³, S.C. Seidel¹⁰⁷, A. Seiden¹³⁹, J.M. Seixas^{26a}, G. Sekhniaidze^{106a},
 K. Sekhon⁹², S.J. Sekula⁴³, N. Semprini-Cesari^{22a,22b}, S. Senkin³⁷, C. Serfon¹²¹, L. Serin¹¹⁹,
 L. Serkin^{167a,167b}, M. Sessa^{136a,136b}, R. Seuster¹⁷², H. Severini¹¹⁵, T. Šfiligoj⁷⁸, F. Sforza¹⁶⁵,
 A. Sfyrila⁵², E. Shabalina⁵⁷, N.W. Shaikh^{148a,148b}, L.Y. Shan^{35a}, R. Shang¹⁶⁹, J.T. Shank²⁴,
 M. Shapiro¹⁶, P.B. Shatalov⁹⁹, K. Shaw^{167a,167b}, S.M. Shaw⁸⁷, A. Shcherbakova^{148a,148b},
 C.Y. Shehu¹⁵¹, Y. Shen¹¹⁵, N. Sherafati³¹, A.D. Sherman²⁴, P. Sherwood⁸¹, L. Shi^{153,an},
 S. Shimizu⁷⁰, C.O. Shimmin¹⁷⁹, M. Shimojima¹⁰⁴, I.P.J. Shipsey¹²², S. Shirabe⁷³,
 M. Shiyakova^{68,ao}, J. Shlomi¹⁷⁵, A. Shmeleva⁹⁸, D. Shoaleh Saadi⁹⁷, M.J. Shochet³³, S. Shojaii⁹¹,
 D.R. Shope¹¹⁵, S. Shrestha¹¹³, E. Shulga¹⁰⁰, M.A. Shupe⁷, P. Sicho¹²⁹, A.M. Sickles¹⁶⁹,
 P.E. Sidebo¹⁴⁹, E. Sideras Haddad^{147c}, O. Sidiropoulou¹⁷⁷, A. Sidoti^{22a,22b}, F. Siegert⁴⁷,
 Dj. Sijacki¹⁴, J. Silva^{128a,128d}, S.B. Silverstein^{148a}, V. Simak¹³⁰, L. Simic⁶⁸, S. Simion¹¹⁹,
 E. Simioni⁸⁶, B. Simmons⁸¹, M. Simon⁸⁶, P. Sinervo¹⁶¹, N.B. Sinev¹¹⁸, M. Sioli^{22a,22b},
 G. Siragusa¹⁷⁷, I. Siral⁹², S.Yu. Sivoklov¹⁰¹, J. Sjölin^{148a,148b}, M.B. Skinner⁷⁵, P. Skubic¹¹⁵,
 M. Slater¹⁹, T. Slavicek¹³⁰, M. Slawinska⁴², K. Sliwa¹⁶⁵, R. Slovak¹³¹, V. Smakhtin¹⁷⁵,
 B.H. Smart⁵, J. Smiesko^{146a}, N. Smirnov¹⁰⁰, S.Yu. Smirnov¹⁰⁰, Y. Smirnov¹⁰⁰,
 L.N. Smirnova^{101,ap}, O. Smirnova⁸⁴, J.W. Smith⁵⁷, M.N.K. Smith³⁸, R.W. Smith³⁸,
 M. Smizanska⁷⁵, K. Smolek¹³⁰, A.A. Snesarev⁹⁸, I.M. Snyder¹¹⁸, S. Snyder²⁷, R. Sobie^{172,o},
 F. Socher⁴⁷, A. Soffer¹⁵⁵, A. Sogaard⁴⁹, D.A. Soh¹⁵³, G. Sokhrannyi⁷⁸, C.A. Solans Sanchez³²,
 M. Solar¹³⁰, E.Yu. Soldatov¹⁰⁰, U. Soldevila¹⁷⁰, A.A. Solodkov¹³², A. Soloshenko⁶⁸,
 O.V. Solovyanov¹³², V. Solovyev¹²⁵, P. Sommer¹⁴¹, H. Son¹⁶⁵, A. Sopczak¹³⁰, D. Sosa^{60b},
 C.L. Sotiropoulou^{126a,126b}, S. Sottocornola^{123a,123b}, R. Soualah^{167a,167c}, A.M. Soukharev^{111,c},
 D. South⁴⁵, B.C. Sowden⁸⁰, S. Spagnolo^{76a,76b}, M. Spalla^{126a,126b}, M. Spangenberg¹⁷³,
 F. Spanò⁸⁰, D. Sperlich¹⁷, F. Spettel¹⁰³, T.M. Spieker^{60a}, R. Spighi^{22a}, G. Spigo³², L.A. Spiller⁹¹,
 M. Spousta¹³¹, R.D. St. Denis^{56,*}, A. Stabile^{94a,94b}, R. Stamen^{60a}, S. Stamm¹⁷, E. Stanecka⁴²,
 R.W. Stanek⁶, C. Stanescu^{136a}, M.M. Stanitzki⁴⁵, B.S. Stapf¹⁰⁹, S. Stapnes¹²¹,
 E.A. Starchenko¹³², G.H. Stark³³, J. Stark⁵⁸, S.H. Stark³⁹, P. Staroba¹²⁹, P. Starovoitov^{60a},
 S. Stärz³², R. Staszewski⁴², M. Stegler⁴⁵, P. Steinberg²⁷, B. Stelzer¹⁴⁴, H.J. Stelzer³²,
 O. Stelzer-Chilton^{163a}, H. Stenzel⁵⁵, T.J. Stevenson⁷⁹, G.A. Stewart⁵⁶, M.C. Stockton¹¹⁸,
 M. Stoebe⁹⁰, G. Stoica^{28b}, P. Stolte⁵⁷, S. Stonjek¹⁰³, A.R. Stradling⁸, A. Straessner⁴⁷,
 M.E. Stramaglia¹⁸, J. Strandberg¹⁴⁹, S. Strandberg^{148a,148b}, M. Strauss¹¹⁵, P. Strizenec^{146b},
 R. Ströhmer¹⁷⁷, D.M. Strom¹¹⁸, R. Stroynowski⁴³, A. Strubig⁴⁹, S.A. Stucci²⁷, B. Stugu¹⁵,
 N.A. Styles⁴⁵, D. Su¹⁴⁵, J. Su¹²⁷, S. Suchek^{60a}, Y. Sugaya¹²⁰, M. Suk¹³⁰, V.V. Sulin⁹⁸,
 DMS Sultan^{162a,162b}, S. Sultansoy^{4c}, T. Sumida⁷¹, S. Sun⁵⁹, X. Sun³, K. Suruliz¹⁵¹,
 C.J.E. Suster¹⁵², M.R. Sutton¹⁵¹, S. Suzuki⁶⁹, M. Svatos¹²⁹, M. Swiatlowski³³, S.P. Swift²,

I. Sykora^{146a}, T. Sykora¹³¹, D. Ta⁵¹, K. Tackmann⁴⁵, J. Taenzer¹⁵⁵, A. Taffard¹⁶⁶,
 R. Tafirout^{163a}, E. Tahirovic⁷⁹, N. Taiblum¹⁵⁵, H. Takai²⁷, R. Takashima⁷², E.H. Takasugi¹⁰³,
 K. Takeda⁷⁰, T. Takeshita¹⁴², Y. Takubo⁶⁹, M. Talby⁸⁸, A.A. Talyshv^{111,c}, J. Tanaka¹⁵⁷,
 M. Tanaka¹⁵⁹, R. Tanaka¹¹⁹, S. Tanaka⁶⁹, R. Tanioka⁷⁰, B.B. Tannenwald¹¹³, S. Tapia Araya^{34b},
 S. Tapprogge⁸⁶, S. Tarem¹⁵⁴, G.F. Tartarelli^{94a}, P. Tas¹³¹, M. Tasevsky¹²⁹, T. Tashiro⁷¹,
 E. Tassi^{40a,40b}, A. Tavares Delgado^{128a,128b}, Y. Tayalati^{137e}, A.C. Taylor¹⁰⁷, A.J. Taylor⁴⁹,
 G.N. Taylor⁹¹, P.T.E. Taylor⁹¹, W. Taylor^{163b}, P. Teixeira-Dias⁸⁰, D. Temple¹⁴⁴, H. Ten Kate³²,
 P.K. Teng¹⁵³, J.J. Teoh¹²⁰, F. Tepel¹⁷⁸, S. Terada⁶⁹, K. Terashi¹⁵⁷, J. Terron⁸⁵, S. Terzo¹³,
 M. Testa⁵⁰, R.J. Teuscher^{161,o}, S.J. Thais¹⁷⁹, T. Thevenaux-Pelzer⁸⁸, F. Thiele³⁹,
 J.P. Thomas¹⁹, J. Thomas-Wilsker⁸⁰, P.D. Thompson¹⁹, A.S. Thompson⁵⁶, L.A. Thomsen¹⁷⁹,
 E. Thomson¹²⁴, Y. Tian³⁸, M.J. Tibbetts¹⁶, R.E. Ticse Torres⁵⁷, V.O. Tikhomirov^{98,aq},
 Yu.A. Tikhonov^{111,c}, S. Timoshenko¹⁰⁰, P. Tipton¹⁷⁹, S. Tisserant⁸⁸, K. Todome¹⁵⁹,
 S. Todorova-Nova⁵, S. Todt⁴⁷, J. Tojo⁷³, S. Tokár^{146a}, K. Tokushuku⁶⁹, E. Tolley¹¹³,
 L. Tomlinson⁸⁷, M. Tomoto¹⁰⁵, L. Tompkins^{145,ar}, K. Toms¹⁰⁷, B. Tong⁵⁹, P. Tornambe⁵¹,
 E. Torrence¹¹⁸, H. Torres⁴⁷, E. Torró Pastor¹⁴⁰, J. Toth^{88,as}, F. Touchard⁸⁸, D.R. Tovey¹⁴¹,
 C.J. Treado¹¹², T. Trefzger¹⁷⁷, F. Tresoldi¹⁵¹, A. Tricoli²⁷, I.M. Trigger^{163a}, S. Trincaz-Duvold⁸³,
 M.F. Tripiana¹³, W. Trischuk¹⁶¹, B. Trocme⁵⁸, A. Trofymov⁴⁵, C. Troncon^{94a},
 M. Trottier-McDonald¹⁶, M. Trovatelli¹⁷², L. Truong^{147b}, M. Trzebinski⁴², A. Trzupek⁴²,
 K.W. Tsang^{62a}, J.C.-L. Tseng¹²², P.V. Tsireshka⁹⁵, G. Tsipolitis¹⁰, N. Tsirintanis⁹,
 S. Tsiskaridze¹³, V. Tsiskaridze⁵¹, E.G. Tskhadadze^{54a}, I.I. Tsukerman⁹⁹, V. Tsulaia¹⁶,
 S. Tsuno⁶⁹, D. Tsybychev¹⁵⁰, Y. Tu^{62b}, A. Tudorache^{28b}, V. Tudorache^{28b}, T.T. Tubbure^{28a},
 A.N. Tuna⁵⁹, S. Turchikhin⁶⁸, D. Turgeman¹⁷⁵, I. Turk Cakir^{4b,at}, R. Turra^{94a}, P.M. Tuts³⁸,
 G. Uccelli^{22a,22b}, I. Ueda⁶⁹, M. Ughetto^{148a,148b}, F. Ukegawa¹⁶⁴, G. Unal³², A. Undrus²⁷,
 G. Unel¹⁶⁶, F.C. Ungaro⁹¹, Y. Unno⁶⁹, K. Uno¹⁵⁷, C. Unverdorben¹⁰², J. Urban^{146b}, P. Urquijo⁹¹,
 P. Urrejola⁸⁶, G. Usai⁸, J. Usui⁶⁹, L. Vacavant⁸⁸, V. Vacek¹³⁰, B. Vachon⁹⁰, K.O.H. Vadla¹²¹,
 A. Vaidya⁸¹, C. Valderanis¹⁰², E. Valdes Santurio^{148a,148b}, M. Valente⁵², S. Valentinetti^{22a,22b},
 A. Valero¹⁷⁰, L. Valéry¹³, S. Valkar¹³¹, A. Vallier⁵, J.A. Valls Ferrer¹⁷⁰,
 W. Van Den Wollenberg¹⁰⁹, H. van der Graaf¹⁰⁹, P. van Gemmeren⁶, J. Van Nieuwkoop¹⁴⁴,
 I. van Vulpen¹⁰⁹, M.C. van Woerden¹⁰⁹, M. Vanadia^{135a,135b}, W. Vandelli³², A. Vaniachine¹⁶⁰,
 P. Vankov¹⁰⁹, G. Vardanyan¹⁸⁰, R. Vari^{134a}, E.W. Varnes⁷, C. Varni^{53a,53b}, T. Varol⁴³,
 D. Varouchas¹¹⁹, A. Vartapetian⁸, K.E. Varvell¹⁵², J.G. Vasquez¹⁷⁹, G.A. Vasquez^{34b},
 F. Vazeille³⁷, D. Vazquez Furelos¹³, T. Vazquez Schroeder⁹⁰, J. Veatch⁵⁷, V. Veeraraghavan⁷,
 L.M. Veloce¹⁶¹, F. Veloso^{128a,128c}, S. Veneziano^{134a}, A. Ventura^{76a,76b}, M. Venturi¹⁷²,
 N. Venturi³², A. Venturini²⁵, V. Vercesi^{123a}, M. Verducci^{136a,136b}, W. Verkerke¹⁰⁹,
 A.T. Vermeulen¹⁰⁹, J.C. Vermeulen¹⁰⁹, M.C. Vetterli^{144,d}, N. Viaux Maira^{34b}, O. Viazlo⁸⁴,
 I. Vichou^{169,*}, T. Vickey¹⁴¹, O.E. Vickey Boeriu¹⁴¹, G.H.A. Viehhauser¹²², S. Viel¹⁶, L. Vignani¹²²,
 M. Villa^{22a,22b}, M. Villaplana Perez^{94a,94b}, E. Vilucchi⁵⁰, M.G. Vinciter³¹, V.B. Vinogradov⁶⁸,
 A. Vishwakarma⁴⁵, C. Vittori^{22a,22b}, I. Vivarelli¹⁵¹, S. Vlachos¹⁰, M. Vogel¹⁷⁸, P. Vokac¹³⁰,
 G. Volpi¹³, H. von der Schmitt¹⁰³, E. von Toerne²³, V. Vorobel¹³¹, K. Vorobev¹⁰⁰, M. Vos¹⁷⁰,
 R. Voss³², J.H. Vosseveld⁷⁷, N. Vranjes¹⁴, M. Vranjes Milosavljevic¹⁴, V. Vrba¹³⁰,
 M. Vreeswijk¹⁰⁹, R. Vuillermet³², I. Vukotic³³, P. Wagner²³, W. Wagner¹⁷⁸, J. Wagner-Kuhr¹⁰²,
 H. Wahlberg⁷⁴, S. Wahrmund⁴⁷, J. Walder⁷⁵, R. Walker¹⁰², W. Walkowiak¹⁴³,
 V. Wallangen^{148a,148b}, C. Wang^{35b}, C. Wang^{36a,q}, F. Wang¹⁷⁶, H. Wang¹⁶, H. Wang³, J. Wang⁴⁵,
 J. Wang¹⁵², Q. Wang¹¹⁵, R.-J. Wang⁸³, R. Wang^{36c}, R. Wang⁶, S.M. Wang¹⁵³, T. Wang³⁸,
 W. Wang^{153,au}, W. Wang^{36c,av}, Z. Wang^{36b}, C. Wanotayaroj⁴⁵, A. Warburton⁹⁰, C.P. Ward³⁰,
 D.R. Wardrope⁸¹, A. Washbrook⁴⁹, P.M. Watkins¹⁹, A.T. Watson¹⁹, M.F. Watson¹⁹, G. Watts¹⁴⁰,
 S. Watts⁸⁷, B.M. Waugh⁸¹, A.F. Webb¹¹, S. Webb⁸⁶, M.S. Weber¹⁸, S.M. Weber^{60a},
 S.W. Weber¹⁷⁷, S.A. Weber³¹, J.S. Webster⁶, A.R. Weidberg¹²², B. Weinert⁶⁴, J. Weingarten⁵⁷,

M. Weirich⁸⁶, C. Weiser⁵¹, H. Weits¹⁰⁹, P.S. Wells³², T. Wenaus²⁷, T. Wengler³², S. Wenig³², N. Wermes²³, M.D. Werner⁶⁷, P. Werner³², M. Wessels^{60a}, T.D. Weston¹⁸, K. Whalen¹¹⁸, N.L. Whallon¹⁴⁰, A.M. Wharton⁷⁵, A.S. White⁹², A. White⁸, M.J. White¹, R. White^{34b}, D. Whiteson¹⁶⁶, B.W. Whitmore⁷⁵, F.J. Wickens¹³³, W. Wiedenmann¹⁷⁶, M. WIELERS¹³³, C. Wiglesworth³⁹, L.A.M. Wiik-Fuchs⁵¹, A. Wildauer¹⁰³, F. Wilk⁸⁷, H.G. Wilkens³², H.H. Williams¹²⁴, S. Williams³⁰, C. Willis⁹³, S. Willocq⁸⁹, J.A. Wilson¹⁹, I. Wingerter-Seez⁵, E. Winkels¹⁵¹, F. Winklmeier¹¹⁸, O.J. Winston¹⁵¹, B.T. Winter²³, M. Wittgen¹⁴⁵, M. Wobisch^{82,v}, T.M.H. Wolf¹⁰⁹, R. Wolff⁸⁸, M.W. Wolter⁴², H. Wolters^{128a,128c}, V.W.S. Wong¹⁷¹, N.L. Woods¹³⁹, S.D. Worm¹⁹, B.K. Wosiek⁴², J. Wotschack³², K.W. Wozniak⁴², M. Wu³³, S.L. Wu¹⁷⁶, X. Wu⁵², Y. Wu⁹², T.R. Wyatt⁸⁷, B.M. Wynne⁴⁹, S. Xella³⁹, Z. Xi⁹², L. Xia^{35c}, D. Xu^{35a}, L. Xu²⁷, T. Xu¹³⁸, W. Xu⁹², B. Yabsley¹⁵², S. Yacoob^{147a}, D. Yamaguchi¹⁵⁹, Y. Yamaguchi¹⁵⁹, A. Yamamoto⁶⁹, S. Yamamoto¹⁵⁷, T. Yamanaka¹⁵⁷, F. Yamane⁷⁰, M. Yamatani¹⁵⁷, T. Yamazaki¹⁵⁷, Y. Yamazaki⁷⁰, Z. Yan²⁴, H. Yang^{36b}, H. Yang¹⁶, Y. Yang¹⁵³, Z. Yang¹⁵, W.-M. Yao¹⁶, Y.C. Yap⁴⁵, Y. Yasu⁶⁹, E. Yatsenko⁵, K.H. Yau Wong²³, J. Ye⁴³, S. Ye²⁷, I. Yeletsikh⁶⁸, E. Yigitbasi²⁴, E. Yildirim⁸⁶, K. Yorita¹⁷⁴, K. Yoshihara¹²⁴, C. Young¹⁴⁵, C.J.S. Young³², J. Yu⁸, J. Yu⁶⁷, S.P.Y. Yuen²³, I. Yusuf^{30,aw}, B. Zabinski⁴², G. Zacharis¹⁰, R. Zaidan¹³, A.M. Zaitsev^{132,ak}, N. Zakharchuk⁴⁵, J. Zalieckas¹⁵, A. Zaman¹⁵⁰, S. Zambito⁵⁹, D. Zanzi⁹¹, C. Zeitnitz¹⁷⁸, G. Zemaityte¹²², A. Zemla^{41a}, J.C. Zeng¹⁶⁹, Q. Zeng¹⁴⁵, O. Zenin¹³², T. Ženiš^{146a}, D. Zerwas¹¹⁹, D. Zhang^{36a}, D. Zhang⁹², F. Zhang¹⁷⁶, G. Zhang^{36c,av}, H. Zhang¹¹⁹, J. Zhang⁶, L. Zhang⁵¹, L. Zhang^{36c}, M. Zhang¹⁶⁹, P. Zhang^{35b}, R. Zhang²³, R. Zhang^{36c,q}, X. Zhang^{36a}, Y. Zhang^{35a,35d}, Z. Zhang¹¹⁹, X. Zhao⁴³, Y. Zhao^{36a,ax}, Z. Zhao^{36c}, A. Zhemchugov⁶⁸, B. Zhou⁹², C. Zhou¹⁷⁶, L. Zhou⁴³, M. Zhou^{35a,35d}, M. Zhou¹⁵⁰, N. Zhou^{36b}, Y. Zhou⁷, C.G. Zhu^{36a}, H. Zhu^{35a}, J. Zhu⁹², Y. Zhu^{36c}, X. Zhuang^{35a}, K. Zhukov⁹⁸, A. Zibell¹⁷⁷, D. Zieminska⁶⁴, N.I. Zimine⁶⁸, C. Zimmermann⁸⁶, S. Zimmermann⁵¹, Z. Zinonos¹⁰³, M. Zinser⁸⁶, M. Ziolkowski¹⁴³, L. Živković¹⁴, G. Zobernig¹⁷⁶, A. Zoccoli^{22a,22b}, R. Zou³³, M. zur Nedden¹⁷ and L. Zwalinski³²

¹ Department of Physics, University of Adelaide, Adelaide, Australia

² Physics Department, SUNY Albany, Albany NY, United States of America

³ Department of Physics, University of Alberta, Edmonton AB, Canada

⁴ (a) Department of Physics, Ankara University, Ankara; (b) Istanbul Aydin University, Istanbul; (c) Division of Physics, TOBB University of Economics and Technology, Ankara, Turkey

⁵ LAPP, CNRS/IN2P3 and Université Savoie Mont Blanc, Annecy-le-Vieux, France

⁶ High Energy Physics Division, Argonne National Laboratory, Argonne IL, United States of America

⁷ Department of Physics, University of Arizona, Tucson AZ, United States of America

⁸ Department of Physics, The University of Texas at Arlington, Arlington TX, United States of America

⁹ Physics Department, National and Kapodistrian University of Athens, Athens, Greece

¹⁰ Physics Department, National Technical University of Athens, Zografou, Greece

¹¹ Department of Physics, The University of Texas at Austin, Austin TX, United States of America

¹² Institute of Physics, Azerbaijan Academy of Sciences, Baku, Azerbaijan

¹³ Institut de Física d'Altes Energies (IFAE), The Barcelona Institute of Science and Technology, Barcelona, Spain

¹⁴ Institute of Physics, University of Belgrade, Belgrade, Serbia

¹⁵ Department for Physics and Technology, University of Bergen, Bergen, Norway

¹⁶ Physics Division, Lawrence Berkeley National Laboratory and University of California, Berkeley CA, United States of America

¹⁷ Department of Physics, Humboldt University, Berlin, Germany

¹⁸ Albert Einstein Center for Fundamental Physics and Laboratory for High Energy Physics, University of Bern, Bern, Switzerland

- ¹⁹ *School of Physics and Astronomy, University of Birmingham, Birmingham, United Kingdom*
- ²⁰ ^(a) *Department of Physics, Bogazici University, Istanbul;* ^(b) *Department of Physics Engineering, Gaziantep University, Gaziantep;* ^(d) *Istanbul Bilgi University, Faculty of Engineering and Natural Sciences, Istanbul;* ^(e) *Bahcesehir University, Faculty of Engineering and Natural Sciences, Istanbul, Turkey*
- ²¹ *Centro de Investigaciones, Universidad Antonio Narino, Bogota, Colombia*
- ²² ^(a) *INFN Sezione di Bologna;* ^(b) *Dipartimento di Fisica e Astronomia, Università di Bologna, Bologna, Italy*
- ²³ *Physikalisches Institut, University of Bonn, Bonn, Germany*
- ²⁴ *Department of Physics, Boston University, Boston MA, United States of America*
- ²⁵ *Department of Physics, Brandeis University, Waltham MA, United States of America*
- ²⁶ ^(a) *Universidade Federal do Rio De Janeiro COPPE/EE/IF, Rio de Janeiro;* ^(b) *Electrical Circuits Department, Federal University of Juiz de Fora (UFJF), Juiz de Fora;* ^(c) *Federal University of Sao Joao del Rei (UFSJ), Sao Joao del Rei;* ^(d) *Instituto de Fisica, Universidade de Sao Paulo, Sao Paulo, Brazil*
- ²⁷ *Physics Department, Brookhaven National Laboratory, Upton NY, United States of America*
- ²⁸ ^(a) *Transilvania University of Brasov, Brasov;* ^(b) *Horia Hulubei National Institute of Physics and Nuclear Engineering, Bucharest;* ^(c) *Department of Physics, Alexandru Ioan Cuza University of Iasi, Iasi;* ^(d) *National Institute for Research and Development of Isotopic and Molecular Technologies, Physics Department, Cluj Napoca;* ^(e) *University Politehnica Bucharest, Bucharest;* ^(f) *West University in Timisoara, Timisoara, Romania*
- ²⁹ *Departamento de Física, Universidad de Buenos Aires, Buenos Aires, Argentina*
- ³⁰ *Cavendish Laboratory, University of Cambridge, Cambridge, United Kingdom*
- ³¹ *Department of Physics, Carleton University, Ottawa ON, Canada*
- ³² *CERN, Geneva, Switzerland*
- ³³ *Enrico Fermi Institute, University of Chicago, Chicago IL, United States of America*
- ³⁴ ^(a) *Departamento de Física, Pontificia Universidad Católica de Chile, Santiago;* ^(b) *Departamento de Física, Universidad Técnica Federico Santa María, Valparaíso, Chile*
- ³⁵ ^(a) *Institute of High Energy Physics, Chinese Academy of Sciences, Beijing;* ^(b) *Department of Physics, Nanjing University, Jiangsu;* ^(c) *Physics Department, Tsinghua University, Beijing 100084;* ^(d) *University of Chinese Academy of Science (UCAS), Beijing, China*
- ³⁶ ^(a) *School of Physics, Shandong University, Shandong;* ^(b) *School of Physics and Astronomy, Key Laboratory for Particle Physics, Astrophysics and Cosmology, Ministry of Education; Shanghai Key Laboratory for Particle Physics and Cosmology, Tsung-Dao Lee Institute, Shanghai Jiao Tong University;* ^(c) *Department of Modern Physics and State Key Laboratory of Particle Detection and Electronics, University of Science and Technology of China, Anhui, China*
- ³⁷ *Université Clermont Auvergne, CNRS/IN2P3, LPC, Clermont-Ferrand, France*
- ³⁸ *Nevis Laboratory, Columbia University, Irvington NY, United States of America*
- ³⁹ *Niels Bohr Institute, University of Copenhagen, Kobenhavn, Denmark*
- ⁴⁰ ^(a) *INFN Gruppo Collegato di Cosenza, Laboratori Nazionali di Frascati;* ^(b) *Dipartimento di Fisica, Università della Calabria, Rende, Italy*
- ⁴¹ ^(a) *AGH University of Science and Technology, Faculty of Physics and Applied Computer Science, Krakow;* ^(b) *Marian Smoluchowski Institute of Physics, Jagiellonian University, Krakow, Poland*
- ⁴² *Institute of Nuclear Physics Polish Academy of Sciences, Krakow, Poland*
- ⁴³ *Physics Department, Southern Methodist University, Dallas TX, United States of America*
- ⁴⁴ *Physics Department, University of Texas at Dallas, Richardson TX, United States of America*
- ⁴⁵ *DESY, Hamburg and Zeuthen, Germany*
- ⁴⁶ *Lehrstuhl für Experimentelle Physik IV, Technische Universität Dortmund, Dortmund, Germany*
- ⁴⁷ *Institut für Kern- und Teilchenphysik, Technische Universität Dresden, Dresden, Germany*
- ⁴⁸ *Department of Physics, Duke University, Durham NC, United States of America*
- ⁴⁹ *SUPA - School of Physics and Astronomy, University of Edinburgh, Edinburgh, United Kingdom*
- ⁵⁰ *INFN e Laboratori Nazionali di Frascati, Frascati, Italy*

- ⁵¹ *Fakultät für Mathematik und Physik, Albert-Ludwigs-Universität, Freiburg, Germany*
- ⁵² *Departement de Physique Nucleaire et Corpusculaire, Université de Genève, Geneva, Switzerland*
- ⁵³ ^(a) *INFN Sezione di Genova;* ^(b) *Dipartimento di Fisica, Università di Genova, Genova, Italy*
- ⁵⁴ ^(a) *E. Andronikashvili Institute of Physics, Iv. Javakhishvili Tbilisi State University, Tbilisi;* ^(b) *High Energy Physics Institute, Tbilisi State University, Tbilisi, Georgia*
- ⁵⁵ *II Physikalisches Institut, Justus-Liebig-Universität Giessen, Giessen, Germany*
- ⁵⁶ *SUPA - School of Physics and Astronomy, University of Glasgow, Glasgow, United Kingdom*
- ⁵⁷ *II Physikalisches Institut, Georg-August-Universität, Göttingen, Germany*
- ⁵⁸ *Laboratoire de Physique Subatomique et de Cosmologie, Université Grenoble-Alpes, CNRS/IN2P3, Grenoble, France*
- ⁵⁹ *Laboratory for Particle Physics and Cosmology, Harvard University, Cambridge MA, United States of America*
- ⁶⁰ ^(a) *Kirchhoff-Institut für Physik, Ruprecht-Karls-Universität Heidelberg, Heidelberg;* ^(b) *Physikalisches Institut, Ruprecht-Karls-Universität Heidelberg, Heidelberg, Germany*
- ⁶¹ *Faculty of Applied Information Science, Hiroshima Institute of Technology, Hiroshima, Japan*
- ⁶² ^(a) *Department of Physics, The Chinese University of Hong Kong, Shatin, N.T., Hong Kong;* ^(b) *Department of Physics, The University of Hong Kong, Hong Kong;* ^(c) *Department of Physics and Institute for Advanced Study, The Hong Kong University of Science and Technology, Clear Water Bay, Kowloon, Hong Kong, China*
- ⁶³ *Department of Physics, National Tsing Hua University, Hsinchu, Taiwan*
- ⁶⁴ *Department of Physics, Indiana University, Bloomington IN, United States of America*
- ⁶⁵ *Institut für Astro- und Teilchenphysik, Leopold-Franzens-Universität, Innsbruck, Austria*
- ⁶⁶ *University of Iowa, Iowa City IA, United States of America*
- ⁶⁷ *Department of Physics and Astronomy, Iowa State University, Ames IA, United States of America*
- ⁶⁸ *Joint Institute for Nuclear Research, JINR Dubna, Dubna, Russia*
- ⁶⁹ *KEK, High Energy Accelerator Research Organization, Tsukuba, Japan*
- ⁷⁰ *Graduate School of Science, Kobe University, Kobe, Japan*
- ⁷¹ *Faculty of Science, Kyoto University, Kyoto, Japan*
- ⁷² *Kyoto University of Education, Kyoto, Japan*
- ⁷³ *Research Center for Advanced Particle Physics and Department of Physics, Kyushu University, Fukuoka, Japan*
- ⁷⁴ *Instituto de Física La Plata, Universidad Nacional de La Plata and CONICET, La Plata, Argentina*
- ⁷⁵ *Physics Department, Lancaster University, Lancaster, United Kingdom*
- ⁷⁶ ^(a) *INFN Sezione di Lecce;* ^(b) *Dipartimento di Matematica e Fisica, Università del Salento, Lecce, Italy*
- ⁷⁷ *Oliver Lodge Laboratory, University of Liverpool, Liverpool, United Kingdom*
- ⁷⁸ *Department of Experimental Particle Physics, Jožef Stefan Institute and Department of Physics, University of Ljubljana, Ljubljana, Slovenia*
- ⁷⁹ *School of Physics and Astronomy, Queen Mary University of London, London, United Kingdom*
- ⁸⁰ *Department of Physics, Royal Holloway University of London, Surrey, United Kingdom*
- ⁸¹ *Department of Physics and Astronomy, University College London, London, United Kingdom*
- ⁸² *Louisiana Tech University, Ruston LA, United States of America*
- ⁸³ *Laboratoire de Physique Nucléaire et de Hautes Energies, UPMC and Université Paris-Diderot and CNRS/IN2P3, Paris, France*
- ⁸⁴ *Fysiska institutionen, Lunds universitet, Lund, Sweden*
- ⁸⁵ *Departamento de Física Teórica C-15, Universidad Autónoma de Madrid, Madrid, Spain*
- ⁸⁶ *Institut für Physik, Universität Mainz, Mainz, Germany*
- ⁸⁷ *School of Physics and Astronomy, University of Manchester, Manchester, United Kingdom*
- ⁸⁸ *CPPM, Aix-Marseille Université and CNRS/IN2P3, Marseille, France*
- ⁸⁹ *Department of Physics, University of Massachusetts, Amherst MA, United States of America*
- ⁹⁰ *Department of Physics, McGill University, Montreal QC, Canada*
- ⁹¹ *School of Physics, University of Melbourne, Victoria, Australia*

- ⁹² *Department of Physics, The University of Michigan, Ann Arbor MI, United States of America*
- ⁹³ *Department of Physics and Astronomy, Michigan State University, East Lansing MI, United States of America*
- ⁹⁴ ^(a) *INFN Sezione di Milano;* ^(b) *Dipartimento di Fisica, Università di Milano, Milano, Italy*
- ⁹⁵ *B.I. Stepanov Institute of Physics, National Academy of Sciences of Belarus, Minsk, Republic of Belarus*
- ⁹⁶ *Research Institute for Nuclear Problems of Byelorussian State University, Minsk, Republic of Belarus*
- ⁹⁷ *Group of Particle Physics, University of Montreal, Montreal QC, Canada*
- ⁹⁸ *P.N. Lebedev Physical Institute of the Russian Academy of Sciences, Moscow, Russia*
- ⁹⁹ *Institute for Theoretical and Experimental Physics (ITEP), Moscow, Russia*
- ¹⁰⁰ *National Research Nuclear University MEPhI, Moscow, Russia*
- ¹⁰¹ *D.V. Skobeltsyn Institute of Nuclear Physics, M.V. Lomonosov Moscow State University, Moscow, Russia*
- ¹⁰² *Fakultät für Physik, Ludwig-Maximilians-Universität München, München, Germany*
- ¹⁰³ *Max-Planck-Institut für Physik (Werner-Heisenberg-Institut), München, Germany*
- ¹⁰⁴ *Nagasaki Institute of Applied Science, Nagasaki, Japan*
- ¹⁰⁵ *Graduate School of Science and Kobayashi-Maskawa Institute, Nagoya University, Nagoya, Japan*
- ¹⁰⁶ ^(a) *INFN Sezione di Napoli;* ^(b) *Dipartimento di Fisica, Università di Napoli, Napoli, Italy*
- ¹⁰⁷ *Department of Physics and Astronomy, University of New Mexico, Albuquerque NM, United States of America*
- ¹⁰⁸ *Institute for Mathematics, Astrophysics and Particle Physics, Radboud University Nijmegen/Nikhef, Nijmegen, Netherlands*
- ¹⁰⁹ *Nikhef National Institute for Subatomic Physics and University of Amsterdam, Amsterdam, Netherlands*
- ¹¹⁰ *Department of Physics, Northern Illinois University, DeKalb IL, United States of America*
- ¹¹¹ *Budker Institute of Nuclear Physics, SB RAS, Novosibirsk, Russia*
- ¹¹² *Department of Physics, New York University, New York NY, United States of America*
- ¹¹³ *Ohio State University, Columbus OH, United States of America*
- ¹¹⁴ *Faculty of Science, Okayama University, Okayama, Japan*
- ¹¹⁵ *Homer L. Dodge Department of Physics and Astronomy, University of Oklahoma, Norman OK, United States of America*
- ¹¹⁶ *Department of Physics, Oklahoma State University, Stillwater OK, United States of America*
- ¹¹⁷ *Palacký University, RCPTM, Olomouc, Czech Republic*
- ¹¹⁸ *Center for High Energy Physics, University of Oregon, Eugene OR, United States of America*
- ¹¹⁹ *LAL, Univ. Paris-Sud, CNRS/IN2P3, Université Paris-Saclay, Orsay, France*
- ¹²⁰ *Graduate School of Science, Osaka University, Osaka, Japan*
- ¹²¹ *Department of Physics, University of Oslo, Oslo, Norway*
- ¹²² *Department of Physics, Oxford University, Oxford, United Kingdom*
- ¹²³ ^(a) *INFN Sezione di Pavia;* ^(b) *Dipartimento di Fisica, Università di Pavia, Pavia, Italy*
- ¹²⁴ *Department of Physics, University of Pennsylvania, Philadelphia PA, United States of America*
- ¹²⁵ *National Research Centre “Kurchatov Institute” B.P.Konstantinov Petersburg Nuclear Physics Institute, St. Petersburg, Russia*
- ¹²⁶ ^(a) *INFN Sezione di Pisa;* ^(b) *Dipartimento di Fisica E. Fermi, Università di Pisa, Pisa, Italy*
- ¹²⁷ *Department of Physics and Astronomy, University of Pittsburgh, Pittsburgh PA, United States of America*
- ¹²⁸ ^(a) *Laboratório de Instrumentação e Física Experimental de Partículas - LIP, Lisboa;* ^(b) *Faculdade de Ciências, Universidade de Lisboa, Lisboa;* ^(c) *Department of Physics, University of Coimbra, Coimbra;* ^(d) *Centro de Física Nuclear da Universidade de Lisboa, Lisboa;* ^(e) *Departamento de Física, Universidade do Minho, Braga;* ^(f) *Departamento de Física Teórica y del Cosmos, Universidad de Granada, Granada;* ^(g) *Dep Física and CEFITEC of Faculdade de Ciências e Tecnologia, Universidade Nova de Lisboa, Caparica, Portugal*

- ¹²⁹ *Institute of Physics, Academy of Sciences of the Czech Republic, Praha, Czech Republic*
¹³⁰ *Czech Technical University in Prague, Praha, Czech Republic*
¹³¹ *Charles University, Faculty of Mathematics and Physics, Prague, Czech Republic*
¹³² *State Research Center Institute for High Energy Physics (Protvino), NRC KI, Russia*
¹³³ *Particle Physics Department, Rutherford Appleton Laboratory, Didcot, United Kingdom*
¹³⁴ ^(a) *INFN Sezione di Roma;* ^(b) *Dipartimento di Fisica, Sapienza Università di Roma, Roma, Italy*
¹³⁵ ^(a) *INFN Sezione di Roma Tor Vergata;* ^(b) *Dipartimento di Fisica, Università di Roma Tor Vergata, Roma, Italy*
¹³⁶ ^(a) *INFN Sezione di Roma Tre;* ^(b) *Dipartimento di Matematica e Fisica, Università Roma Tre, Roma, Italy*
¹³⁷ ^(a) *Faculté des Sciences Ain Chock, Réseau Universitaire de Physique des Hautes Energies - Université Hassan II, Casablanca;* ^(b) *Centre National de l'Energie des Sciences Techniques Nucleaires, Rabat;* ^(c) *Faculté des Sciences Semlalia, Université Cadi Ayyad, LPHEA-Marrakech;* ^(d) *Faculté des Sciences, Université Mohamed Premier and LPTPM, Oujda;* ^(e) *Faculté des sciences, Université Mohammed V, Rabat, Morocco*
¹³⁸ *DSM/IRFU (Institut de Recherches sur les Lois Fondamentales de l'Univers), CEA Saclay (Commissariat à l'Energie Atomique et aux Energies Alternatives), Gif-sur-Yvette, France*
¹³⁹ *Santa Cruz Institute for Particle Physics, University of California Santa Cruz, Santa Cruz CA, United States of America*
¹⁴⁰ *Department of Physics, University of Washington, Seattle WA, United States of America*
¹⁴¹ *Department of Physics and Astronomy, University of Sheffield, Sheffield, United Kingdom*
¹⁴² *Department of Physics, Shinshu University, Nagano, Japan*
¹⁴³ *Department Physik, Universität Siegen, Siegen, Germany*
¹⁴⁴ *Department of Physics, Simon Fraser University, Burnaby BC, Canada*
¹⁴⁵ *SLAC National Accelerator Laboratory, Stanford CA, United States of America*
¹⁴⁶ ^(a) *Faculty of Mathematics, Physics & Informatics, Comenius University, Bratislava;* ^(b) *Department of Subnuclear Physics, Institute of Experimental Physics of the Slovak Academy of Sciences, Kosice, Slovak Republic*
¹⁴⁷ ^(a) *Department of Physics, University of Cape Town, Cape Town;* ^(b) *Department of Physics, University of Johannesburg, Johannesburg;* ^(c) *School of Physics, University of the Witwatersrand, Johannesburg, South Africa*
¹⁴⁸ ^(a) *Department of Physics, Stockholm University;* ^(b) *The Oskar Klein Centre, Stockholm, Sweden*
¹⁴⁹ *Physics Department, Royal Institute of Technology, Stockholm, Sweden*
¹⁵⁰ *Departments of Physics & Astronomy and Chemistry, Stony Brook University, Stony Brook NY, United States of America*
¹⁵¹ *Department of Physics and Astronomy, University of Sussex, Brighton, United Kingdom*
¹⁵² *School of Physics, University of Sydney, Sydney, Australia*
¹⁵³ *Institute of Physics, Academia Sinica, Taipei, Taiwan*
¹⁵⁴ *Department of Physics, Technion: Israel Institute of Technology, Haifa, Israel*
¹⁵⁵ *Raymond and Beverly Sackler School of Physics and Astronomy, Tel Aviv University, Tel Aviv, Israel*
¹⁵⁶ *Department of Physics, Aristotle University of Thessaloniki, Thessaloniki, Greece*
¹⁵⁷ *International Center for Elementary Particle Physics and Department of Physics, The University of Tokyo, Tokyo, Japan*
¹⁵⁸ *Graduate School of Science and Technology, Tokyo Metropolitan University, Tokyo, Japan*
¹⁵⁹ *Department of Physics, Tokyo Institute of Technology, Tokyo, Japan*
¹⁶⁰ *Tomsk State University, Tomsk, Russia*
¹⁶¹ *Department of Physics, University of Toronto, Toronto ON, Canada*
¹⁶² ^(a) *INFN-TIFPA;* ^(b) *University of Trento, Trento, Italy*
¹⁶³ ^(a) *TRIUMF, Vancouver BC;* ^(b) *Department of Physics and Astronomy, York University, Toronto ON, Canada*
¹⁶⁴ *Faculty of Pure and Applied Sciences, and Center for Integrated Research in Fundamental Science*

- and Engineering, University of Tsukuba, Tsukuba, Japan
- ¹⁶⁵ Department of Physics and Astronomy, Tufts University, Medford MA, United States of America
- ¹⁶⁶ Department of Physics and Astronomy, University of California Irvine, Irvine CA, United States of America
- ¹⁶⁷ ^(a) INFN Gruppo Collegato di Udine, Sezione di Trieste, Udine; ^(b) ICTP, Trieste; ^(c) Dipartimento di Chimica, Fisica e Ambiente, Università di Udine, Udine, Italy
- ¹⁶⁸ Department of Physics and Astronomy, University of Uppsala, Uppsala, Sweden
- ¹⁶⁹ Department of Physics, University of Illinois, Urbana IL, United States of America
- ¹⁷⁰ Instituto de Fisica Corpuscular (IFIC), Centro Mixto Universidad de Valencia - CSIC, Spain
- ¹⁷¹ Department of Physics, University of British Columbia, Vancouver BC, Canada
- ¹⁷² Department of Physics and Astronomy, University of Victoria, Victoria BC, Canada
- ¹⁷³ Department of Physics, University of Warwick, Coventry, United Kingdom
- ¹⁷⁴ Waseda University, Tokyo, Japan
- ¹⁷⁵ Department of Particle Physics, The Weizmann Institute of Science, Rehovot, Israel
- ¹⁷⁶ Department of Physics, University of Wisconsin, Madison WI, United States of America
- ¹⁷⁷ Fakultät für Physik und Astronomie, Julius-Maximilians-Universität, Würzburg, Germany
- ¹⁷⁸ Fakultät für Mathematik und Naturwissenschaften, Fachgruppe Physik, Bergische Universität Wuppertal, Wuppertal, Germany
- ¹⁷⁹ Department of Physics, Yale University, New Haven CT, United States of America
- ¹⁸⁰ Yerevan Physics Institute, Yerevan, Armenia
- ¹⁸¹ Centre de Calcul de l'Institut National de Physique Nucléaire et de Physique des Particules (IN2P3), Villeurbanne, France
- ¹⁸² Academia Sinica Grid Computing, Institute of Physics, Academia Sinica, Taipei, Taiwan
- ^a Also at Department of Physics, King's College London, London, United Kingdom
- ^b Also at Institute of Physics, Azerbaijan Academy of Sciences, Baku, Azerbaijan
- ^c Also at Novosibirsk State University, Novosibirsk, Russia
- ^d Also at TRIUMF, Vancouver BC, Canada
- ^e Also at Department of Physics & Astronomy, University of Louisville, Louisville, KY, United States of America
- ^f Also at Physics Department, An-Najah National University, Nablus, Palestine
- ^g Also at Department of Physics, California State University, Fresno CA, United States of America
- ^h Also at Department of Physics, University of Fribourg, Fribourg, Switzerland
- ⁱ Also at II Physikalisches Institut, Georg-August-Universität, Göttingen, Germany
- ^j Also at Departament de Física de la Universitat Autònoma de Barcelona, Barcelona, Spain
- ^k Also at Departamento de Física e Astronomia, Faculdade de Ciências, Universidade do Porto, Portugal
- ^l Also at Tomsk State University, Tomsk, and Moscow Institute of Physics and Technology State University, Dolgoprudny, Russia
- ^m Also at The Collaborative Innovation Center of Quantum Matter (CICQM), Beijing, China
- ⁿ Also at Università di Napoli Parthenope, Napoli, Italy
- ^o Also at Institute of Particle Physics (IPP), Canada
- ^p Also at Horia Hulubei National Institute of Physics and Nuclear Engineering, Bucharest, Romania
- ^q Also at CPPM, Aix-Marseille Université and CNRS/IN2P3, Marseille, France
- ^r Also at Department of Physics, St. Petersburg State Polytechnical University, St. Petersburg, Russia
- ^s Also at Borough of Manhattan Community College, City University of New York, New York City, United States of America
- ^t Also at Department of Financial and Management Engineering, University of the Aegean, Chios, Greece
- ^u Also at Centre for High Performance Computing, CSIR Campus, Rosebank, Cape Town, South Africa

- ^v Also at Louisiana Tech University, Ruston LA, United States of America
- ^w Also at Institutio Catalana de Recerca i Estudis Avancats, ICREA, Barcelona, Spain
- ^x Also at Department of Physics, The University of Michigan, Ann Arbor MI, United States of America
- ^y Also at Graduate School of Science, Osaka University, Osaka, Japan
- ^z Also at Fakultät für Mathematik und Physik, Albert-Ludwigs-Universität, Freiburg, Germany
- ^{aa} Also at Institute for Mathematics, Astrophysics and Particle Physics, Radboud University Nijmegen/Nikhef, Nijmegen, Netherlands
- ^{ab} Also at Department of Physics, The University of Texas at Austin, Austin TX, United States of America
- ^{ac} Also at Institute of Theoretical Physics, Ilia State University, Tbilisi, Georgia
- ^{ad} Also at CERN, Geneva, Switzerland
- ^{ae} Also at Georgian Technical University (GTU), Tbilisi, Georgia
- ^{af} Also at Ochadai Academic Production, Ochanomizu University, Tokyo, Japan
- ^{ag} Also at Manhattan College, New York NY, United States of America
- ^{ah} Also at The City College of New York, New York NY, United States of America
- ^{ai} Also at Departamento de Física Teórica y del Cosmos, Universidad de Granada, Granada, Spain
- ^{aj} Also at Department of Physics, California State University, Sacramento CA, United States of America
- ^{ak} Also at Moscow Institute of Physics and Technology State University, Dolgoprudny, Russia
- ^{al} Also at Departement de Physique Nucleaire et Corpusculaire, Université de Genève, Geneva, Switzerland
- ^{am} Also at Institut de Física d'Altes Energies (IFAE), The Barcelona Institute of Science and Technology, Barcelona, Spain
- ^{an} Also at School of Physics, Sun Yat-sen University, Guangzhou, China
- ^{ao} Also at Institute for Nuclear Research and Nuclear Energy (INRNE) of the Bulgarian Academy of Sciences, Sofia, Bulgaria
- ^{ap} Also at Faculty of Physics, M.V.Lomonosov Moscow State University, Moscow, Russia
- ^{aq} Also at National Research Nuclear University MEPhI, Moscow, Russia
- ^{ar} Also at Department of Physics, Stanford University, Stanford CA, United States of America
- ^{as} Also at Institute for Particle and Nuclear Physics, Wigner Research Centre for Physics, Budapest, Hungary
- ^{at} Also at Giresun University, Faculty of Engineering, Turkey
- ^{au} Also at Department of Physics, Nanjing University, Jiangsu, China
- ^{av} Also at Institute of Physics, Academia Sinica, Taipei, Taiwan
- ^{aw} Also at University of Malaya, Department of Physics, Kuala Lumpur, Malaysia
- ^{ax} Also at LAL, Univ. Paris-Sud, CNRS/IN2P3, Université Paris-Saclay, Orsay, France
- * Deceased